Interactions between Cucumber mosaic virus proteins and host proteins

Lewis G. Watt

Darwin College

University of Cambridge

This dissertation is submitted for the degree of Doctor of Philosophy

March 2020

Dedication

This thesis is dedicated to my parents for their continuous support.

Acknowledgments

I would like to thank my supervisor John Carr for all his advice, for being supportive throughout my PhD and for allowing to follow my research interests. I will miss lab meeting MPSW cocktails and virology themed jokes during Part II virology practicals. I would like to take this opportunity to thank Alex Murphy for her help during my PhD learning various techniques, and providing me with transgenic Arabidopsis lines. Many thanks to Sam Crawshaw for being a hard working Part II student and contributing to my PhD by carrying out confocal imaging. It was great fun working with you. I am happy to see the work we started being continued during your PhD, and wish you all the best. I am also very grateful for Sun-Ju for helping me with my project and expert cloning advice. I would like to thank Nina for help with interpreting imaging results and providing me with constructs.

I would like to thank past members of the Virology lab for providing advice and making the lab a fun place to work. I am thankful for the help of Adrienne for getting me started in the lab and always being kind and making the lab a welcoming environment. I am especially thankful for the help of Ana, Sanjie, Trisna and Deusa, who helped me greatly at the start of my PhD and taught me the joys of aphid experiments. I would like to thank current lab members Anna and Warren for their support, discussion and company.

I would like to thank friends who have supported me during my PhD, especially Ben. I am also grateful to the Darwin College community and the 2015 BBSRC DTP cohort for many memorable times throughout my PhD. Finally, I thankful for the support of my parents and brothers. I would not be able to complete my PhD without the selflessness of my parents, especially my mum for donating her kidney to me, and my dad for caring for us both.

Declaration

This dissertation is the result of my own work and includes nothing which is the outcome of work done in collaboration except where specifically indicated in the text or Acknowledgements. None of its parts have been submitted for any other qualification. The dissertation does not exceed the word limit set by the Degree Committee for Biology.

Lewis G. Watt
Darwin College

Summary

Cucumber mosaic virus (CMV) infects over a thousand plant species including many crops. CMV is mainly transmitted between plants by aphids, insects with probing mouthparts that introduce virus particles directly into host cells. The 2b viral suppressor of RNA silencing (VSR) encoded by CMV is a potent counterdefence and pathogenicity factor that inhibits antiviral silencing by titration of short double-stranded RNAs. The 2b VSR not only influences infection, but also host interactions with one of the main insect vectors of CMV, the generalist aphid *Myzus persicae*. The 2b protein disrupts microRNA-mediated regulation of host gene expression by binding ARGONAUTE 1 (AGO1). In Arabidopsis, complete inhibition of AGO1 activity is counterproductive to CMV since this triggers antibiosis against aphids and stimulates resistance mechanisms by AGO2. The CMV 1a protein (a replicase component) is able to moderate antibiosis induction by the 2b VSR. This ensures that aphid vectors are deterred from feeding but not poisoned when they feed on CMV-infected Arabidopsis plants.

I found that the CMV 1a protein is able to directly inhibit the 2b-AGO1 interaction. By binding 2b protein molecules and sequestering them in processing-bodies, the 1a protein decreases the proportion of 2b protein molecules available for binding AGO1. This ameliorates 2b-induced viral symptoms and moderates the induction of aphid resistance. However, the 1a-2b protein interaction does not inhibit the VSR activity of the 2b protein. The interaction between the CMV 1a and 2b proteins represents a novel viral regulatory system for VSRs. The finding also provides a mechanism that may explain how CMV, and possibly other viruses, modulate symptom induction and manipulate host-vector interactions.

Contents

List of Figures

List of Tables

List of Abbreviations

4MI3M	4-methoxy-indol-3-ylmethylglucosinolate
ABA	abscisic acid
AGO	Argonaute
BAK1	BRI1-ASSOCIATED RECEPTOR KINASE
BiFC	bimolecular fluorescence complementation
BMV	Brome mosaic virus
BR	brassinosteroid
CaMV	cauliflower mosaic virus
CMV	cucumber mosaic virus
CP	coat protein
DAMP	damage-associated molecular patterns
DCL	dicer-like proteins
dsRNA	double-stranded RNA
ETI	effector-triggered immunity
flg22	22 amino acid epitope of flagellin
Fny-CMV	(see also CMV) CMV strain Fast New York
GFP	green fluorescent protein
HR	hypersensitive response
I3M	indol-3-ylmethyl glucosinolate
JA	jasmonic acid
LS-CMV	CMV strain Lactuca sativa
MAMP	microbe-associated molecular pattern
MAPK	mitogen-activated protein kinases
miRNA	microRNA
MP	movement protein
MRGR	mean relative growth rate
NLR	nucleotide-binding site leucine-rich repeat
NLS	nuclear localisation sequences
NT	non-transgenic
ORF	open reading frame
ORMV	oilseed rape mosaic virus
P-bodies	processing bodies
PAD3	PHYTOALEXIN DEFICIENT 3
PAMP	pathogen-associated molecular pattern
PRR	pattern recognition receptor
PTGS	posttranscriptional gene silencing

PTI	PAMP-triggered immunity
RdRp	RNA-dependent RNA-polymerase
RFP	red fluorescent protein
RISC	RNA-induced silencing complex
RLK	receptor-like kinases
RLKs	receptor-like kinases
RNAi	RNA interference
ROS	reactive oxygen species
SA	salicylic acid
siRNA	short interfering RNA
ssRNA	single stranded RNA
TCV	turnip crinkle virus
TF	transcription factor
TLR	toll-like receptor
TMV	tobacco mosaic virus
TuMV	turnip mosaic virus
VSR	viral suppressor of RNA silencing
YFP	yellow fluorescent protein

Chapter. 1 General Introduction

1.1 Background

Plant viruses are agriculturally and economically important pathogens since they decrease crop yield and quality (Loebenstein, 2009). The use of intensive monoculture-based agriculture combined with warmer temperatures (allowing insects vectors to spread), has increased the impact viruses have on agriculture (Elad and Pertot, 2014; Fereres and Raccah 2015). This problem is likely to increase as viruses are responsible for causing approximately half of all emerging crop diseases worldwide (Anderson et al., 2004; Scholthof et al., 2011). The global population is expected to increase by 2.3 billion people by 2050, and will require agricultural production to increase significantly (Fess et al., 2011). Thus, research in plant viruses is crucial for protecting food security.

Recent work suggests that viruses are able to alter the physiological characteristics of their host plant which influence the behaviour and performance of insect vectors (Groen et al., 2016; Westwood et al., 2013b; Yang et al., 2008). Viruses must replicate efficiently to generate inoculum for further transmission, while also avoiding triggering the host immune system or causing excessive damage to the host. Viral genomes are small and, consequently, viral proteins often have multiple functions. Studying the interactions between viral and host factors may aid efforts to engineer or breed virus resistant crops, as well as providing a useful tool to study pathogen-host interactions at the fundamental level (Culver and Padmanabhan, 2007).

In this study, I used the model system of cucumber mosaic virus (CMV), the peach-potato aphid (*Myzus persicae*) and the model plant *Arabidopsis thaliana* to investigate how the interactions between viral proteins and host factors are able to alter the host defence response in order to promote virus transmission by aphids.

1.2 Cucumber mosaic virus

Cucumber mosaic virus is the type species of the genus *Cucumovirus* in the family *Bromoviridae* (Palukaitis and García-Arenal, 2003). Other virus species belonging to the *Cucumovirus* genus include *Tomato aspermy virus* and *Peanut stunt virus*. CMV has one of the broadest host ranges of all plant viruses and can infect more than 1200 species (Carrère et al., 1999; Yoon et al., 2019). This host range includes many important agricultural crops including beans (broad, lima, snap), cucurbits (cucumber, melon, pumpkin, summer and winter squash, watermelon), pepper, potato and tomato (Palukaitis and García-Arenal, 2019). CMV is globally distributed and is considered an important disease in temperate, tropic and subtropical regions (Palukaitis and García-Arenal, 2003). Due to its large host range and economic importance, CMV has received considerable research attention over several decades. Many molecular techniques can be used to determine components of viral pathogenesis. Reverse genetic studies, where the pathogen is genetically modified (for example by site directed mutagenesis), can be used to identify how viral gene products contribute to pathogenicity, the ability to replicate, or infect specific hosts.

The CMV genome comprises three positive-sense RNAs (Peden and Symons, 1973). Due to this segmented CMV genome it is possible to create reassortant (also called pseudorecombinant) viruses, comprised of genomic RNAs from different strains. The mixing of genomic RNA molecules can also naturally occur and is thought to have contributed to the evolution of CMV (Lin et al., 2004). A crucial step in CMV research was the reverse transcription and complementary DNA (cDNA) cloning of the full-length CMV RNAs (Rizzo and Palukaitis, 1990). Viral cDNA clones are easily propagated in plasmid vectors and can be genetically modified easily to produce chimeric viruses and introduce point mutations in order to map virus function to specific genetic elements (reviewed by Jacquemond, 2012). Infectious mixtures of virus RNAs can be reconstituted using *in vitro*-synthesised transcripts from viral cDNA clones or by launching infection *in planta* by agroinfection (Hayes and Buck, 1990; Palukaitis and García-Arenal, 2019).

1.2.1 CMV genome organisation and replication

The current genetic map of CMV (Fig. 1.1) incorporates the information derived from the studies on translation, sequence and mutational analysis and biochemical analysis of the viral proteins. The CMV genome is split over three RNAs designated 1, 2, and 3, and contains five genes (*1a, 2a, 2b, 3a* and *3b*). Each of these three positive sense RNA molecules possess 7-methyl-guanosine cap structures at their 5' termini and tRNA-like structures at their 3' termini (Jacquemond, 2012). RNA 1 is monocistronic and acts as the mRNA for the 1a protein (Palukaitis and Garcia-Arenal, 2003). RNA 2 encodes the 2a and 2b proteins, the 2b open reading frame (ORF) overlaps the C-terminal coding region of the 2a ORF but in a different reading frame (Ding et al., 1994). RNA 3 encodes the 3a movement protein (MP), while the 3'-proximal ORF for the 3b coat protein (CP) is produced by translation of the RNA 3 derived subgenomic RNA 4. Each genomic RNA is encapsidated in a separate T = 3 icosahedral particle (Palukaitis and García-Arenal, 2003). Cucumoviral particles are 29 nm in diameter, and made up of 180 CP subunits and have an RNA content of about 18 % (Habili and Francki, 1974a, b). The sizes of these genomic RNAs vary slightly depending on the CMV isolate, although the overall genome organisation is identical (Balaji et al., 2008; Roossinck, 2002).

Upon entry of the host cell from an aphid vector, from a neighbouring cell via plasmodesmata, or experimentally by inoculation, virus particles are uncoated. Viral genomic RNAs are released into the cytoplasm where they are translated for production of viral proteins. RNA 1 and RNA 2 are directly transcribed to produce the 1a and 2a protein, respectively, which initiate formation of the replication complex in association with host proteins.

Progeny + strand (sub)genomic, and messenger RNAs are formed via complementary and double- stranded RNA intermediates. These (+) strands have several functions: mRNA for translation, template for further transcription, and production of virions. In Cowpea protoplasts infected with CMV CP can be detected 15 hours after infection (Gonda & Symons, 1979). In the case of CMV, (−) strand accumulation reaches a plateau soon after infection, while (+) strand accumulation

continues to increase and can reach a level nearly 100-fold that of (−) strands (Seo et al., 2009). It was demonstrated that, while both proteins 1a and 2a are required for synthesis of the (−) strand, protein 2a alone can produce (+) strands from a (−) template of either the genomic or the subgenomic RNAs (Seo et al., 2009). This possibility could account not only for the presence of free protein 2a in the cytoplasm but also for the higher proportion of (+) strands in infected cells.

Table 1.0. Role of CMV proteins during infection.

Protein	Encoded by	Function(s)	Localisation	Reported interactions	Reference
1a	RNA1	Involved in CMV replication Interaction with host proteins Systemic movement of CMV	Vacuolar membrane Processing bodies	2a protein 2b protein Tcoi1 BRP1 TIP1 /TIP2 NtTLP1	O'Reilly et al., 1998 Watt et al., in preparation Kim et al., 2006b, 2008 Chaturvedi et al., 2016 Kim et al., 2006a Kim et al., 2005
2a	RNA2	RNA polymerase Induction of antixenosis	Vacuolar membrane Cytoplasmic	1a protein CIPK12 MP	O'Reilly et al., 1998 Kang et al., 2012 Hwang et al., 2005
2b	RNA2	Viral suppresor of RNA silencing Binding sRNA AGO binding activity	Nucleous Nucleolous Cytoplasm	1a protein AGO1 (Subgroup I stains) AGO4 CAT3	Watt et al., in preparation Zhang et al., 2006 Gonzalez et al., 2012 Inaba et al., 2011
CP	RNA3	Formation of virus particles Cell-to-cell and systemic movement Plant-to-plant transmission by aphids	Cytoplasmic Bundle sheath cells	Chloroplast ferredoxin I	Qiu et al., 2018
MP	RNA3	Cell-to-cell and systemic movement	Plasmodesmata Partial sieve elements	2a	Hwang et al., 2005

1.2.2 Classification of CMV subgroups

Initially, CMV strains were classified into two Subgroups, Subgroup I and Subgroup II, according to serological data, peptide mapping of the CP and nucleic acid hybridisation (Kaplan et al., 1997; Owen and Palukaitis, 1988; Roossinck, 2002). CMV strains have since been further divided into three Subgroups IA, IB, and II based upon comparisons of the 5'-untranslated regions (Balaji et al., 2008; Owen et al., 1990; Roossinck et al., 1999). The Fny strain of CMV used in this study is classified into Subgroup IA (Rizzo and Palukaitis, 1988).

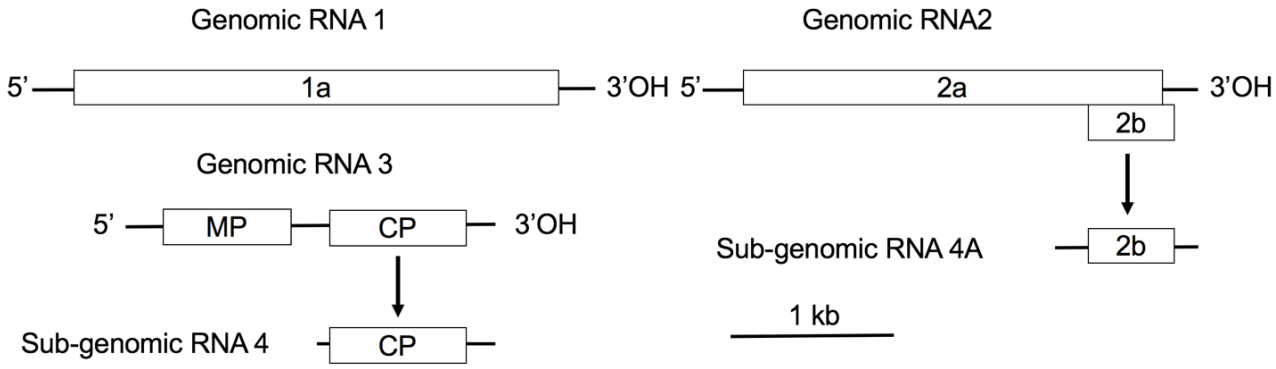

Figure 1.1. Genome organisation of CMV.

The genome consists of three RNAs designated RNA 1, 2 and 3. Five genes designated 1a, 2a, 2b, 3a and 3b encode corresponding proteins. RNA 1 encodes the 1a protein. RNA 2 encodes the 2a and 2b proteins. The 2b protein is translated from a subgenomic RNA designated RNA 4A. RNA 3 encodes the 3a protein and the 3b coat protein (CP). The CP is translated from the subgenomic RNA 4 (Figure courtesy of J. Carr).

1.2.3 CMV gene products

1.2.3.1 The 1a protein

CMV RNA 1 encodes the 1a protein, which has a mass of 111 kDa. The 1a protein has two functional domains based on sequence similarity to other viruses: a methyltransferase domain at the N-terminus and helicase domain at the C-terminal which displays RNA-binding and ATPase activity (Gal-On et al., 1994; Palukaitis and García-Arenal, 2003). Helicases are enzymes that bind and may even remodel nucleic acid or nucleic acid protein complexes. The 1a protein helicase domain is likely important in “unwinding” the double stranded RNA that develops during viral replication. The 1a protein interacts with the 2a protein through the helicase domain in the yeast-two hybrid system (O’Reilly et al., 1998). Deletion of the helicase domain or fusion of a protein to the helicase domain prevents virus replication, suggesting that this domain is important in replicase formation. This demonstrates that the C-terminal region of the helicase domain is responsible for systemic infection by controlling virus replication and cell-to-cell movement. This region contains a putative hinge, based on comparison to the orthologous BMV 1a protein, between the methyltransferase and helicase domains (O’Reilly et al., 1998). Protein methylation in an important posttranslational modification involved in regulating protein-protein interactions, and can influence a number of effects during cellular events. Mutations affecting the amino acid composition of the methyltransferase domain of the 1a protein disrupt capping activities and virus replication, whereas single amino acid substitutions at the N- and C-terminal regions around the methyltransferase domain do not appear to affect virus replication and systemic virus spread (Seo et al., 2009). The N-terminal region of the hinge located between the methyltransferase and helicase domains of the 1a protein appears to self-interact to form homodimers in a yeast two-hybrid system (O’Reilly et al., 1998). Changes in the degree of self-interaction or conformational modification of the homodimer structure of the 1a protein has been shown to be associated with the induction of necrotic cell death in Arabidopsis leaves in response to the CMV(Y) strain carrying single amino acid substitutions around the methyltransferase domain (Tian et al., 2020). The N-terminal region of the 1a protein (amino acids 1-533) can

interact with itself (O'Reilly et al., 1998). It was shown that the C-terminal region (amino acids 584-933) interacts with the 2a protein (O'Reilly et al., 1998). The 1a protein is a component of the viral replicase complex together with the 2a protein and additional host factors (Hayes and Buck, 1990). Besides its role in replication, it is also involved in the systemic movement of CMV (Canto and Palukaitis, 2001; Gal-On et al., 1994), and has a number of effects in virus-host interactions (discussed further in Section 1.6 Plant immunity triggered by CMV).

As is common for other plus-strand RNA viruses, CMV RNA replication occurs in close association with intracellular membranes (den Boon and Ahlquist, 2010; Jaspars et al., 1986; Nagy et al., 2016). Previous studies have determined the localisation of the 1a protein to associate with vacuolar membranes in tobacco (*Nicotiana tabacum*) and cucumber (*Cucumis sativus*) (Cillo et al., 2002). It is thought that the 1a protein acts as an anchor in order to recruit the 2a protein, and additional host factors, to the replicase complex (Cillo et al., 2002; Gal-On et al., 1994).

Several host factors that interact with the 1a protein have been identified. In Arabidopsis, two tonoplast intrinsic proteins (TIP1 and TIP2) were confirmed to interact with the 1a protein (Kim et al., 2006a). It was hypothesised that TIP1 and TIP2 are involved in facilitating the interaction of 1a protein with intracellular membranes. Using co-immunoprecipitation and liquid chromatography-tandem mass spectrometry (LC-MS/MS) assays it was shown that the *Nicotiana benthamiana* scaffolding protein bromodomain-containing RNAbinding protein 1 (BRP1) interacted with the 1a protein (Chaturvedi et al., 2016). When mutant Arabidopsis *brp1* plants were infected with CMV the replication efficiency was reduced, but not completely abolished. In the same study it was shown that a cytosolic variant of glyceraldehyde 3-phosphate dehydrogenase (GapC2) was essential for CMV replication. It was hypothesised that BRP1 assists in stabilizing the CMV replication complex while GapC2 is required for interaction of the 1a and 2a proteins. In tobacco, a methyltransferase and a kinase, named Tcoi1 and Tcoi2, respectively, were shown to bind to the methyltransferase domain of the 1a protein (Kim et al., 2006b, 2008). It was suggested that Tcoi1 facilitates virus replication and movement. Although the exact significance of the Tcoi1-CMV 1a interaction

and the methylation of sites of the 1a protein is unclear was not identified in this study (Kim et al., 2008). Taken together, CMV infection induced increased expression of the Tcoi1 gene. This suggests that Tcoi1 may be involved in modulating the replication and or spread of the virus, although it remains to be determined if it is thought its capacity to methylate the 1a protein. Modification of 1a protein activity, via post translational modifications, is likely to affect the interaction with other viral proteins such as the 2a or 1a protein, as well as other host proteins. It was shown that the 1a protein interacts with the *N. tabacum* thaumatin-like protein 1 (NtTLP1) (Kim et al., 2005). In CMV-infected tobacco the expression of *NtTLP* is increased, although the role of NtTLP in the tobacco-CMV interaction is not known. Interestingly, NtTLP interacts with the CMV MP and CP, suggesting it may play several roles in CMV replication and movement.

1.2.3.2 The 2a protein

RNA 2 encodes the 2a protein (97 kDa), which is an RNA-dependent RNA polymerase (RdRp) for genome replication and subgenomic RNA transcription (Palukaitis and García-Arenal, 2003). The RdRp activity is dependent on the GDD (gly-asp-asp) motif, which is highly conserved amoung RNA viruses. The 2a protein is a component of the CMV replicase (Mine and Okuno, 2012). A compatible interaction between the 1a and 2a proteins is essential for RNA replication *in vivo*. The N-terminal 126 amino acids of the 2a protein are required for the interaction between the 1a and the 2a proteins, *in vitro* as well as *in vivo* (Kim et al., 2002). Phosphorylation of the N-terminal domain prevents the 2a protein from associating with the 1a protein (Kim et al., 2002).

The 2a protein occurs in cytoplasmic and membrane-associated cellular fractions (Gal-On et al., 2000). It has been shown that a tobacco homologue of the CBL-interacting protein kinase 12 is involved in phosphorylation of the N-terminal domain of the 2a protein (Kang et al., 2012). It is thought that phosphorylation of the 2a protein has a regulatory role in limiting replicase formation so that the 2a protein can fulfil additional roles in the cytoplasm (Kim et al., 2002). The 2a protein also

interacts with the MP (Hwang et al., 2005), with the N-terminal 21 amino acids and the region surrounding the GDD motif of the 2a required for this interaction (Hwang et al., 2007).

1.2.3.3 The 2b protein

The 2b protein is encoded by the 3' proximal ORF of RNA 2. This overlaps the 3' portion of the 2a ORF (Fig. 1.1). The 2b protein is the smallest protein of CMV with a predicted mass of 12-13 kDa but it can migrate with an apparent mass of c. 17 kDa during sodium dodecyl sulphate-polyacrylamide gel electrophoresis (SDS-PAGE) (Mayers et al., 2000). It was first described as a pathogenicity determinant by Ding et al. (1994, 1996). The 2b protein was one of the first viral suppressors of RNA silencing (VSR) to be discovered and since then studies have implicated the 2b protein in almost all steps of the viral infection cycle including symptom induction (Lewsey et al., 2009), virus movement (Palukaitis and García-Arenal, 2003), and interference with the host's salicylic acid (SA)- and jasmonic acid (JA)-mediated defence mechanisms (Ji and Ding, 2001; Lewsey et al., 2010) (Fig 1.2).

The amino acid sequences of 2b proteins from different CMV strains have high conservation of sequence identity within Subgroups but distinct differences in amino acid sequence between Subgroups I and II (Lucy et al., 2000; Mayers et al., 2000). The intracellular localisation of the 2b protein has been well studied but there are differences in localisation between 2b proteins of Subgroup I and II stains (Du et al., 2014a; Lucy et al., 2000). Subgroup I and II CMV 2b proteins accumulate in the nucleus but for Subgroup I strains there is also an association with the nucleolus, cytoplasm and cytoskeleton (Du et al., 2014a; González et al., 2010; Mayers et al., 2000).

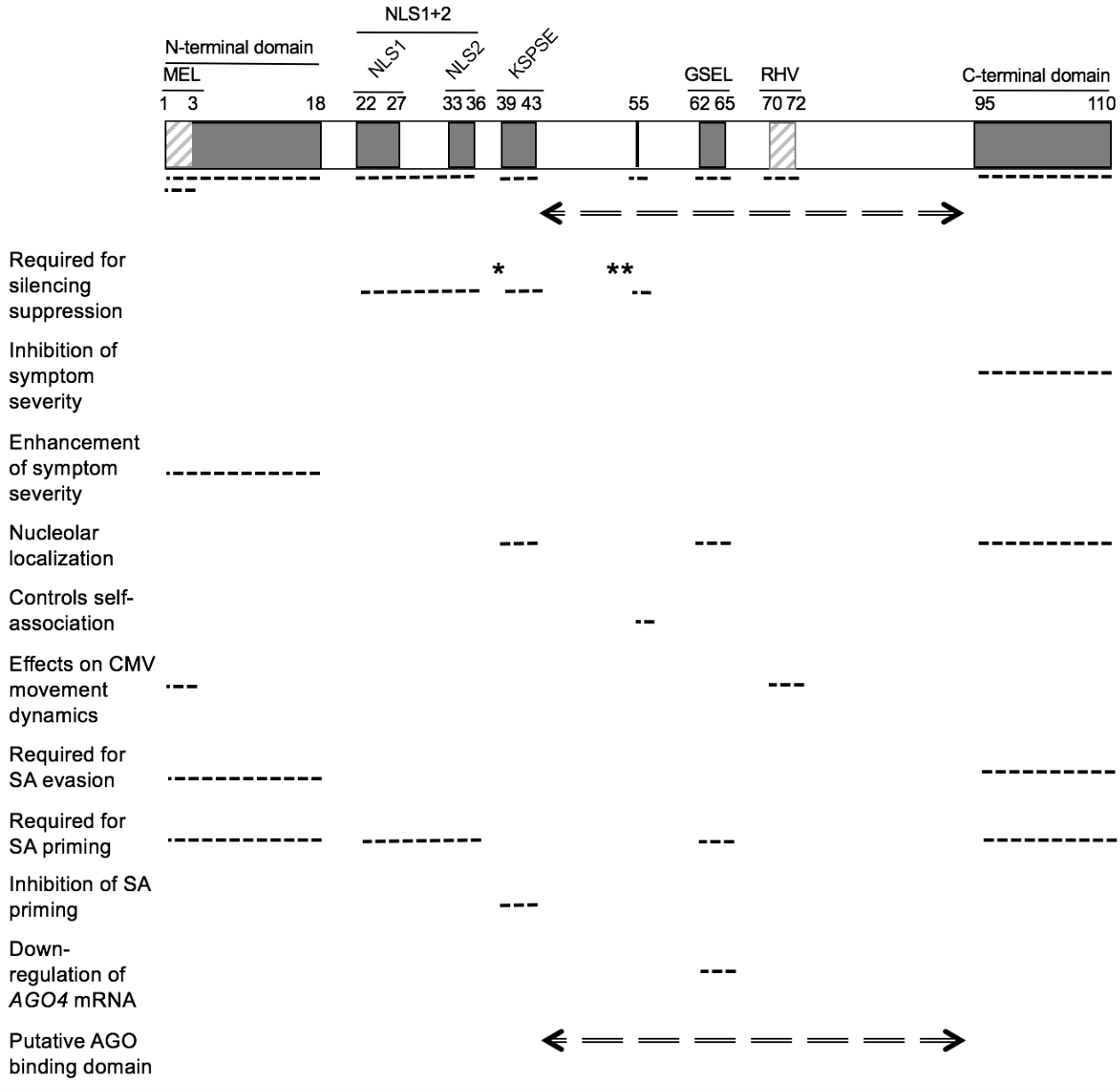
NLS1+2
N-terminal domain
MEL
NLS1
NLS2
KSPSE
GSEL
RHV
C-terminal domain
1 3
18
22 27
33 36
39 43
55
62 65
70 72
95
110
*
**
Required for silencing suppression
Inhibition of symptom severity
Enhancement of symptom severity
Nucleolar localization
Controls self-association
Effects on CMV movement dynamics
Required for SA evasion
Required for SA priming
Inhibition of SA priming
Down-regulation of AGO4 mRNA
Putative AGO binding domain

Figure 1.2. The CMV 2b protein is a multifunctional protein with roles in counterdefence and the elicitation of host defences.

The amino acid residue numbering is based on the 2b protein of the Subgroup IA Fny strain of CMV (110 amino acids). Domains and residues with known biological activities are listed at the left of the figure. Positions of nuclear localisation sequences (NLS) 1 and 2 and the N- and C-terminal domains are indicated, and the double-headed arrow indicates the region of the 2b protein though to be involved in binding to Argonaute (AGO) proteins. Single-letter codes for amino acids are used to indicate conserved functional amino acid sequence. Functional domains are indicated with shaded boxes; two of these (the N-terminal MEL sequence and the sequence RHV at residues 70-72) are indicated with light shading. These sequences are distinguished since they affect CMV movement dynamics without affecting RNA silencing suppression. *KSPSE is a putative phosphorylation domain. Deletion of the entire domain abolishes silencing suppression, indicative of the regulatory role. Residue 55 is essential for the self-interaction of 2b and indirectly affects RNA silencing suppression, since monomeric 2b proteins are inefficient suppressor the RNA silencing. Figure adapted from Carr and Murphy 2019.

1.2.3.4 The movement protein

The MP is encoded by RNA 3 and is required for cell-to-cell and systemic movement (Boccard and Baulcombe, 1993; Canto et al., 1997; Lucas, 1995). The MP localises to plasmosdesmata between infected cells (Vaquero et al., 1996), as well as to larger aggregates inside sieve elements (Blackman et al., 1997). The MP can bind single stranded RNA (ssRNA) and a putative RNA binding domain has been described (Li and Palukaitis, 1996; Vaquero et al., 1997). The MP binds to viral RNA, forming a ribonucleoprotein complex. The MP complex is able to interact with host plasmodesmal proteins, increasing plasmodesmal size exclusion limits, allowing the ribonucleoprotein complex through into the neighbouring cell where viral RNA is unloaded (Vaquero et al., 1994).

A role for the MP in subverting plant immunity was recently described by Kong et al. (2018). Tobacco plants transiently expressing MP were compromised in reactive oxygen species (ROS) production when various defence elicitor compounds were applied. In the same paper transgenic Arabidopsis plants expressing the MP displayed multiple defects in their PAMP-triggered immunity (PTI) response (Kong et al., 2018).

1.2.3.5 The coat protein

The CP is required for the formation of virus particles, but is also required for cell-to-cell movement, systemic movement and plant-to-plant transmission by aphids (Boccard and Baulcombe, 1993; Canto et al., 1997; Chen and Francki, 1990). For many viruses, including cucumoviruses, the CP is the sole determinant of virion binding to insect mouthparts (Perry et al., 1994; Perry et al., 1998; Liu et al., 2002). Specific amino acid sequences in the CP have been identified as influencing the efficiency of transmission by *M. persicae* and *Aphis gossypii* (Perry et al., 1994; Perry et al., 1998).

1.3 CMV transmission by aphid vectors

The success of insect-borne pathogen dispersal relies on the frequency of contact between their primary hosts and insect vectors. Important factors determining the frequency of contact between host and vector is the survival and reproductive success of both. Since infection of new hosts is imperative for the continuation of pathogen populations, natural selection may be expected to favour pathogen genes that promote insect vector - and potentially host - survival and reproduction, that promote attraction of insect vectors to infected hosts, or that modify host suitability to facilitate pathogen uptake by insects.

Aphids are the most prevalent insect vectors of plant viruses, and are responsible for transmission of c. 50% of these viruses (Brault et al., 2010). Aphids are particularly adapted to transmit viruses due to their unique probing behaviour. (Ng and Perry, 2004). In addition, a high reproductive rate, ability to reproduce asexually and broad host range makes aphids efficient at vectoring plant viruses (Ng and Perry, 2004).

Aphids vector viruses through two main modes of transmission, depending on whether the viron is ingested (circulative transmission) or not internalised (non-circulative transmission) by the aphid. In the circulative mode, the virus is taken up through the gut wall and is transported to the salivary glands via the haemolymph (Ng and Perry, 2004). The virus is then exported from the salivary glands during feeding, where it can infect a new host. The non-circulative pathway is a more transient association, in which viral particles are confined to the aphid's stylet (Drucker and Then, 2015).

Aphids of over 80 species vector CMV in the non-persistent manner, i.e. virions bind receptors within the aphid stylet and are acquired and lost rapidly during short probes of plant epidermal cells and the virus is not internalised (Hull, 2009; Krenz et al., 2015). During the non-persistent mode of aphid-mediated virus transmission, viral particles bind to receptors in the stylets of the insects (Mulot et a., 2018; Deshoux et al., 2018). Upon feeding on an infected plant the attachment of viral particles to these receptors occurs rapidly, i.e. within seconds. Thus, virus

acquisition does not require prolonged feeding from vascular tissues; virus particles are acquired most efficiently as the aphid probes the plant for palatability by briefly feeding from the epidermal cells (Powell, 2005). However, virus particles can be easily dislodged from the stylet during salivation, which increases in likelihood if prolonged feeding occurs on a suitable host (Martin et al., 1997). Rapid, local transmission is most efficient when aphids alight briefly on infected plants, sample the epidermal cell contents and disperse (Donnelly et al., 2019; Groen et al., 2017; Mauck et al., 2016). However, epidemiological modelling indicates that while rejection of a host following a brief sampling feed encourages rapid localised transmission by wingless aphids, if aphids settle and reproduce on plants this will eventually favour longer distance virus dissemination by winged aphids (Donnelly et al., 2019).

CMV seems to be able to manipulate host-aphid interactions to promote its own transmission. There is increasing evidence that certain genes of plant viruses exert extended phenotypes i.e., these parasite genes influence the expression of host genes in ways that ultimately benefit the virus (Dawkins, 1982). Among the host genes altered in expression by infection are those involved in the biosynthesis of insect-attracting and insect-repelling secondary metabolites and genes involved in defence against insect infestation. The resulting changes in plant biochemistry and defence alter the interactions of infected host plants with vectors and may have profound effects on epidemiological processes that benefit the virus. Although changes in plant biochemistry and defence status that favour transmission were previously assumed to be only secondary effects of virus infection, this assumption has become less plausible as more evidence accumulates of virus-host-vector co-evolution (Carr et al., 2018; Donnelly et al., 2019; Groen et al., 2017; Mauck et al., 2016; Ziebell et al., 2011; Westwood et al., 2013a,b).

The effects of CMV on plant-aphid interactions are host-specific. For example, in squash (*Cucurbita pepo*) and tobacco the Subgroup IA CMV strain Fny (Fny-CMV) induces changes in the emission of plant volatile organic compounds (VOCs) although only those produced by infected cucurbits appear to influence aphid foraging behaviour (Carmo-Sousa et al., 2014; Mauck et al., 2010; Tungadi et al., 2017). Fny-CMV induces production of distasteful substances (antixenosis) in

squash and *Arabidopsis thaliana* plants. Antixenosis promotes virus acquisition from epidermal cells, inhibits phloem feeding, and promotes aphid dispersal (Donnelly et al., 2019; Mauck et al., 2010; Westwood et al., 2013ab).

1.4 Plant innate immunity

Plants have evolved a powerful, multilayered innate immune system capable of responding to, and discriminating between, beneficial and detrimental organisms (Boller and He, 2009; Dodds and Rathjen, 2010; Zipfel, 2008). Aside from constitutive defences such as trichomes, further defence mechanisms can be induced following pathogen or insect attack (van Loon et al., 2006). The first layer of innate immunity is activated upon host recognition of highly conserved molecules expressed by pathogens, pathogen- or microbe-associated molecular patterns (PAMPs or MAMPs) (Jones and Dangl, 2006). During wounding or pathogenic attack damage-associated molecular patterns (DAMPs) released by the host can also trigger defences (Macho and Zipfel, 2014). PAMPs and DAMPs are recognised by membrane-bound pattern-recognition receptors (PRRs) which activate immune signalling resulting in PTI (Jones and Dangl, 2006). PTI is effective against the majority of plant pathogens. The best characterised bacterial and fungal PAMPs are bacterial flagellin (or its derived peptide flg22), bacterial elongation factor (EF)-Tu and fungal chitin oligosaccharides (Boller and He, 2009; Kunze, 2004). Similarly, DAMPs such as oligogalacturonides and oligopeptide signals such as systemins and AtPep1 accumulate as a result of pathogen or insect-induced enzymatic degradation of plant cell walls or proteins (Boller and Felix, 2009; Ferrari et al., 2013; Lotze et al., 2007).

Plant PRRs can be classed as receptor-like kinases (RLKs) or receptor-like proteins. RLKs have a conserved receptor configuration consisting of a peptide signal, a transmembrane segment that connects a variable extracellular domain with specific ligand binding capacity to a cytosolic kinase domain that phosphorylates threonine/serine residues and, in some cases tyrosine residues, on protein substrates (Antolin-Llovera et al., 2012; Greeff et al., 2012). RLK-mediated

signalling is often initiated by a ligand-dependent dimerisation or oligomerisation of the receptor (Antolín-Llovera et al., 2014). PTI is primarily triggered by nucleotide binding site leucine-rich repeat (NLR) PRRs which require association with the BRI1-ASSOCIATED RECEPTOR KINASE (BAK1) (Chinchilla et al., 2009; Heese et al., 2007). BAK1 belongs to the RLK family and is comprised of an N-terminal extracellular leucine-rich repeat domain (which is related to mammalian Toll-like receptor (TLR) immune sensors) a transmembrane segment, and an intracellular kinase domain (Chinchilla et al., 2009). In Arabidopsis, flg22 binds to FLAGELLIN SENSITIVE 2 (FLS2) which rapidly heterodimerises with BAK1 (Heese et al., 2007; Sun et al., 2013). BAK1 is necessary for effective downstream immune signalling, such as mitogen-activated protein kinases (MAPK) activation, ROS bursts, callose depositions, induction of defence genes and induced resistance (Boller and Felix, 2009; Heese et al., 2007). BAK1 functions as a positive regulator of innate immune responses triggered by the Arabidopsis PRRs PEPR1 and PEPR2 that recognise the Arabidopsis-derived DAMP AtPep1 (Krol et al., 2010). Therefore, BAK1 is a central component of plant immunity, through co-activation of numerous PRRs it is essential for complete immunity against a number of bacterial, fungal and oomycete pathogens.

1.4.1 Plant antiviral immunity

The role of innate immunity in virus-host interactions is well characterised in animal systems (Seth et al., 2006). TLRs are the best characterised PRRs in mammals, and have important roles in antiviral defence (Takeda and Akira, 2004; Yoneyama and Fujita, 2010). Several recent studies have described a role for PTI in antiviral immunity (Gouveia et al., 2017; Jia et al., 2016; Kørner et al., 2013; Nicaise and Candresse, 2016; Niehl et al., 2016). In mammalian and insect cells, the TLRs comprise a large family of nucleic acid-sensing PRRs, which are similar to NLRs (Kawai and Akira, 2006; Yoneyama and Fujita, 2010). Various members of the TLR family recognise specific biochemical features typically present in viral, but not in host, nucleic acids, such as uncapped single-stranded RNA, double-stranded RNA

(dsRNA), or unmethylated DNA (Jensen and Thomsen, 2012; Yoneyama and Fujita, 2010).

One of the first instances of resistance to plant viruses was reported in Tobacco plants infected with *Tobacco mosaic virus* (TMV). Tobacco plants that possess the *N* gene (Whitham et al., 1994) are resistant to TMV and exhibit the hypersensitive response (HR) after inoculation with that virus. The HR is followed by an increase in SA and induction of systemic acquired resistance throughout the plant (Ross, 1961a, 1961b). However, in plants it was assumed that antiviral defence was largely dependent on RNA silencing. Recent studies have uncovered several novel PTI signalling mechanisms that can inhibit viral infection in a similar manner to non-viral pathogens (Calil and Fontes, 2016; Gouveia et al., 2017; Kørner et al., 2013). During infection, certain plant viruses induce a complex set of PTI responses, including ROS production, ion fluxes, SA accumulation, defence gene activation, such as *PR1*, and callose deposition (Allan et al., 2001; Mandadi and Scholthof, 2013). Components of the PTI signalling pathway have been shown to play a role in antiviral defence. Kørner et al. (2013) observed that PTI was triggered by positive-sense RNA viruses in a BAK1-dependent manner. The involvement of BAK1 in antiviral immunity suggests that recognition of a viral PAMP or virus-induced DAMPs occurs through direct interaction with BAK1 or an BAK1-interacting co-receptor. More recently it was demonstrated that dsRNA associated with viral infection can act as PAMPs and can activate typical PTI responses (Niehl et al., 2016). Niehl et al. (2016) demonstrated that *in vitro*-generated dsRNAs, dsRNAs from virus-infected plants and a synthetic dsRNA induced PTI responses that were dependent on the co-receptor SERK1, but independent of dicer-like proteins (DCL: see Section 1.5) in Arabidopsis.

The nuclear shuttle protein (NSP)-interacting kinase 1 (NIK1) has been implicated in antiviral immunity (Zorzatto et al., 2015). NIK1 was originally identified as a virulence target of the NSP of bipartite geminiviruses (begomoviruses) (Fontes et al., 2004). NIK1 is a transmembrane RLK, which is thought to dimerise or multimerise with itself and/or co-receptors to promote transphosphorylation (Santos et al., 2009). However, the mechanism underlying the antiviral function of NIK1 is

different from the classical BAK1-mediated PTI. Activation of NIK1 signalling leads to the translocation of the ribosomal protein L10 to the nucleus, where it binds to L10-interacting myb domain-containing protein to repress the expression of translational machinery-related genes and global host translation (Carvalho et al., 2008). During infection, the NIK1-mediated translational regulatory mechanism results in reduced translation efficiency of begomovirus mRNAs (Zorzatto et al., 2015).

Plasma membrane-localised PRRs, such as BAK1, NIK1 and SERK1, have been shown to be involved in antiviral PTI (Kørner et al., 2013; Niehl et al., 2016; Zorzatto et al., 2015). Yet it remains to be determined how viral pathogens, which replicate intracellularly, are perceived by extracellular receptors. However, the process of viral infection may release endogenous DAMPs which may be perceived by plasma membrane PRRs. Similarly, there is a lack of information regarding whether or not viral proteins have the ability to interact with the intracellular domains of plant PRRs.

The PRR co-receptors BAK1 and BAK1-LIKE1 (BKK1) have been implicated in antiviral defence in Arabidopsis, as loss-of-function mutations in BAK1 and BKK1 result in enhanced susceptibility to turnip crinkle virus (TCV) infection (Yang et al., 2010). It was shown that Arabidopsis *bak1* mutants have increased susceptibility to three RNA viruses, while crude extracts of virus-infected leaf tissue also induced a typical PTI responses in a BAK1-dependent manner (Kørner et al., 2013). When inoculated with plum pox virus the double mutant *bak1-5 bkk1* supported increased viral titres (Nicaise and Candresse, 2016). The *bak1-4* mutant has pleiotropic effects on cell death control, whereas the *bak1-5* mutant contains a point mutation which abolishes its role in defence but minimises the cell death pleiotropy (Schwessinger et al., 2011).

A major question raised is how CMV and other RNA viruses activate PTI-signalling. Currently research suggests that viral factors can act as PAMPs but this does not eliminate the possibility that DAMPs produced in response to virus infection are responsible for inducing antiviral defence in plants. Several mechanisms have been suggested, although direct binding of viral proteins to PPRs or other cell-surface

receptors has not yet been demonstrated. It was proposed by Kørner et al. (2013) that viral infection may trigger production of endogenous DAMPs, such as AtPeps which are encoded by the *PROPEP* genes, and that AtPeps trigger PTI by binding to PEPR1 and PEPR2 in a BAK1-dependent manner. Although it was observed that there was no difference in susceptibility of *pepr1 pepr2* double mutants to TCV infection (Kørner et al., 2013). It was concluded that AtPep signalling is not sufficient to suppress or attenuate TCV infection. It is unknown if DAMPs activate PTI during CMV infection. *PROPEP3* was up-regulated in response to CMV infection, although expression of *PEPR1* and *PEPR2* was not induced (Ziebell et al., 2011).

More recently, dsRNA and virus-derived dsRNA were shown to act as viral PAMPs in Arabidopsis and induce PTI (Niehl et al., 2016). Application of dsRNA or the synthetic dsRNA analogue polyinosinic–polycytidylic acid to Arabidopsis leaf disks induced typical PTI responses, including MAPK activation and defence gene expression. Pre-treatment with dsRNA conferred protection against oilseed rape mosaic virus (ORMV) which showed significantly reduced viral accumulation in treated leaves (Niehl et al., 2016). PTI triggered by dsRNA is dependent on the co-receptor kinase SERK1, and functions independently of the RNA silencing pathway (Niehl et al., 2016).

A viral component was shown to act as a suppressor of PTI signalling (Nicaise and Candresse, 2016). The capsid protein from PPV appears to act as a virulence factor during infection, and supressed early immune responses such as the ROS burst and expression of PTI marker genes (Nicaise and Candresse, 2016). A role for the CMV MP in plant immunity was recently described (Zhu et al., 2018). Tobacco plants transiently expressing the CMV MP were compromised in ROS production when various defence elicitor compounds were applied. Whereas transgenic Arabidopsis plants expressing the MP displayed multiple defects in their PTI response. A direct interaction between the CMV MP and host proteins was not confirmed, but it was demonstrated that the MP can serve as effector proteins to suppress host immune signalling (Zhu et al., 2018). The 2a protein of Subgroup I strain Fny-CMV, but not the Subgroup II strain LS-CMV, also activates defence signalling (Westwood et al., 2013a) (discussed in Section 1.6 Plant immunity triggered by CMV).

1.5 RNA silencing

RNA silencing [also known as posttranscriptional gene silencing (PTGS)] is a mechanism of gene regulation and antiviral defence (Hannon, 2002; Baulcombe, 2004; Ding, 2010; Drinnenberg et al., 2011). RNA silencing forms an additional layer of plant immunity that is distinct from PTI or ETI (Baulcombe, 2004; Agius et al., 2012). RNA silencing comprises a set of related RNA degradation and translation inhibiting pathways that are directed by small (s) RNAs, 20-25 nucleotides in size, which are complementary to target sequences. RNA silencing is present in a broad range of eukaryotic organisms, but was first discovered in plants and thought to have evolved as an adaptive defence response against viral pathogens (Baulcombe, 2004; Shabalina and Koonin, 2008; Drinnenberg et al., 2011). In plants, RNA silencing can target viral gene expression in several ways; by sequence-specific transcript degradation, inhibiting translation of mRNAs, or by promoting targeted methylation of viral DNA which results in transcriptional gene silencing (Ding, 2010; Li and Ding, 2006).

DCL proteins recognise and cleave double-stranded endogenous or foreign RNA (dsRNA) into short 21-25 nucleotide small-interfering RNAs (siRNA) or microRNA (miRNA) duplexes (Sabin et al., 2013). In Arabidopsis, four DCL enzymes (DCLs 1-4) have been identified, which generate short dsRNAs of 20-25, 22, 24 and 21 nucleotides, respectively (Blevins et al., 2006; Fukudome and Fukuhara, 2017). In response to positive strand RNA viruses including CMV, the DCLs act in a hierarchical manner with the 21 nt siRNA-producing DCL4 being the main dicer involved, with DLC2 also involved (Bouche et al., 2006; Diaz-Pendon et al., 2007). The processed siRNA or miRNA are subsequently loaded into a multiprotein effector complex, the RNA-induced silencing complex (RISC) (Filipowicz, 2005; Schuck et al., 2013).

Members of each clade specifically recruit siRNAs depending on the 5’ terminal nucleotide (Mi et al., 2008). Either strand of the siRNA duplex can then be

incorporated into the RISC. The RISC is then guided to target nucleic acids in a sequence-specific manner (Baumberger and Baulcombe, 2005). RICSs can cleave target mRNAs or repress their translation, direct DNA methylation, or mediate antiviral defence (Garcia-Ruiz et al., 2015; Zilberman et al., 2003). AGO is the slicer component of the RISC, which inhibits the expression of target RNAs. The AGO family has expanded during plant evolution (Singh et al., 2015), leading to the functional specialisation of plant AGOs. The role of each AGO in different sRNA pathways and biological processes can be attributed to their biochemical properties, expression patterns, and other proteins and/or sRNA which they interact with. AGO proteins are divided into three clades 1) AGOs 1, 5 and 10; 2) AGOs 2, 3 and 7; 3) AGOs 4, 6, 8 and 9 (Vaucheret, 2008). Members of the first clade (AGO1/AGO5/AGO10 in Arabidopsis) primarily bind 21-nt small RNAs and are the main executors of PTGS. AGO1 is the effector protein for miRNAs and trans acting (ta) -siRNAs (Vaucheret et al., 2004; Baumberger and Baulcombe, 2005). AGO1 is guided by miRNAs and ta-siRNAs, and regulates the expression of genes that are involved in numerous developmental and physiological processes (described further in section 1.5.2 MicroRNA antiviral signalling). The expression of Arabidopsis AGO5 is confined to the somatic cells around megaspore mother cells as well as in the megaspores. AGO5 can also bind virus-derived siRNAs of CMV (Takeda et al., 2008), suggesting a role in antiviral defence. However, AGO5 appears to play a minor role in antiviral resistance to TuMV, that was predominantly effective in leaf tissue (Garcia-Ruiz et al., 2015).

The 24-nt siRNAs that derive mostly from transposons and repetitive sequences are incorporated into AGOs that belong to clade 3 (AGO4/AGO6/AGO9 in Arabidopsis). Arabidopsis AGO2 is induced by viruses and plays a major role in antiviral defence and has been shown to act cooperatively with AGO1 or AGO5 to provide broad spectrum of plant viruses (Harvey et al., 2011; Jaubert et al., 2011). Experiments using cytoplasmic extracts of evacuolated tobacco protoplasts revealed that AGO2 loaded with synthetic virus-derived siRNAs can target viral RNAs for cleavage, thereby inhibiting viral replication (Schuck et al., 2013). AGO2 also binds miR393b* to silence a Golgi-localized gene MEMB12 likely via translational repression, resulting in exocytosis of antimicrobial pathogenesis-related protein PR1 and increased antibacterial activity (Zhang et al., 2011). The

role of AGO2 in response to CMV infection is discussed further in Section 6.). The Arabidopsis AGO2 and AGO3 genes are very similar to each other and are likely the result of an evolutionarily recent duplication event. AGO3 binds siRNAs derived from Potato spindle tuber viroid (Minoia et al., 2014), and AGO3 programmed with exogenous siRNAs can cleave viral RNAs in vitro (Schuck et al., 2013).

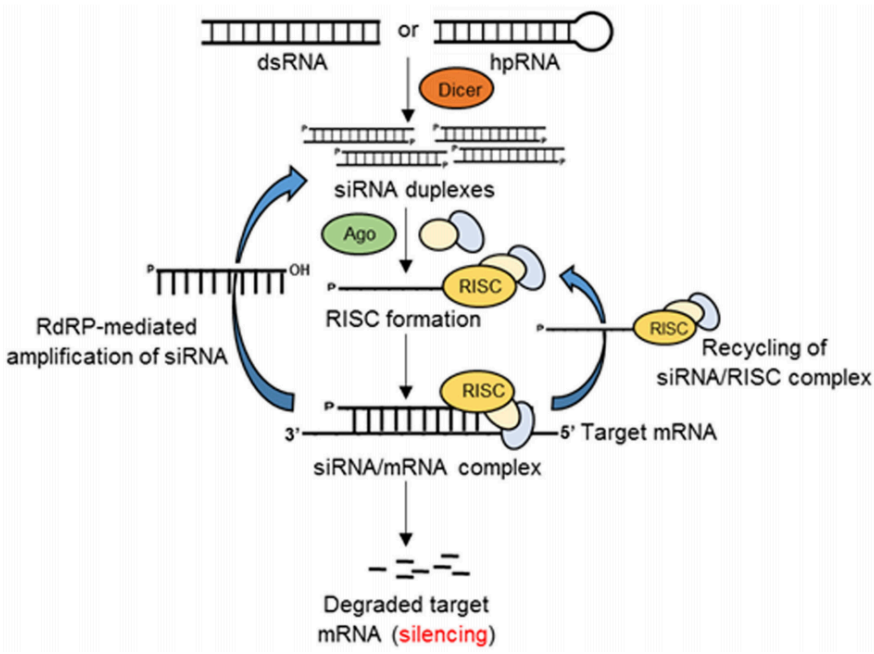

Figure 1.3. RNA-based immunity in plants.

Double-stranded RNAs (dsRNA) or hairpin RNAs generate siRNA duplexes by the action of Dicer (DCL, dicer-like). The guide RNA strand binds with Argonaute (AGO) proteins to form an RNA-induced silencing complex (RISC). The siRNA/RISC complex then binds the complementary sequence of the target mRNA resulting in the degradation of the target transcript or inhibition of translation. The components of siRNA/mRNA complex can be recycled to the RISC complex or generate siRNA duplexes by the action of RNA-dependent RNA-polymerase (RdRP) (Figure adapted from Majumdar et al., 2017).

1.5.1 Viral suppressors of RNA silencing

Most plant viruses encode at least one VSR. The CMV 2b protein was one of the first VSRs described and prevents initiation of silencing (Beclin et al., 1998; Csorba et al., 2015). CMV mutants that lack the 2b protein (CMVΔ2b), are unable to replicate efficiently and accumulate to a much lower titre than wild-type CMV. Accumulation of these mutant viruses can be rescued by disrupting the plant's antiviral silencing machinery. CMVΔ2b mutants accumulate to titres comparable to WT CMV in *dcl2 dcl4* and *rdr1 rdr6* double mutants of Arabidopsis (Wang et al., 2010; Westwood et al., 2013a).

It was initially thought that cucumoviral 2b VSRs inhibit antiviral RNA silencing by binding to AGO1 (Zhang et al., 2006) until subsequent work showed that 2b protein VSR activity is actually dependent upon its ability to titrate double-stranded siRNAs (Chen et al., 2008; González et al., 2010, 2012; Goto et al., 2007; Rashid et al., 2008; Xu et al., 2013). Cucumoviral 2b proteins can self-interact, forming dimers or tetramers *in vivo,* with the latter showing significant preference for binding short dsRNA (Chen et al., 2008; González et al., 2012; Goto et al., 2007; Rashid et al., 2008; Xu et al., 2013). The 2b protein also can directly interact with host proteins in order to suppress host anti-viral signalling. AGO1 is targeted by VSRs encoded by several viruses and inhibition of AGO1 activity for some viruses can provide an effective means of diminishing antiviral RNA silencing (Csorba et al., 2009). The 2b protein was also shown to interact with AGO4 from Arabidopsis (Hamera et al., 2012). The 2b protein specifically interacts with the RNA-binding module PAZ and catalytic PIWI domains, and thereby inhibits sRNA-mediated transcript cleavage of AGO4 (Hamera et al., 2012). It was also shown that the in vitro suppression of AGO1 and AGO4 slicing activities by CMV 2b requires its physical interaction with AGOs, although this interaction was dispensable for RNA silencing suppression by CMV 2b (Hamera et al., 2012).

The 2b protein has distinct activities in different cellular compartments. The cytoplasmic fraction of the 2b protein is predominantly responsible for its VSR activity and by using a mutated version of Fny 2b protein which is confined to the

nucleus and nucleolus siRNA-mediated local RNA silencing, antiviral silencing, and miRNA activity was shown to be greatly reduced (Du et al., 2014a; González et al., 2010). Although the VSR activity of the 2b protein is reduced when confined to the nucleus, nuclear localised Fny 2b was shown to suppress JA-mediated gene expression (Lewsey et al., 2010).

1.5.2 MicroRNA antiviral signalling

miRNAs are formed when endogenous transcripts fold back on themselves producing hairpin structures with imperfect base-pairing. These primary miRNAs are processed by DCL1 to form short miRNA duplexes which are then transported from the nucleus to the cytosol (Park et al., 2002b). Once in the cytosol, single-stranded miRNAs are assembled into RISCs, that predominantly contain AGO1 (Vaucheret et al., 2004) (Fig 1.4).

Several Arabidopsis miRNAs are known to regulate innate immune responses. Recognition of PAMPs induces the transcription of MIR160a, MIR167 and MIR393 (Li et al., 2010). These MIR transcripts produce miRNAs that target mRNAs encoding AUXIN RESPONSE FACTORS (ARFs) 10, 16 and 17 [miR160a (Mallory et al., 2005)] and 6 and 8 [miR167 (Rhoades et al., 2002; Jones-Rhoades and Bartel, 2004)], and the auxin receptors TIR1, AFB2 and AFB3 [miR393 (Parry et al., 2009)]. This represses auxin signalling, which results in the prioritisation of defence over developmental signalling (Soto-Suárez et al., 2017) .

The miRNA pathway is important in the regulation of plant growth and development. Mutants of AGO1 or DCL1 in Arabidopsis are embryonically lethal, and to study their function viable hypomorphic mutants are used. An example of this is the abnormal growth phenotypes caused by VSRs when expressed in Arabidopsis, which was initially thought to be due to misregulation of the auxin-responsive transcription factor (TF) ARF8 by miR167 (Wu et al., 2006), but this was later found to be incorrect (Mlotshwa et al., 2016). In *2b*-transgenic Arabidopsis plants the 2b protein induces stunting of shoots and roots, and developmental abnormalities, including floral deformation (Lewsey et al., 2007). These effects occur in part

through inhibition of AGO1 activity (in particular, inhibition of mRNA slicing directed by miR159) and also through effects that the 2b protein has within the host cell nucleus (Du et al., 2014a,b; Lewsey et al., 2007, 2009). VSRs can alleviate AGO1 antiviral function by interfering with its homeostatic regulatory loop. Suppression of RNA silencing by inhibiting AGO1 is an effective strategy of many plant viruses. Several plant RNA viruses induce expression of MIR168 (Varallyay et al., 2010). miR168 directs the cleavage of AGO1 mRNAs, indicating that miRNAs themselves can regulate the feedback of the miRNA pathway (Vaucheret et al., 2004). The Tombusvirus p19 VSR causes over-accumulation of miR168, which results in downregulation of AGO1 protein level (Varallyay et al., 2010). Several unrelated VSRs induce miR168 induction and the subsequent disruption of AGO1 regulation (Varallyay et al., 2013). However, inhibiting AGO1 activity may be counterproductive in some instances. In Arabidopsis, AGO2 is regulated by a miRNA (miR403) (Allen et al., 2005). Disruption of AGO1 activity during virus infection results in the de-repression of *AGO2* mRNA levels by miR403 (Harvey et al., 2011). This leads to higher levels of AGO2 and, consequently, triggers the establishment of another layer of antiviral silencing (Harvey et al., 2011).

Several NLRs that contribute to antiviral immunity are directly or indirectly regulated by miRNAs (Yi and Richards, 2007). Disruption of the miRNA pathway by VSRs can lead to an enhanced immune response. This defence feedback loop is particularly effective when it is the VSRs that are recognised by these NLR proteins. Several VSRs including the CMV 2b protein induce a HR in certain host plants (Li et al., 1999; Ren et al., 2000). Viral infection may lead to activation of enhanced defence signalling if AGO1 or other host components of the miRNA pathways are perturbed. In order to avoid disrupting the miRNA pathway, viruses subvert RNA silencing via other mechanisms, such as sequestration of siRNAs. MiRNAs are highly variable between plant species (Cuperus et al., 2011), and the disruption of the miRNA pathway by the 2b protein is likely to have different effects in separate plant species. This may explain why VSRs do not completely inhibit the miRNA pathway in all plants, as is the case with CMV strains from Subgroup II [e.g. LS- and Q-CMV (Lewsey et al., 2007; Zhang et al., 2006)]. Although the LS-CMV 2b protein does not interact with AGO1 in Arabidopsis, it was shown alter the expression levels of certain miRNAs in tomato (Cillo et al., 2009).

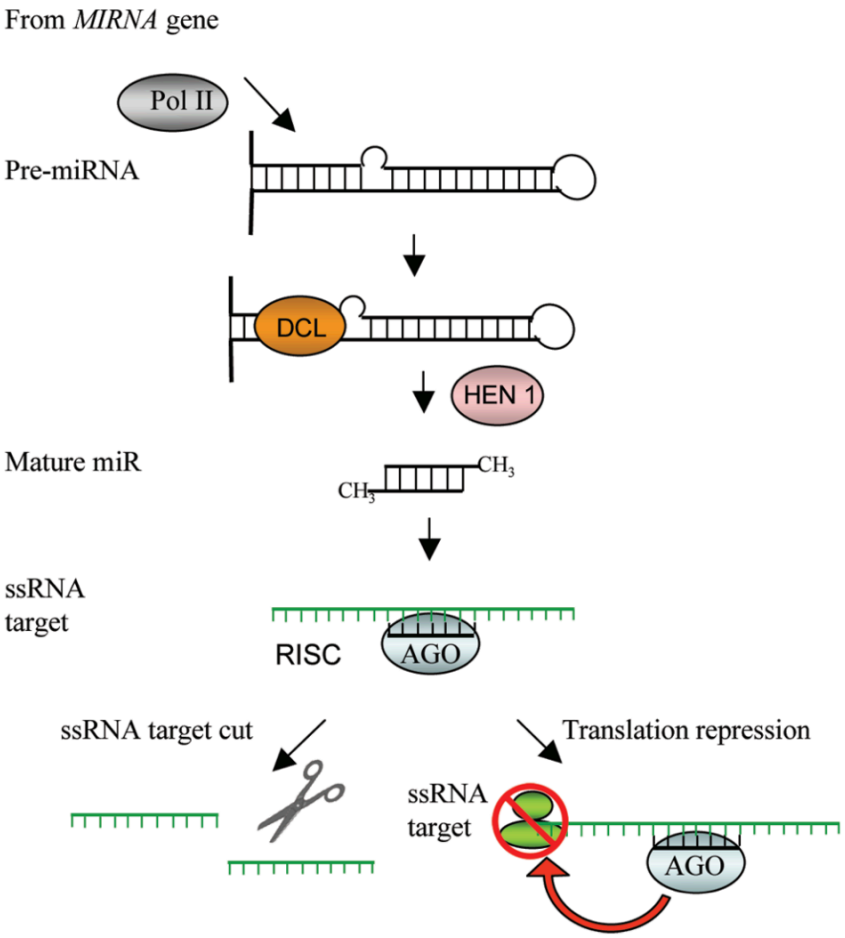

Figure 1.4. MicroRNA biosynthesis and modes of action in plants.

In Arabidopsis, the transcribed *MIR* genes form hairpin structures with imperfect base-pairing. These are cleaved by DCL1 to produce miRNAs. HEN1 directly methylates the 3' end of the DCL-produced small RNA duplexes. The mature miRNA duplex binds to AGO1, which is able to slice and inhibit translation of target mRNA. Diagram adapted from Ilardi and Nicola-Negri, 2011.

1.6 Plant immunity triggered by CMV

Virus infection results in the induction of plant defence responses and the reprogramming of host plant biochemistry (Handford and Carr, 2006). Formerly, this may have been seen as incidental to the infection process but work in our group and that of others show that altered primary and secondary host metabolism can alter the dynamics between infected plants and aphid vectors (reviewed in Brault et al., 2010). In Arabidopsis and other Brassicaceae an important class of metabolites that affects aphids are glucosinolates (Cole, 1997; Zust et al., 2012). Accumulation of aliphatic glucosinolates is regulated by development and sugar signalling (Gigolashvili et al., 2007a; Miao et al., 2013), whereas indole glucosinolate levels rise after biotic stress (Gigolashvili et al., 2007b). JA-signalling regulates both basal glucosinolate levels and induction of glucosinolate biosynthesis (Mikkelsen et al., 2003).

1.6.1 Immunity to aphid transmission

The Fny 2b protein interacts with and inhibits AGO1 (Zhang et al., 2006). AGO1 positively regulates expression of the P450 enzyme *CYP81F2*, the product of which catalyses the formation of the aphid feeding deterrent compound 4-methoxy-indol3yl-methylglucosinolate (4MI3M) from its precursor indol-3-yl-methylglucosinolate (I3M) (Fig. 1.5) (Kim and Jander, 2007; Clay et al., 2009; Pfalz et al., 2009). Accumulation of I3M relies on basal JA signalling (Mewis et al., 2006).The conversion of I3M to 4MI3M is positively regulated by SA and ethylene signalling (Kliebenstein et al., 2002; Clay et al., 2009). During PTI the production of 4MI3M from I3M is dependent on EDS1, the TF MYB51 (Dombrecht et al., 2007; Frerigmann et al., 2016; Schlaeppi et al., 2010; Xu et al., 2016).

The induction of feeding deterrence against *M. persicae* in Arabidopsis by infection with Fny-CMV appears to be an emergent property of the direct or indirect interactions of three viral gene products with the host and each other. It was observed using *2b*-transgenic Arabidopsis plants that the 2b protein induces strong resistance to aphids (Westwood et al., 2013a). This form of resistance is termed

(antibiosis) and is based on the accumulation of toxic compounds which aphids cannot recover from feeding on. Antibiosis is deleterious to aphid-mediated transmission as aphids will continue to ingest toxic compounds and not disperse to uninfected host plants (Westwood et al., 2013a). In Arabidopsis, AGO1 negatively regulates antibiosis against aphids (Kettles et al., 2013; Westwood et al., 2013a) and the inhibition of AGO1 by the Fny 2b protein allows this form of insect resistance to become active (Watt et al., unpublished data; Westwood et al., 2013a). In tobacco plants infected with the mutant CMVΔ2b, aphids reproduced poorly and exhibited increased mortality (Ziebell et al., 2011). It appears that in tobacco, the 1a protein has the ability to trigger antibiosis against aphids. But during infection with wild-type CMV induction of antibiosis is counteracted by the 2b protein (Tungadi et al 2019; Ziebell et al., 2011).

1.6.2 Immunity to virus replication

Fny-CMV infection induces antixenosis in Arabidopsis plants. This form of resistance is based on increased 4MI3M biosynthesis and aphid feeding deterrence. Using transgenic plants and pseudorecombinant virus the induction antixenosis was mapped to the 2a protein from Fny-CMV (Westwood et al., 2013a). As the production of 4MI3M is advantageous to CMV (promoting transmission by aphids) the 2a protein although acting as a PAMP has properties of an effector; a pathogen molecule that defeats or manipulates defence in order to benefit pathogen, or in this case, viral fitness.

As the immune response triggered by the 2a protein does not inhibit CMV replication it suggests that CMV is able to tolerate or evade the host immune response (Westwood et al., 2013a). Viruses are able to form viral replication factories in order to prevent viral RNAs from detection and subsequent degradation by the hosts RNA silencing machinery (den Boon and Ahlquist, 2010). Viral factories cause the modification of intracellular membranes into spherules and have been well studied in RNA plant virus brome mosaic virus (BMV) (taxonomically placed with CMV in the Bromoviridae). For CMV and BMV, replicase formation involves accumulation of the 1a replicase protein to membranes and recruitment of the 2a replicase protein

and viral RNA. The location of these viral factories differs between the two viruses: BMV replicates at the endoplasmic reticulum (ER), whereas CMV replicates at the tonoplast (Palukaitis and Garcia-Arenal, 2019). The formation of too many viral factories may be detrimental to CMV as disruption of the tonoplast intrinsic protein 1 (TIP1), which is targeted by the 1a replicase, induces cellular toxicity (Ma et al., 2004).

Viral proteins are increasingly recognised as more than replication components, but additionally as agents to subvert host immune responses, evidently to influence their interaction with vectors (Ingwell et al., 2012; Mauck et al., 2012; Nicaise and Candresse, 2016). During infection there is interplay between three CMV proteins (1a, 2a and 2b protein) which determines whether feeding deterrence or antibiosis is triggered in Arabidopsis (Fig. 1.5) (Westwood et al., 2013a). In Arabidopsis, it is the 2b protein that must be prevented from inducing antibiosis through its interaction with AGO1. A direct interaction between the 1a protein and the 2b protein was shown to limit the inhibition of AGO1 by the 2b protein, thus preventing induction of antibiosis while also preventing inhibition of 4MI3M biosynthesis (Chapters 4 and 5; Westwood et al., 2013a). This results in 2a-induced feeding deterrence as the dominant anti-aphid resistance mechanism induced by CMV infection in Arabidopsis (Westwood et al., 2013a). There are numerous scenarios whereby the CMV 2a protein could be activating PTI, either by the production of DAMPs as a consequence of infection or, conversely, or through interaction with host factors.

The Fny-CMV 1a protein's previously documented effect on host-aphid interactions, in Arabidopsis, contrasts markedly with its effect in tobacco, as does the effect of the 2b protein. In Arabidopsis, it is the Fny-CMV 2b protein that induces antibiosis against aphids while the 1a protein is the factor that limits 2b-induced antibiosis induction (Watt et al., unpublished results; Westwood et al., 2013a). In both plant hosts, the 1a and 2b proteins have antagonistic roles in conditioning CMV-induced effects on aphid-plant interactions suggesting the interplay of the 1a and 2b proteins determines the outcome (induction of aphid resistance or aphid susceptibility) of CMV infection on plant-aphid interactions in different hosts. This reinforces previous work showing that the effects of viral proteins on plant-aphid interactions are complex and combinatorial (Tungadi et al., 2020; Westwood et al., 2013a, 2014).

In Arabidopsis, anti-aphid resistance has also been shown to be partly regulated by PAD4, SA, ethylene, as well as miRNA-mediated signalling (Kettles et al., 2013; Mewis et al., 2006; Moran and Thompson, 2001; Smith and Boyko, 2006). BAK1 has also been shown to be necessary for activating PTI in response to aphids (Prince et al., 2014). Furthermore, it was observed that extracts of *M. persicae* trigger plant defence responses in Arabidopsis that resemble PTI. One of the defence genes induced encodes PHYTOALEXIN DEFICIENT 3 (PAD3), a cytochrome P450 that converts dihydrocamalexic acid to camalexin, a major phytoalexin that is toxic to *M. persicae* (Prince et al., 2014). The involvement of BAK1 may be significant in the CMV-Arabidopsis-*M. persicae* pathosystem as BAK1 has been shown to be important in antiviral resistance to several RNA viruses (Kørner et al., 2013; Yang et al., 2010).

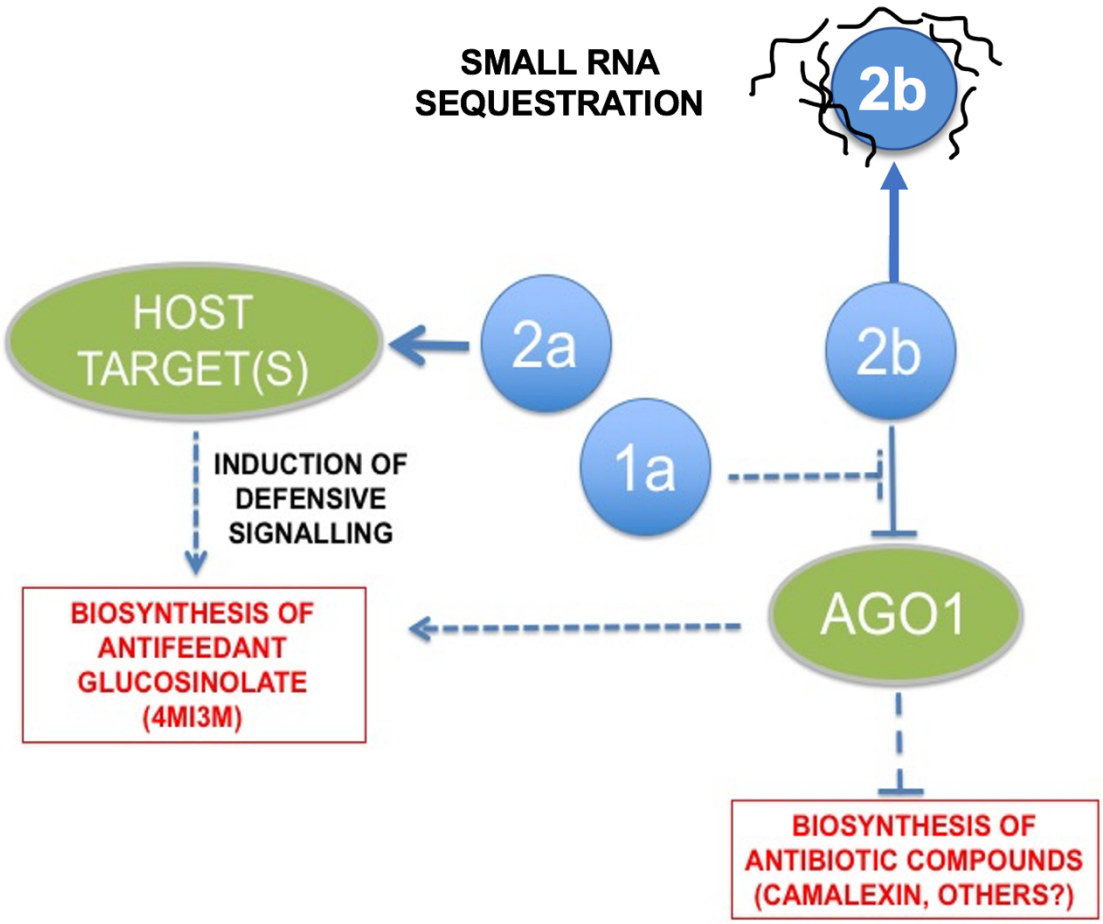

Figure 1.5. Model depicting the interaction between the CMV proteins and host components central to defence signalling.

The 2b RNA silencing suppressor protein of CMV inhibits antiviral silencing through binding of virus-derived siRNAs, allowing viral gene products, including the 1a and 2a replicase proteins to accumulate. The 2b protein can also bind to and inhibit AGO1, which positively regulates biosynthesis of the aphid feeding deterrent compound 4-methoxy-indol3yl-methylglucosinolate (4MI3M). AGO1 also negatively regulates induction of a toxicity-based resistance to aphids (antibiosis). The 1a replicase protein is able to moderate inhibition of AGO1 by the 2b protein, preventing induction of antibiosis and preventing inhibition of 4MI3M biosynthesis. The 2a protein stimulates PTI- and ETI-related signalling, which results in increased accumulation of 4MI3M. Model adapted from Westwood et al. (2013a).

1.7 Aims and objectives

The main objective of my research was to investigate the interactions between plants, viruses and insect vectors, with a particular focus on how the interaction of viral proteins with host factors, and each other, can trigger different forms of aphid resistance. This work continues the research of Westwood et al. (2013), who demonstrated that during CMV infection induces defence signalling and accumulation of the aphid-repellent metabolite 4MI3M in Arabidopsis. Below a more detailed overview of the aims for each chapter will be given.

Determine the role of the 2a protein in anti-aphid resistance in Arabidopsis.

Westwood et al. (2013) demonstrated that the CMV 2a protein induces anti-aphid resistance. More recent work from our group, suggested that CMV-induced anti-aphid resistance may be dependent on BAK1 (Groen et al., unpublished results).

My first objective was to further investigate the role of the 2a protein in CMV-induced anti-aphid resistance. And secondly to determine if BAK1 is required for CMV-induced anti-aphid resistance. This work will be discussed in Chapter 3.

How does the 1a protein prevent 2b-induced antibiosis in Arabidopsis?

Co-expression of 1a and 2b proteins in transgenic plants inhibited aphid resistance and also ameliorated the 2b-induced developmental abnormalities that occur in *2b*-transgenic Arabidopsis plants (Lewsey et al. 2007; Westwood et al., 2013a). This suggested that the CMV 1a protein negatively regulates the ability of the 2b protein to inhibit AGO1 activity (Westwood et al., 2013a).

My second objective was to investigate if the 1a protein inhibits 2b-AGO1 interactions indirectly or by directly interacting with either the 2b protein or AGO1 and if these interactions affect the 2b protein's VSR activity. This work will be discussed in Chapters 4 and 5.

Chapter 2. General Materials and Methods

2.1 Chemicals and molecular biology reagents

2.1.1 Sterilisation of solutions and equipment

Chemicals used were obtained from Merck (Gillingham, Dorset, UK), Duchefa (Melford Labratories, Chelsworth, Ipswich, UK), Thermo Fisher Scientific (Paisley, UK) unless otherwise indicated. All bottles, metals and plastic equipment were sterilised by autoclaving for 15 minutes at 121°C and 15 pounds per square inch pressure. Other glassware and ceramics were soaked in 10 % (w/v) sodium hypochlorite for at least one hour, then rinsed with distilled water before being baked at 180°C for two hours. Solutions and media were prepared using deionised water and sterilised by autoclaving, apart from antibiotics and plant hormone solutions which were filter sterilised before being added to autoclaved media.

2.2 Plant materials

2.2.1 Brassicaceae

Chinese cabbage (*Brassica rapa* L. subspecies *pekinensis* cv. Green Rocket) seeds were sown onto Levington M3 compost (Fisons Plc, Ipswich, UK). After 7 days, germinated seedlings were transplanted into individual pots. Cabbage plants were grown under a 16 hour photoperiod (using Sylvania Activa 172 Professional 36W bulbs) at 22°C ± 1°C, 60 % relative humidity and a light intensity of 200 $\mu E.m^{-2}.s^{-1}$. Plants were housed in a custom-built walk-in growth chamber with an automated watering system on a 36 hour watering regime (Conviron, Manitoba, Canada) at the Department of Plant Sciences Plant Growth Facility, Botanic Garden, University of Cambridge (Cambridge, UK).

Arabidopsis thaliana (L.) Heynh. (Arabidopsis) accession Col-0 plants were grown under the same conditions and in the same location as described above for the Chinese cabbage plants, except that photoperiod was 8 hours rather than 16 hours. Arabidopsis seeds were sown in small circular pots on F2 compost and subsequently cold-stratified for 3 days at 4°C. Seeds for Arabidopsis mutants with transgenes linked to antibiotic resistance genes or with T-DNA inserts containing these genes were sowed on 1.5 % (w/v) agar plates containing the appropriate antibiotic and concentration (50 µg/ml kanamycin; 30 µg/ml hygromycin). Seeds for other Arabidopsis lines were germinated without antibiotics. After seven days, seedlings were transferred to P24 tray inserts with cell dimensions of 50 x 48 mm (Desch Plantpak, Mundon Maldon, UK) containing a 4 : 1 M3 compost : sand (washed, lime free, horticultural quartzite sharp sand: J. Arthur Bowers, Lincoln, UK) mixture. Trays were placed under plastic propagation lids to facilitate seedling growth. After two more weeks of growth in trays, plants used for experiments involving virus infections were inoculated (Section 2.3.4) and grown for another two weeks to develop systemic infection. Plants not requiring inoculation were allowed to grow in trays for two more weeks. Both the inoculated and non-treated Arabidopsis plants were 5-6 weeks old and still in the pre-bolting vegetative stage when used in experiments.

2.2.2 Arabidopsis accessions and mutants

Experiments on Arabidopsis were done using the accession Columbia-0 (Col-0). All Arabidopsis mutants used were in the Col-0 genetic background unless indicated, and seeds for these mutants were from pools previously authenticated for the presence of mutant alleles. Transgenic Arabidopsis plants expressing CMV 2b sequences were previously generated by Dr. Mathew G. Lewsey (Lewsey et al., 2007). The Arabidopsis lines containing Fny2b and LS2b transgenes, LS2b 5.7D and 4.3B; Fny2b 2.30F, and 3.13F have been described (Lewsey et al., 2007; Lewsey et al., 2010).

Transgenic Arabidopsis plants expressing the genes encoding the Fny 1a protein and 2a protein, were obtained from Dr. Alex M. Murphy (University of Cambridge,

Cambridge, UK). Like the previously described *2b*-transgenic Arabidopsis lines these *1a* and *2a* transgenic lines were created by transformation of Arabidopsis with *Agrobacterium tumefaciens* [GV3101 (Koncz and Schell, 1986)] containing the appropriate recombinant Ti plasmids through floral dipping (Clough and Bent, 1998). The plasmids contain the ORFs of the genes encoding the Fny 1a protein derived from the vector pT149 (which was provided by Dr. Tomas Canto, Biological Research Centre, Madrid, Spain), and the ORF of the gene encoding the 2a protein from the vector pFny209 (Rizzo and Palukaitis, 1990). The 1a and 2a ORFs were subcloned into the plant expression vector pMDC32 (GenBank reference FJ172534) (Curtis and Grossniklaus, 2003) via the gateway entry vector pDONR207 (Thermo Fisher Scientific, Paisley, UK), the cloning procedure is described in detail in Section 2.5.6. This placed them under the control of the Cauliflower mosaic virus (CaMV) 35S promoter and allows *in planta* selection for resistance to hygromycin for transformants containing the pMDC32-derived constructs. The *2b*-transgenic plants described at the beginning of this Section were selected for resistance to kanamycin. Fny2b/Fny1a double transgenic lines were created by supertransformation of the Fny*2b*-transgenic line 2.30F through floral dipping in the same manner the *1a*-transgenic lines had been created. However, in this instance a derivative of the vector pDJSn had been used (Gilliland et al., 2003), which also places the 1a ORF under the control of the CaMV 35S promoter, but allows *in planta* selection of Fny2b / Fny1a double transformants by the use of hygromycin. The *bak1-5* and *bkk1-1* single and double mutants used in this study were provided by the Nottingham Arabidopsis Stock Centre (NASC) and have been previously characterized (He et al., 2007; Schwessinger et al., 2011).

2.2.3 Solanaceae

Nicotiana benthamiana Domin seeds were sown onto Levington M3 compost. After 10 days, germinated seedlings were transplanted into individual pots containing a soil mixture made up of Levington M3 compost and sand, at a ratio of 4 : 1. Plants were kept in a controlled growth room at 22°C at 60 % humidity with a 16 hour photoperiod. Plants were grown under the same conditions and in the same location as described above for the Chinese cabbage plants. *N. benthamiana* plants were used to bulk up virus stocks when they were at the 3-4 leaf stage of development

(approximately 3 weeks old), and for agroinfiltration when they were at the 4-5 leaf stage (approximately 4 weeks old).

2.3 Cucumber mosaic virus

2.3.1 Strains

CMV strain Fast New York (Fny-CMV) was first isolated from *Cucumis melo* in New York State, USA (Roossinck and Palukaitis, 1990) and strain *Lactuca sativa* (LS-CMV) was first isolated from *Lactuca sativa,* also in New York State (Provvidenti et al., 1980; Zaitlin et al., 1994). The Fny strain of cucumber mosaic virus (Fny-CMV) (Roossinck and Palukaitis, 1990) was used in this work for aphid experiments. Infectious clones of Fny-CMV RNA1 (pFny109), RNA2 (pFny209) and RNA3 (pFny309) were used to inoculate and propagate the virus in *N. benthamiana* via agroinoculation for later virion purification. The original infectious clones were constructed by Rizzo and Palukaitis (1990) but were modified for agroinfiltration by replacing the T7 promoter with the CaMV 35S promoter (Zhiyou Du, unpublished results). Infectious clones of LS-CMV genomic RNA1 (pLS109), RNA2 (pLS209) and RNA3 (pLS309) used in this study are described by Zhang et al. (1994).

2.3.2 Virus preparation

The CMV purification method was adapted from Roossinck and White (1998). Systemically infected leaves from five-to-six-week old *N. benthamiana* plants were weighed and blended in a pre-chilled blender (Magimix, Farnham, UK) with ice-cold Buffer A [0.5 M sodium citrate pH 6.5-7.0, 5 mM disodium ethylenediaminetetraacetic acid (EDTA), 0.5 % (v/v) thioglycolic acid] and chloroform, at a ratio of plant tissue : Buffer A : chloroform = 1g : 1 ml : 1 ml. The mixture was centrifuged at 18 500 g in a Beckman JLA-10,500 rotor for 15 minutes at 4°C. The aqueous phase was removed and filtered through two layers of Miracloth pre-soaked with distilled water. Ten grams of polyethylene glycol (PEG) was added to every 100 ml of aqueous extract to precipitate and concentrate the virus. The mixture was shaken for approximately 40 minutes at 4°C until the PEG was completely dissolved. The mixture was then centrifuged at 18 500 g in a

Beckman JLA-10,500 rotor for 10 minutes at 4°C. The pelleted virus was drained and residual PEG solution removed. The pellet was resuspended in Buffer B [5 mM sodium borate pH 9.0, 0.5 mM disodium EDTA, 2 % v/v Triton-X 100] using approximately 25% of the original volume of Buffer A used. The mixture was then stirred for 40 minutes at 4°C, before being centrifuged at 6600 g using a Beckman JLA-10,500 rotor for 10 minutes at 4°C. Ultracentrifugation of the supernatant was carried out at 100,000 g in a Beckman Ti70 rotor for 75 minutes at 4°C. The aqueous phase was underlaid with 5 ml of Buffer A and 10 % (w/v) sucrose. The pellet was dried and resuspended in 3 ml Buffer B and left shaking overnight at 4°C. The following day, the viron suspension was centrifuged at 6600 g using a Beckman JLA-10,500 rotor for 20 minutes at 4°C. The supernatant was centrifuged at 100,000 g for 1 hour and 15 minutes in a Beckman Ti70 rotor over a 5 ml cushion of Buffer C [5 mM sodium borate pH 9.0m 0.5 mM disodium EDTA]. The pellet was resuspended in 200 µl Buffer C. The concentration of the virus (mg/ml) was determined by measuring the absorption at 260 nm and dividing this value by the 1 mg/ml extinction coefficient (Lot and Kaper, 1976). Virion preparations were stored at 4°C and remained infectious for approximately 3 months.

2.3.3 Inoculation

After Arabidopsis plants were inoculated with purified CMV virions when they were 4-5 weeks old. For inoculation, purified CMV virions were diluted to 10 µg/ml using 0.1 M potassium phosphate buffer, pH 7. Carborundum powder [i.e. silicon carbide (SiC)], was dusted onto the third and fourth leaves of each plant in order to increase inoculation efficiency. A pipette was used to deliver 2 µl of virion suspension onto the surface of the third and fourth leaves. The leaves were gently rubbed with a gloved fingertip in order to inoculate the plants. This procedure was repeated for mock-inoculated plants, using sterilised water instead of virion suspension. Inoculated plants were kept in a controlled growth room at 21°C with an 8 hour photoperiod and covered with a propagator lid for 2 days to maintain humidity around the wounded plants. Virus-inoculated plants were used for aphid experiments at 2 weeks post-inoculation.

N. benthamiana plants were inoculated at the 3-4 leaf stage of development (approximately 3 weeks old). One cotyledon and the oldest true leaf were dusted with Carborundum which was used to gently abrade the leaf surface to facilitate virus entry. Ten µl of a 10 µg/ml purified viron suspension was pipetted onto the Carborundum-dusted leaves and gently rubbed with a gloved finger. Plants were left to develop systemic infection for seven days.

2.4 Aphid experiments

2.4.1 Aphid species

The green-peach or peach-potato aphid *Myzus persicae* Sulz. (referred to as "aphid" throughout the text) was used for most aphid-plant interaction experiments in this report. The *M. persicae* clone US1L is an insecticide susceptible clone that was first described by Devonshire et al. (1977). Aphid cultures were maintained on Chinese cabbage (Section 2.2.1). In addition, virus-free cultures of apterous individuals of the oligophagous Brassicaceae specialists, the mealy cabbage aphid *Brevicoryne brassicae* L. and the turnip aphid *Lipaphis erysimi* Kaltenbach were reared on Chinese cabbage for use in some experiments with Arabidopsis. Clones of these specialist aphids were provided by Rothamstead Research, Harpenden, UK. Stock plants were individually contained in micro-perforated plastic bags (Associated Packaging Ltd., Tonbridge, UK) and placed inside a bench-top fabric insect cage (Insect Cage Net, Carmarthen, Dyfed, UK) at the Department of Plant Sciences Plant Growth Facility, University of Cambridge (Cambridge, UK). To obtain aphids of standardised developmental stage for use in experiments, adults were transferred to non-infested stock plants and allowed to reproduce for no longer than 24 hours. Nymphs produced were transferred to experimental plants using fine paintbrushes and contained using micro-perforated plastic bags.

2.4.2 Aphid colony growth assay

Approximately 100 adult aphids were transferred to a fresh uninfested Chinese cabbage plant one day prior to the start of the experiment. On the day of the experiment single freshly produced nymphs were transferred to individual

Arabidopsis plants using a fine paintbrush. Nymphs were placed on the middle rosette, and each aphid-infested Arabidopsis plant was contained in a microperforated bread bag. Nymphs were left to feed on the plants for 10 days before recording the number of offspring produced. As an additional containment measure aphid-infested plants were kept inside a rectangular Nylon mesh insect cage.

2.4.2 Aphid mean relative growth rate assay

One-day-old first instar nymphs were individually weighed on a microbalance (MX5, Mettler-Toledo, Columbus, OH, USA) just before being placed on test plants. Nymphs were contained on experimental plants using micro-perforated plastic bags secured at the base of each pot with an elastic band. The final weight of each aphid was measured five days post- infestation immediately after having been allowed to feed on the test plants. This period was chosen to maximise the time the aphids could spend on the plants without starting to reach adulthood and reproduce. Aphid mean relative growth rate (MRGR) was calculated using the formula MRGR = ()/ *t*, where *t* = time in days between the initial and final measurements of each aphid's fresh weight (*W*) (Leather and Dixon, 1984; Stewart et al, 2009). At least 15 replicates per treatment group were used and experiments performed three times in total.

2.5 Nucleic acid manipulations

2.5.1 Polymerase chain reaction (PCR) conditions

For routine PCR reactions DNA sequences were amplified by PCR using the BioMix Red (Bioline/ Scientific Laboratory Supplies Limited, Hessel, UK) reagent mix. Unless otherwise stated, the reaction volumes were 20 µl, comprising 10 µl 2 x BioMix Red master mix, 8.5 µl distilled water, 0.5 µl of 10 µM mixture of primer sets, and 1 µl of DNA template typically containing 50 to 150 ng/µl of DNA. DNA targets from total nucleic extracts were amplified using the following PCR programme: 94°C, 5 min, 30 cycles of amplification (94°C 30 s, 57°C 30 s, and 72°C 1 min). 72°C, 5 min, and finally 4°C for 5 min. The annealing temperatures were adjusted

according to the basic melting temperatures from Primer3 (Untergasser et al., 2012) of the primers of interest. Likewise, the extension time was calculated to cover the length of the expected product based on the extension speed of 1000 bp/minute specified in the manufacturer's instructions. The amplification of DNA for molecular cloning was carried out using Q5 high fidelity polymerase (New England Biolabs, Hitchin, UK). Unless otherwise stated, the reaction volumes were 50 µl, containing 10 µl 5 x Q5 reaction buffer, 1 µl of 10 mM dNTPs, 10 µM mixture of primer set, 1 µl of DNA template typically 100 ng/µl of DNA, 0.5 µl of Q5 High-Fidelity DNA polymerase and the remaining volume made up with nuclease-free water. DNA targets from total nucleic extracts were amplified using the following PCR programme: 98°C, 30 seconds, 30 cycles of amplification (98°C 10 s, 50-72°C 30 s, and 72°C 30 seconds/kb), 72°C 2 min, and finally 4°C for 5 min.

2.5.2 Gel electrophoresis of DNA

For visualisation on agarose gels, 5 µl of each PCR reaction was mixed with 1 µl 6 x Gel Loading Dye (New England Biolabs, Hitchin, UK) and loaded into wells of a 1 % (w/v) agarose gel in TAE buffer [0.04 M Tris, 0.001 M EDTA pH 8.0, 0.1142 % (v/v) glacial acetic acid] containing 0.05 µg/ml ethidium bromide. Gels were submerged in TAE buffer and run in a gel rig (Flowgen / Scientific Laboratory Supplies, Hessle, UK) at up to 100 V using a Power Pac 3000 (Bio-Rad Laboratories Ltd, Hemel Hempstead, UK). Adjacent lanes were loaded with 5 µl 1 kb ladder or 10 kb ladder (Bioline) depending on the expected size of the PCR products. Gels were examined under UV illumination to reveal bands using an InGenius3 gel analysis system (SynGene, Cambridge, UK).

2.5.3 Extraction of DNA from agarose gel

DNA sequences were extracted from agarose gels when required for molecular cloning. The gel was run as in Section 2.5.2 except that visualisation was carried out on a UV transilluminator light box. Bands of the correct size were excised from the gel using a scalpel and transferred to a 2 ml microcentrifuge tube. The Monarch DNA gel extraction kit (New England Biolabs, Hitchin, UK) was used to dissolve and purify DNA according to the manufacturer's instructions.

2.5.4 Plasmid DNA purification

Escherichia coli (E. coli) DH5α was cultured overnight in Luria-Bertani (LB) media containing appropriate antibiotics. The New England Biolabs Monarch plasmid purification kit was used for mini-preparations which is based on alkaline lysis, neutralisation and subsequent washing to quickly purify plasmids. In total 4 ml of *E. coli* was pelleted by centrifugation for 4 minutes at 10000 rpm in a bench top centrifuge. Following steps were carried out according to manufacturers instructions (New England Biolabs, Hitchin, UK). The purified plasmid DNA was eluted in 20 µl sterilised distilled water.

2.5.5 DNA sequencing

Plasmids and for sequencing were purified by mini-prep (Section 2.5.4) and PCR amplicons for sequencing were purified from gel extraction (Section 2.5.3). Sequencing reactions were prepared in individual PCR reaction tubes and contained 5 µl of plasmid (100 ng/µl) or PCR amplicon (10 ng/µl). Five µl of sequencing primers 3.2 pmol/µl were sent in separate tubes. Reactions were sent for automated sanger sequencing to Source BioScience, UK Ltd (Cambridge, UK) (Sanger et al., 1977; Smith et al., 1986)

2.5.6 Generation of expression vectors

Several vectors used in bimolecular fluorescence complementation (BiFC) experiments were originally were produced in the lab of Tomas Canto (Centro de Investigaciones Biológicas, Madrid, Spain) and were previously gifted to the lab. These include several containing the AGO1, Fny2b and LS2b ORFs (described below). The pROK2-based vectors for BiFC were originally generated by amplifying the N- and C-terminal domains from the yellow fluorescent protein (YFP) ORF, which were cloned into the XbaI and BamHI linearised pROK2 vector (Bracha-Drori et al., 2004). This insertion left a BamHI-XmaI-KpnI-SacI polylinker downstream of the inserted N- and C-terminal halves of the YFP sequence into which the amplified viral ORFs were inserted.

Primers were designed (Table 1.1) to amplify the following fragments Fny 2a, Fny 1a (Fny 2a and Fny 1a are referred to as 2a and 1a from herein) from pFny 209 and

pFny109 constructs. The LS 1a fragment was amplified from the previously described pLS109 construct. The amplified fragments were digested with appropriate restriction enzymes (BamHI and XmaI) and then purified after gel extraction. The purified fragments were ligated into the BamHI and XmaI digested pROK-sYFP backbone to generate the pROK constructs sYFPn-1a and sYFPc-1a, sYFPn-1aLS and sYFPc-1aLS, sYFPn-2a and sYFPc-2a. Additional pROK constructs expressing sYFPn-2b, sYFPc-2b, sYFPn-AGO1 and sYFPc-AGO1 were previously described by González et al. (2010).

The enhanced version of *Green fluorescent protein* (*GFP*) or monomeric *red fluorescent protein* (*RFP*) sequences were amplified to introduce BamHI and ApaI overhangs (Table 1) and then cloned into the BamHI and ApaI digested 1a-pMDC32 vector to generate the GFP-1a and RFP-1a fusions which were expressed from the pMDC32 vector. This approach followed previous work by Dr. Alex M. Murphy (University of Cambridge, Cambridge, UK) who previously constructed the pMDC32 construct expressing the untagged Fny 1a protein (described in detail in Section 2.2.2). Molecular cloning was carried out using the Gateway recombinational cloning method (Thermo Fisher Scientific, Paisley, UK) (Karimi et al., 2007). PCR amplification of the desired fragment with primers added 5' and 3' attB sites to the PCR product to permit recombination with Gateway-compatible entry vectors. The gel purified PCR product was mixed with the gateway entry vector pDONR221 and 0.5 µl of BP clonase II and the reaction was incubated at 25ºC for 1 hour. To end the BP reaction 0.5 µl of Proteinase K solution was added to the reaction and incubated for 10 min at 37°C. Two µl of this reaction was used to transform *E.coli* and after plating on kanamycin selection agar plates positive colonies were confirmed by PCR and sequencing of the purified plasmid. Confirmed entry clones containing the gene of interest were then mixed with an appropriate destination vector in a LR reaction with 0.5 µl of LR clonase II and incubated at 25ºC for 1 hour. To end the LR reaction 0.5 µl of proteinase K solution was added to the reaction and incubated for 10 min at 37°C. Two µl of the LR reaction was used to transform *E.coli* and after plating on agar plates containing the appropriate antibiotic to select the destination vector positive colonies were confirmed by PCR and sequencing of the purified plasmid.

In order to generate GFP or RFP fusion proteins a set of vectors based on the pSAT system was used (Chakrabarty et al., 2007). These “pSITE” vectors were modified to contain the destination fragment required for Gateway LR recombination in place of the multiple cloning site in the pSAT-6 AFP cassettes (Hartley et al., 2000). The pSITE system was demonstrated to be effective in transient and stable expression of viral proteins from the sonchus yellow net virus (Chakrabarty et al., 2007). The pSITE vectors and corresponding GenBank reference used in this study were pSITE-2NB (EF212296), pSITE-2CA(EF212294), pSITE-4CA (EF212292). The pSITE vectors were used to construct the GFP-2a, RFP 2a fusion proteins and the AGO1-GFP and DCP1-GFP and DCP1-RFP fusion proteins. The Arabidopsis AGO1 (AT1G48410) and DCP1 (AT1G08370) ORFs were amplified from Arabidopsis cDNA using forward and reverse primers that contained 5’ extensions corresponding to the attB site (Table 2.1). The purified attB-PCR fragments were then introduced into the entry vector pDONR221 before being subcloned into pSITE-2NB, pSITE-2CA and pSITE-4CA vectors as described above.

Table 2.1. Primers used in the construction of fusion protein vectors.

Primer name	**Sequence 5'-3'**
mRFP-BamHI-Fw	GGGCCCGGATCCATGGCCTCCTCCGAGGAC
mRFP-ApaI-Rv	GGCGCGCCGGGCCCAGGCGCCGGTGGAGTG
GFP-BamH1-Fw	TAGGGCCCGGGATCCTGATGGTGAGCAAGGGCGAG
GFP-ApaI-Rv	GATCCCGGGCCCTATACTTGTACAGCTCGTCCAT
1a-BamHI-Fw	CTGCTAGGATCCATGGCGACGTCCTCGTTCAACATC
1a-XmaI-Rv	ATCTAGCCCGGGCTAAGCACGAGCAACACATT
DCP1-att-Fw	GGGGACAAGTTTGTACAAAAAAGCAGGCTTAATGTCTCAAAACGGGAAGATAATCCCA
DCP1-att-Rv	GGGGACCACTTTGTACAAGAAAGCTGGGTTTTATTGTTGAAGTGCATTTTGTAAAGTTCGG
DCP1-Cterm-RFP-att-Rv	GGGGACCACTTTGTACAAGAAAGCTGGGTGTTGTTGAAGTGCATTTTGTAAAGTTCGG
AGO1-att-Fw	GGGGACAAGTTTGTACAAAAAAGCAGGCTTAATGGTGAGAAAGAGAAGAACGGATG
AGO1-att-Rv	GGGGACCACTTTGTACAAGAAAGCTGGGTTGCAGTAGAACATGACACGCT

2.5.7 Mutagenesis of plasmids

For the generation of small mutations or deletions in plasmids the Q5 Site-Directed Mutagenesis Kit (New England Biolabs) was used. This method is based on the Q5 high fidelity DNA Polymerase (described in Section 2.5.1) along with custom mutagenic primers that allow the site-specific creation of insertions, deletions and substitutions in the target DNA sequence (Kalnins et al., 1983). Reactions were carried out according to manufacturer's instructions (New England Biolabs, Hitchin, UK).

2.6 Molecular biology techniques

2.6.1 Transformation of *E. coli*

A 50 µl aliquot of *E. coli* DH5α 5-alpha high efficient competent cells (New England Biolabs) was thawed on ice, 20-50 ng of plasmid DNA was added and left on ice for 30 minutes. The tube was transferred to a 42ºC water bath for 45 s before being returned to ice for 2 mins. The culture was made up to 500 µl with LB and incubated in a shaking 37ºC incubator for 1 hour. Approximately 20-150 µl of the transformed cells were plated on LB plates containing the appropriate antibiotic for selection.

2.6.2 *A. tumefaciens* competent cell preparation

A single colony of *A. tumefaciens* strain GV3101 was selected from gentamicin 10 µg/ml /rifampicin 50 µg/ml plates and used to inoculate 20 ml of LB media containing gentamicin 10 µg/ml and rifampicin 50 µg/ml, which was cultured overnight at 28°C with shaking. Two 500 ml flasks of LB were inoculated with 9 ml of the overnight culture, and grown at 28°C with shaking until the OD_{600} was 0.7. The *A. tumefaciens* culture was then chilled on ice for 20 minutes. The flasks were centrifuged at 4000 g for 15 minutes at 4°C. The supernatant was removed and the pellet resuspended in 10 ml of ice cold water. The flasks were centrifuged at 4000 g for 15 minutes at 4°C. The supernatant was removed and pellet resuspended in 25 ml of ice cold water. The flasks were centrifuged at 4000 g for 15 minutes at 4°C. The supernatant was removed and pellet resuspended in 5 ml ice cold 10 % glycerol. The resuspended pellets were combined and transferred into one 50 ml Falcon conical

tube and centrifuged at 4000 g for 15 minutes at 4°C. The supernatant was removed and pellet resuspended in 3 ml of ice cold 10 % glycerol. The resuspended pellet was divided into 50 µl aliquots in 1.5 ml microfuge tubes, and immediately frozen in liquid nitrogen, competent *A. tumefaciens* cells stored at -80°C remained viable for at least 6 months.

2.6.3 Transformation of *A. tumefaciens*

The transformation of *A. tumefaciens* was carried out using a protocol adapted from Weigel and Glazebrook (2006). Plasmids were diluted to 15 ng/µL using sterile distilled water. Two µl of diluted plasmid was mixed with 50 µl of competent *A. tumefaciens* GV3101 in a 1.5 ml microfuge tube and placed on ice before transfer to a prechilled MicroPulser electroporation cuvette (Bio-Rad Laboratories Ltd, Hemel Hempstead, UK) with a 0.1 cm gap, and left to chill on ice for 20 minutes. A Gene Pulser Xcell™ (Bio-Rad Laboratories Ltd, Hemel Hempstead, UK) was set using the pre-programmed *A. tumafaciens* electroporation protocol (200 Ω, capacitance extender 250 µF, capacitance 25 µF). After electroporation 1 ml of LB media was added to the cuvette and then transferred to a 2 ml microcentrifuge tube. Electroporated cells were incubated at 28°C for 2-3 hours before plating 70 µl on LB plates containing rifampicin 50 µg/ml, gentamycin 10 µg/ml and the plasmid specific antibiotic. Plates were wrapped with Parafilm tape and incubated at 28°C for 2-3 days.

2.6.4 *A. tumefaciens* transient expression assay

Expression vectors containing genes of interest were transferred to *A. tumefaciens* GV3101 using electroportation (described in Section 2.6.3). To prepare cells for agroinfiltration 5 ml of LB, containing the appropriate antibiotic for selection of the expression vector and rifampicin 50 µg/ml, gentamycin 10 µg/ml was inoculated from a glycerol stock of the desired construct by means of a pipette tip. The 5 ml starter culture was incubated at 28°C overnight, 1 ml of this culture was used to inoculate 50 ml LB containing antibiotics which was cultured overnight. The *A. tumefaciens* cultures were centrifuged for 15 min at 5000 g and then resuspended in MMA buffer [10 mM $MgCl_2$, 10 mM 2-(*N*-morpholino)ethanesulfonic acid (MES), 100 µM acetosyringone]. The OD_{600} of the *A. tumefaciens* suspension

was adjusted to 0.5 with MMA buffer, and the resuspended cells then rested at room temperature for 2 h prior to agroinfiltration. *A. tumefaciens* suspensions were infiltrated using a syringe without a needle onto the abaxial side of a *N. benthamiana* leaf. The infiltrated plants were covered with a clear plastic propagation tray for one day. Plants were examined for protein expression by microscopy or by immunoblotting 3-4 days after agroinfiltration.

2.7 Protein methods

2.7.1 Extraction and quantification of proteins from plants

Protein was extracted from approximately 100 mg of leaf tissue using protein extraction buffer [10% glycerol, 25 mM Tris-HCl (pH 7.5), 200 mM NaCl, 1 mM EDTA, 0.15% IGEPAL CA-630 (Sigma), 10 mM Dithiothreitol (DTT) and protease inhibitor cocktail]. Frozen leaf tissue was ground to a fine powder using a pre-chilled pestle and mortar and liquid nitrogen. One ml of extraction buffer was added for every 100 mg of leaf tissue. The ground tissue was centrifuged at 10,000 g for 5 minutes at 4°C using an Eppendorf 5415 R centrifuge (Eppendorf, Stevenage, UK). The supernatant was transferred to a clean 1.5 ml micro centrifuge tube and centrifuged once more at 10,000 g for 5 minutes at 4°C to remove any remaining debris. The supernatant was removed to a clean tube and the amount of protein in the samples quantified using Bradford's dye binding assay (Bradford, 1976). A suitable volume of protein extract (1-2 µl/ml) was added to 200 µl Bio-Rad protein assay solution [0.02% (w/v) Coomassie Brilliant Blue G-250, 4.75% (v/v) ethanol, 10% (v/v) phosphoric acid]. The sample was made up to 1 ml with water and left to stand for 5 minutes. The OD_{595} of the sample was measured in a Helios Gamma spectrophotometer. The concentration of protein was then estimated using a calibration curve prepared with bovine serum albumin (BSA) standards (0.1-20 mg/ml).

2.7.2 SDS-polyacrylamide gel electrophoresis

Protein extracted from plant tissue was resolved by sodium dodecyl sulfate-polyacrylamide gel electrophoresis (SDS-PAGE; Laemmli, 1970). Slab gels

comprising an upper 5% (w/v) acrylamide (stacking gel) over a 10% (w/v) acrylamide separation gel were prepared from stock solutions of 30% (w/v) acrylamide and 1% (w/v) N,N'-bis-methylene acrylamide. The separating gels contained 0.37 M Tris-HCL pH 8.7 and 0.1% (w/v) SDS and the stacking gels contained 0.143 M Tris-HCL pH 6.8 and 0.1% (w/v) SDS. Gels were polymerised by the addition of 0.12% (w/v) Tetramethylethylenediamine (TEMED) and 0.12% (v/v) ammonium persulphate. Gels were cast and electrophosed using the Mini-Protean II Dual Slab Cell system with 10 well combs (Bio-Rad Laboratories Ltd, Hemel Hempstead, UK). Gels were polymerised at room temperature for approximately 30 minutes. The appropriate amount of protein (1-10 µg) was mixed with an at least equal volume of SDS-PAGE sample buffer [50 mM Tris-HCL pH 6.8, 2% (w/v) SDS, 10% (v/v) glycerol, 100 mM DTT and 0.1% (w/v) bromophenol blue]. Before the samples were loaded onto the gel, the protein sample was denatured by incubating the samples at 70-90°C for 10 minutes. Gels were run in running buffer [0.125 M Tris-HCl pH 8.3, 0.2 M glycine, 0.1% (w/v) SDS] at 150 V until the gel front had run off the bottom of the gel.

2.7.3 Immunoblot analysis

SDS-PAGE gels were transferred to PROTRAN nitrocellulose membrane, pore size 45 µm (Merck) and probed according to the method of Towbin et al. (1979). Electroblotting was carried out using the Mini Trans-Blot electrophoretic transfer cell (Bio-Rad). Transfer was carried out at 100 V for 1 hour in transfer buffer [15.6 mM Tris-HCl pH 8.3, 120 mM glycine, 20% (v/v) methanol] (Gershoni and Palade, 1982). Blots were stained with Ponceau S stain [0.1% (w/v) Ponceau S, 5% (w/v) acetic acid] to assess equal loading.

For probing and detection of proteins, membranes were gently shaken in 25 ml blocking buffer [phosphate buffered saline with Tween-20 (PBST) (140mM sodium chloride, 2.7 mM potassium chloride, 10 mM NaH_2PO_4, 2 mM KH_2PO_4, 5% (w/v) skimmed milk powder, 0.1% Tween-20)] for 1 hour at room temperature. The blots were washed twice for 5 minutes in 20 ml PBST. Blots were then incubated with 10 ml blocking buffer containing primary antibody [rabbit polyclonal anti-GFP (PABG1) (1:1000), mouse monoclonal anti-RFP (6G6) (1:2000) (Chromotek, Planegg-

Martinsried, Germany), mouse monoclonal anti-GFP (B-2) 1:200 (Santa Cruz Biotechnology Inc, Heidelberg, Germany)] and gently shaken overnight at 4°C. The blots were washed 3 times for 5 minutes in 20 ml PBST. After washing, blots were incubated with 10 ml blocking buffer containing secondary antibody (anti-rabbit or anti-mouse IgG conjugated to horseradish peroxidase (HRP) (Promega) 1:10000 dilution). The blots were shaken gently for 1 hour at room temperature and then blots were washed 3 times for 10 minutes in 20 ml PBST. The binding of the conjugated HRP-anti-rabbit or -mouse IgG was detected with a chemiluminesence assay using the Pierce ECL Western Blotting Substrate according to the manufacturers' instructions (Thermo Fischer Scientific, Paisley, UK). Blots were then exposed to Fujifilm super RX-N medical film (FUJIFILM UK Ltd, Bedford, UK) and the film developed using an automatic X-ray processor (X-ograph, Compact X2)

2.7.4 Immunoprecipitation

Plant tissue samples for immunoprecipitation experiments were processed as described above in Section 2.7.1. Approximately 500-700 µg (around 200-500 µl) of total protein was used as input for immunoprecipitation experiments. RFP- or GFP-Trap magnetic agarose beads (Chromotek, Planegg-Martinsried, Germany) were used for the immunoprecipitation of RFP- or GFP-tagged proteins and anti-flag M2 magnetic agarose beads (Thermo Fisher Scientific) were used for the immunoprecipitation of FLAG-tagged proteins. Before use, magnetic agarose beads were equilibrated by washing 3 times in 500 µl ice-cold dilution buffer [10 mM Tris-HCl (pH 7.5), 150 mM NaCl, 0.5 mM EDTA], a magnetic rack was used at all stages during the experiment to capture the magnetic beads while the supernatant was removed. The equilibrated beads were resuspended in dilution buffer to their original volume and 25 µl of magnetic beads were combined with the protein extraction supernatant (approximately 200-500 µl depending on protein concentration) in a 2 ml microcentrifuge tube. The supernatant and magnetic bead mixture was then filled to 1.5ml with ice-cold dilution buffer, and placed on a rotary incubator for 1 hour at 4°C. The magnetic agarose beads were then washed three times with 500 µl ice-cold dilution buffer. After the final wash the remaining dilution buffer was removed and magnetic agarose beads were resuspended in 50 µl SDS-

PAGE sample buffer (Laemmli, 1970) (Section 2.7.2). The re-suspended magnetic agarose beads were then boiled for 10 minutes at 95°C to dissociate immunocomplexes from the beads. After boiling, microcentrifuge tubes were returned to a magnetic rack and the sample buffer was collected and analysed via SDS-PAGE or stored in an -80°C freezer for further use.

2.8 Confocal laser scanning microscopy

All confocal microscopy was performed on a Leica Model SP5 (Leica Microsystems Ltd, Milton Keynes, UK). GFP was imaged using an excitation maxima of 488 nm and emission maxima of 509 nm, RFP at 561 nm and 583 nm and YFP at 514 nm and 527 nm, respectively. Image acquisition was conducted at a resolution of 512 x 512 pixels and a scan rate of 10 µs/pixel. Control of the microscope, as well as image acquisition and export as TIFF files, was controlled by Leica LAS software. Image analysis was conducted using ImageJ (Version 2.0.0: http://imagej.net). Leaf Sections from *N. benthamiana* were prepared with a scalpel and stuck to a microscope slide with double sided sticky tape so that the abaxial surface was facing up.

2.8.2 Staining of plant tissue

Staining of the endoplasmic reticulum was achieved with ER-tracker (Invitrogen). A concentration of 1 µM was prepared in PBS and infiltrated with a 1 ml needle-less syringe into *N. benthamiana* through the abaxial leaf surface. Dye was left for 30 min before re-infiltrating with PBS to remove excess dye. Leaf Sections were then imaged using an excitation and emission maxima at 587 nm and 615 nm, respectively. The styryl dye FM-4-64 (Invitrogen) was used for the staining of membranes. A solution of 25 mM FM-4-64 was prepared in distilled water and infiltrated into the leaf through the abaxial surface of *N. benthamiana* leaves. Images were taken 1 hour after infiltration. Leaf Section were then imaged using an excitation and emission maxima at 515 nm and 640 nm, respectively.

2.9 Arabidopsis PTI assays

2.9.1 Bacterial inoculation by infiltration

Bacterial inoculum was prepared by streaking out a plate of bacterial colonies one day prior to the experiment (Tornero and Dangl, 2001). On the day of the experiment, the grown plate of bacterial culture was resuspended in 10 mM $MgCl_2$ and diluted in a 1:10 ratio prior to optical density measurements at 600nm (OD_{600}) with a Helios Gamma spectrophotometer (previously Unicam of Cambridge, currently known as Thermo Electron Spectroscopy, Cambridge, UK). An OD_{600} reading of 0.1 approximately equates to 1 x 10^8 colony forming units (CFU)/ml (Masclaux and Expert, 1995). The bacterial suspension was diluted appropriately to achieve 10^5 CFU/ml for all infiltration experiments unless otherwise stated. Leaves from approximately 4 week old plants grown under short day conditions were inoculated with a 1 ml (needle-less) syringe from the tip of the leaf with the prepared bacterial suspension (Klement, 1963). Infected plants were covered with propagating lids for at least 1 h and were returned to the growth rooms until the day of sampling. At two days post inoculation (dpi), unless otherwise stated, leaf samples were taken to determine bacterial growth titres. Plant tissue samples were taken by recording fresh weight (mg) per leaf. Samples typically containing 20 to 40 mg of tissue was ground in 400 µl of 10 mM $MgCl_2$ and serially diluted in a 96-well V-bottom microtitre plate (Thermo Scientific). A volume of 4 µl from each diluent were gently placed on LB agar plates with appropriate selecting antibiotics and grown at 25°C for 1-2 days. Corresponding sample diluents with visibly discrete bacterial colonies were counted to calculate final CFU. Bacterial growth titres were then expressed in CFU/mg, calculations of which are shown below:

$$\text{CFU} = \frac{10^n \text{ x number of colonies x extraction volume (µl)}}{4\text{µl}}$$

where *n* is the dilution factor of the sample used to count discrete bacterial colonies.

2.9.2 Preparation of crude extracts from CMV infected plants

WT Arabidopsis plants were inoculated with Fny-CMV, as described in Section 2.3.3. After 2-weeks infected systemic tissue was harvested and was frozen in liquid nitrogen. The tissue was ground and extracted in 1/10 (wt/vol) PBS-Tween (0.5%) overnight on a rotation wheel at 4°C. The extracts were centrifuged three times at 4000 x g for 15 min to remove cellular debris and were analysed by SDS-PAGE and Coomassie staining. Extracts were produced at least three times independently. The mock extract derived from mock-inoculated plants was treated exactly the same way as extracts derived from virus-infected plants.

2.9.3 Root growth experiments

For root growth inhibition experiments, growth conditions were set to a 16 h light/8 h dark cycle at 21°C, 50% light intensity and at 20°C, respectively (Percival growth chamber). Surface-sterilized seeds were sown on 0.5 x MS with 1% (w/v) agar (Phyto Agar, Duchefa Biochemie, distributed by Melford Laboratories Ltd.) and stratified at 4°C for 2-3 days. Seeds were allowed to germinate vertically in square tissue culture plates (Sarstedt Ltd., Leicester, UK). After one week seedlings were transferred to new MS plates. Seedlings were imaged immediately after transfer to new plants and imaged after 3 and 5 days of further growth. Images were saved in JPEG format and analysed by ImageJ (Version 2.0.0: http://imagej.net). Total root lengths were traced using the freehand line feature in the software and measured.

2.10 Statistical analysis

The R statistical package 3.2.2 (CRAN-Ma, Imperial College London, UK, www.R-project.org.) was used for all statistical analysis and tests. Graphs were constructed using Microsoft Excel for Mac OS. For all displayed data, mean and standard error of the mean (SEM) were calculated. Multiple comparisons of the mean were calculated using analysis of variance (ANOVA) and post-hoc analysis of significance calculated using Tukey's HSD test. For conservation plot for Fny- and LS-2a protein sequences (Fig. 3.1), plotcon program (EMBOSS package) was used with comparison matrix EBLOSUM62 (default) and window size of 10 residues.

Chapter 3. Characterising PAMP-triggered immunity induced by Fny-CMV in Arabidopsis

3.1 Introduction

The Fny strain of CMV has the potential to induce two types of anti-aphid resistance in Arabidopsis: feeding deterrence (antixenosis), and antibiosis (which is toxic to aphids) (Westwood et al., 2013a). Previous work carried out in our lab used transgenic plants and reassortant viruses consisting of combinations of RNA1, RNA2 and RNA3 from Fny- and LS-CMV to study CMV-induced aphid resistance. As LS-CMV does not induce aphid resistance in Arabidopsis ecotype Col-0 it was possible to map the viral inducer of feeding deterrence encoded by Fny-CMV to RNA2 by creating reassortant CMV genomes containing mixtures of genomic RNAs derived from either Fny-CMV, or LS-CMV.

In Arabidopsis, feeding deterrence is induced by the Fny-CMV 2a protein, whereas antibiosis is triggered by the Fny-CMV 2b protein (Westwood et al., 2013a). During CMV infection the 1a protein supresses 2b-induced antibiosis (discussed in Chapter 4 and 5) resulting in 2a-induced feeding deterrence becoming the dominant anti-aphid resistance mechanism. During infection with Fny-CMV, several PAMP-responsive genes, including those induced by PAMPs such as flg22, elf26 and chitin, were up-regulated (Groen et al., unpublished results; Westwood et al., 2013a). This suggested that CMV infection is able to activate some aspects of PTI signalling in Arabidopsis, although we do not know if these PTI responses contribute

towards aphid resistance. To further characterise the nature of the resistance induced by the 2a protein I carried out aphid performance experiments, as well as assays to determine how PTI might contribute towards CMV-induced anti-aphid resistance. I also carried out experiments to determine if BAK1, a key factor in PAMP perception, has any role in CMV-induced anti-aphid resistance. BAK1 was previously found to be implicated in resistance to several RNA viruses (discussed in Section 1.4.1 Plant antiviral immunity)

3.2 Results

3.2.1 Identifying domains of the Fny 2a protein responsible for induction of antixenotic resistance to aphids

In order to determine which domains of the 2a protein may be responsible for the activation of antixenosis, I compared the Fny-CMV and LS-CMV 2a protein coding sequences in order to identify differences (Fig. 3.1). The RdRp domain (roughly residues 300-720) was highly conserved between the two strains suggesting that the RdRp is unlikely to be involved directly in inducing antixenosis. The N-terminal (residues 1-300) was highly dissimilar between the two strains. This was most marked in the sequences flanking residues 70, 160 and 260, which included sequences where similarity was low as 20%. The part of the 2a protein ORF encoding the C-terminal region which overlaps the 2b ORF was also highly dissimilar. However, this region of the 2a protein is unlikely to be responsible for the induction of antixenosis, because a truncated version of the 2a protein (encoded by the CMV∆2b mutant, which lacks nucleotides 2419-2713 of the Fny-CMV RNA2 sequence) induced anti-aphid resistance when transgenically expressed in Arabidopsis (Westwood et al., 2013a). Additionally, when the *dcl2/4* mutant (which is deficient in antiviral signalling) were inoculated with CMV∆2b and used in aphid performance assays, feeding deterrence was observed (Westwood et al., 2013a). The *dcl2/4* mutant allows CMV∆2b to accumulate to levels comparable to wild-type Fny-CMV (Lewsey et al., 2009).

I hypothesised that the region spanning residues 1-300 of the 2a protein was most likely to contain amino acid(s) that determine antixenosis induction. From this point a colleague (Dr Sun-Ju Rhee) carried out the molecular work for this project. Five recombinant cDNA clones encoding chimeric RNA 2 molecules were constructed in which the regions encoding the N-proximal 300 residues of the 2a protein comprised sequences exchanged between the RNA 2 sequences of Fny-CMV and LS-CMV. Constructs were derived from plasmids pFny206 and pLS-CMV2, the respective infectious cDNA clones for the Fny-CMV and LS-CMV RNA2 molecules (Rizzo and Palukaitis, 1990). Wild-type or recombinant RNA2 molecules were synthesized by in vitro transcription using T7 RNA polymerase, and infectious RNA mixtures produced by mixing these with in vitro-synthesized Fny-CMV RNAs 1 and 3.

Infectious RNA mixtures for these reassortant and recombinant viruses were used to inoculate *N. benthamiana* plants for preparation of virions to use as inoculum for experiments with *A. thaliana*. The symptoms induced by these recombinant and reassortant viruses in N. benthamiana and *A. thaliana* are shown in Fig. 3.0. In Arabidopsis the chimeric viruses accumulated to similar levels, indicating that none were compromised in their ability to replicate or spread through the host.

Future work in our lab will aim to characterise the specific host proteins that interact with the 2a protein. Several strategies will be used in order to further this research theme, including Co-IP and yeast 2-hybrid. A yeast 2-hybrid assay was conducted by Choi *et al*. (2016), who selectively used the CMV-1a helicase domain as bait to screen a yeast two-hybrid library derived from a *Capsicum annuum* cDNA library. However, without a clear idea of which 2a sequences are involved this approach would be very labour intensive. I initially cloned an infectious clone of RNA2 containing, so that Co-IP with FLAG tagged 2a proteins from Fny- and LS-CMV to develop a proteomic database of plant proteins, which interact with 2a. This method uses an antibody raised against a specific antigen (in this case the FLAG tag) to specifically bind that protein in the sample. Once host targets are identified, Arabidopsis mutants can be produced to test whether aphid performance is affects.

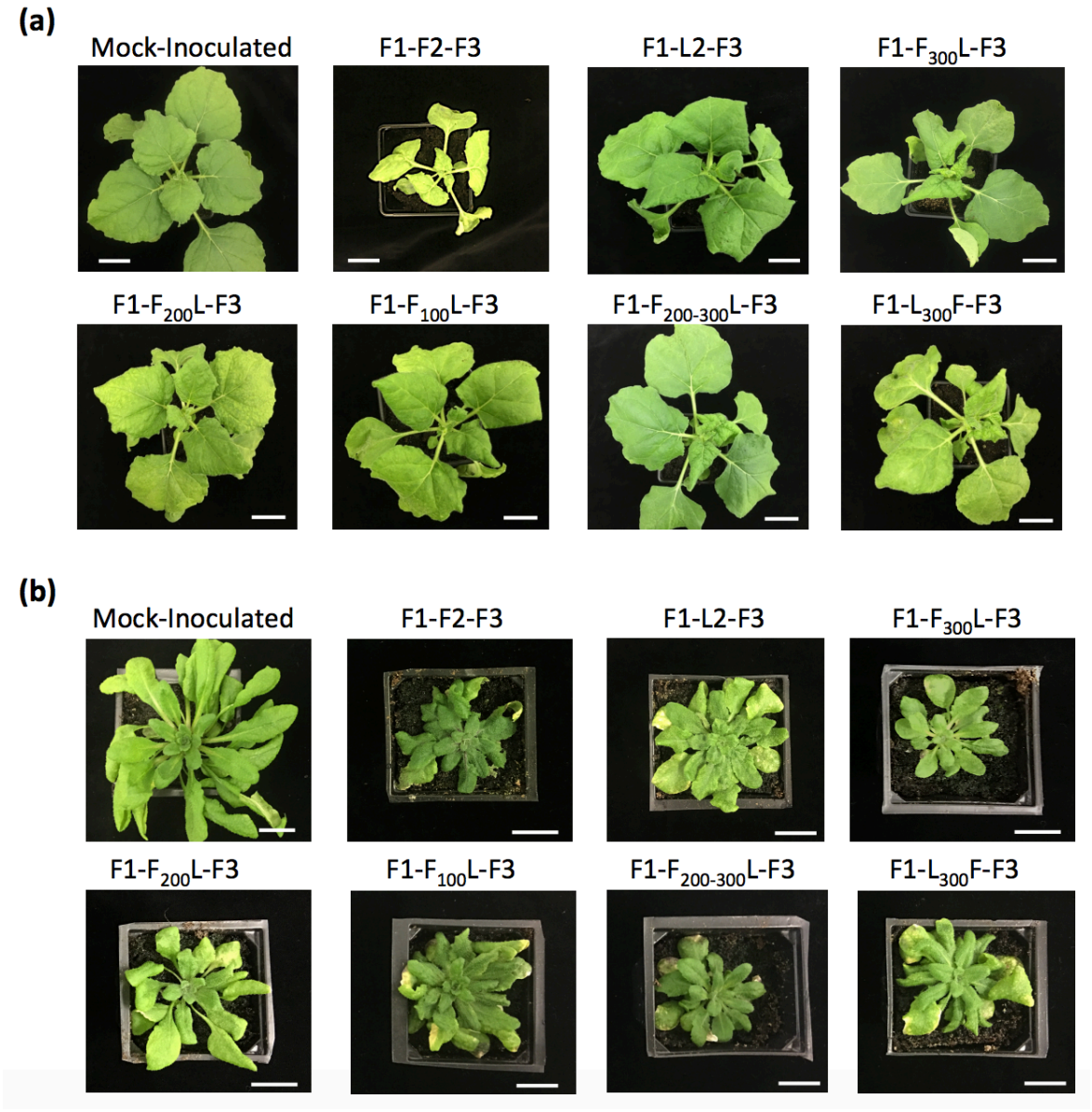

Figure 3.0. Systemic disease symptoms on plants infected with reconsulted viruses and viral reassortant, and recombinant viruses.

The Fny strain of cucumber mosaic virus reconsulted by mixing synthetic RNAs generated by in vitro transcription of clones for Fny-CMV RNAs 1, 2, and 3 (F1-F2-F3) induced stunting, leaf deformation, and chlorosis in *Nicotiana benthamiana* plants (a) and stunting and leaf deformation in plants of Arabidopsis thaliana Col-0 (b). A reassortant virus constituted of the RNAs 1 and 3 of Fny-CMV and LS-CMV RNA2 (F1-L2-F3) induced milder disease symptoms in both host plants, as reassortant viruses possessing recombinant RNAs 2 possessing sequences

derived from the RNAs 2 of LS-CMV and Fny-CMV. N*. benthamiana* plants were inoculated with synthetic viral RNA mixtures on lower leaves 2 weeks after germination, and plants photographed 11 days later (a). *A. thaliana* plants were inoculated with purified virions (800 ng.µl-1) at the 2-3 leaf stage, and photographed 22 days later. Mock-inoculated plants were mechanically inoculated with sterile water. Scale bars represent 2cm.

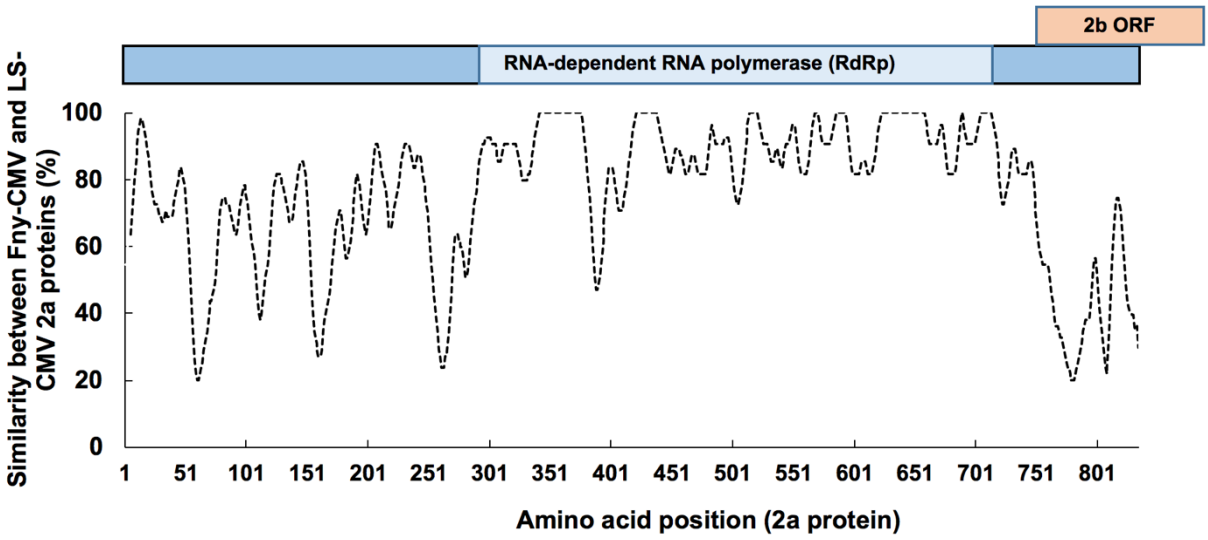

Figure 3.1. Amino acid sequence alignment and similarity between the Fny- and LS-2a protein.

The line graph illustrates the degree of conservation with the window size of ten residues obtained using plotcon program (EMBOSS). A diagram of the 2a protein ORF is displayed above the conservation plot showing the RNA-dependent RNA polymerase (RdRp) domain, and the overlapping 2b ORF.

3.2.2 The 2a protein induces antixenosis when transgenically expressed in Arabidopsis

During infection, the 2a protein elicits enhanced biosynthesis of an aphid feeding deterrent, 4MI3M (Westwood et al., 2013a). In that study, only MRGR was used as a measure of aphid performance. I additionally investigated the effects of the 2a and 2b protein on aphid reproduction. When 1 day old aphid nymphs were confined on transgenic plants expressing viral proteins I observed various effects on aphid MRGR and progeny produced (colony size). The 2a protein was previously shown to induce 4MI3M production and antixenosis in Arabidopsis, in this experiment I observed a significant reduction in MRGR of aphids grown on 2a-transgenic plants compared to WT Col-0 plants (Fig. 3.2). In the same experiment the colony size of aphids grown on 2a-transgenic plants was significantly reduced after 9 and 12 days compared to colony sizes of aphids reared on WT plants. The 2b protein is known to induce antibiosis against aphids in Arabidopsis (Westwood et al., 2013a). I confirmed that aphid growth rate was significantly decreased on *2b*-transgenic plants (Fig. 3.3). Similarly, I observed that colony growth was also significantly reduced when aphids were maintained on *2b*-transgenic plants compared to WT Col-0 plants.

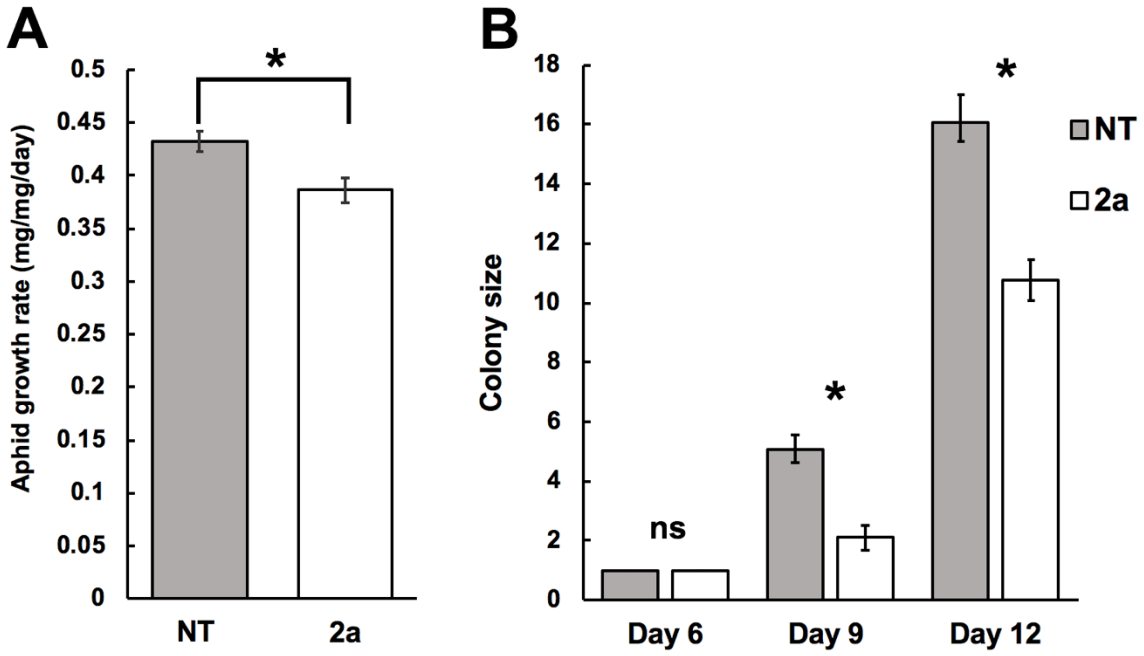

Figure 3.2. The 2a protein inhibits aphid reproduction, as well as growth rate.

A single aphid nymph was placed on an individual four-week old non-transgenic (NT) Col-0 Arabidopsis plants and a transgenic plant expressing the CMV 2a protein. The mean relative growth rate (MRGR) was calculated after 6 days (A) and the number of progeny produced were recorded after 6 and 10 days (B). Error bars represent standard error of the mean (n=16). Significant differences ($P < 0.05$, Student's t-test) are marked by an asterisk, non-significant is displayed as (ns). Comparisons were made between NT and 2a transgenic plants at each time point (B).

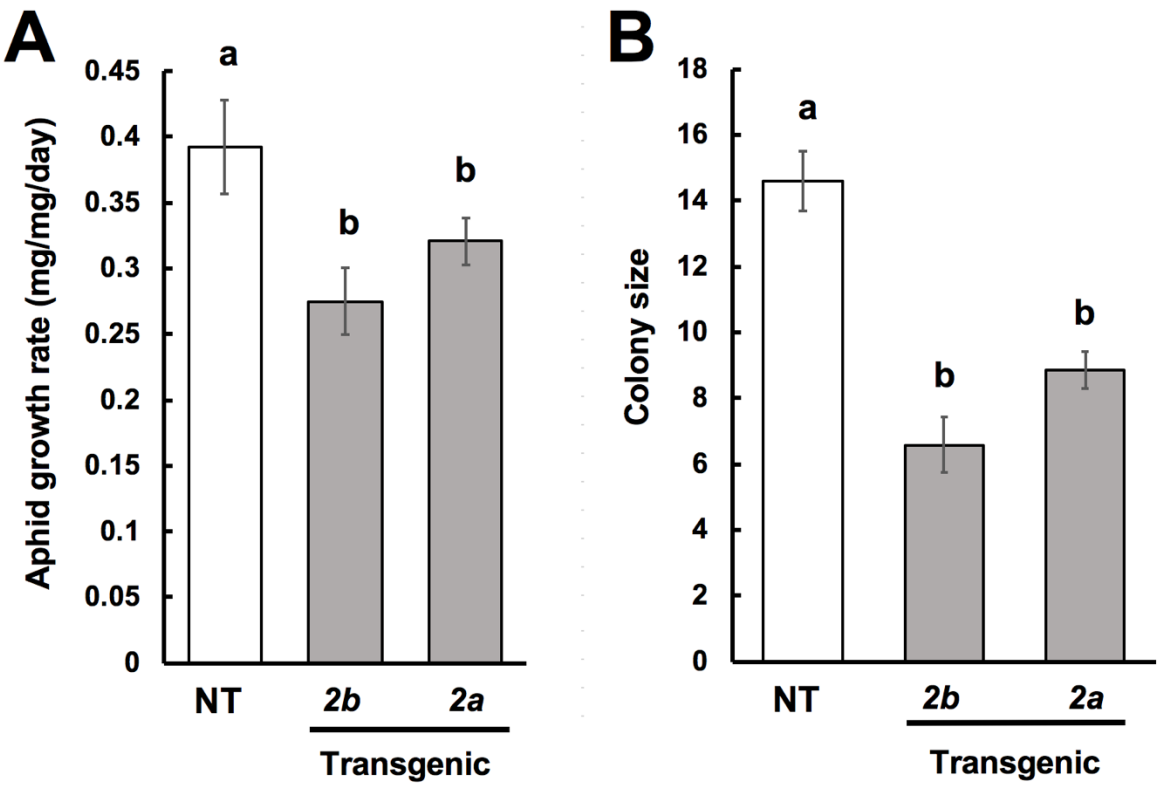

Figure 3.3. Aphid reproduction as well as growth rate is decreased on transgenic Arabidopsis plants expressing viral proteins.

A, the mean relative growth rate (MRGR) of individual aphids placed on transgenic Arabidopsis plants expressing either the Fny-CMV 2b or the Fny-CMV 2a protein or non-transgenic (NT) plants. B, sizes of aphid colonies produced from initial infestations of single one-day-old nymph at 10 days post-infestation. Different letters are assigned to significantly different groups (One-way ANOVA with post-hoc Tukey's tests: $P < 0.05$). Error bars represent standard error of the mean calculated from the measurement of 20 aphids for (A), and the mean number of aphids from 20 plants (B).

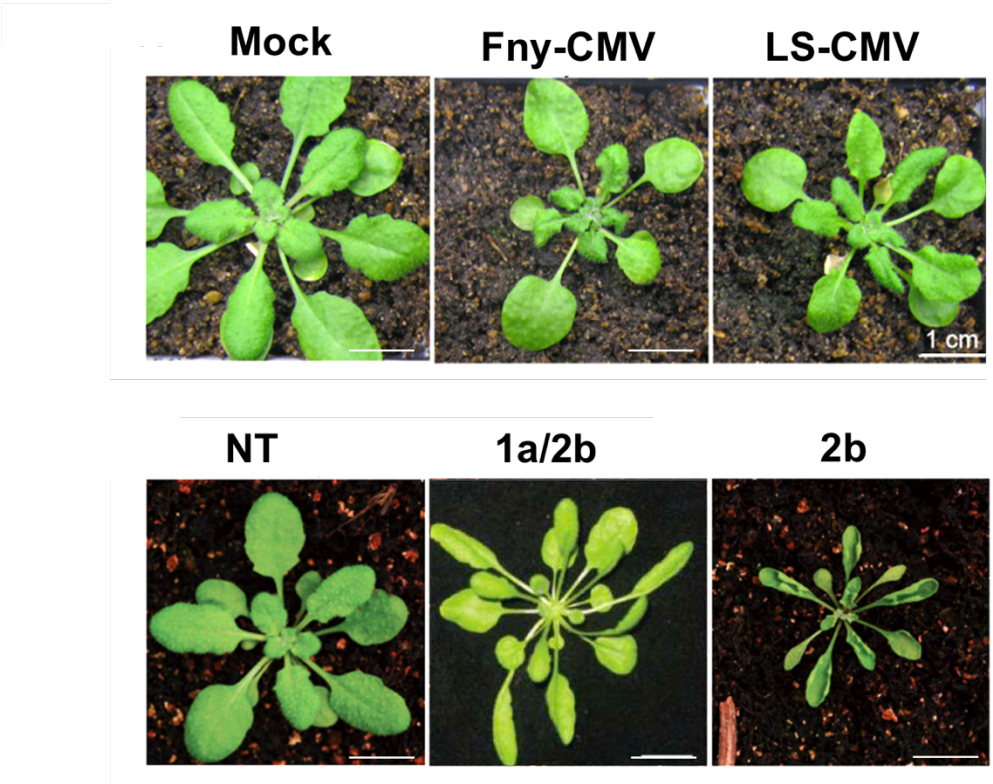

Figure 3.4. Symptoms of CMV-infected and phenotypes of transgenic Arabidopsis plants constitutively expressing various Fny-CMV proteins.

Upper panel, mock indicates a mock-inoculated plant. Plants inoculayed with Fny-CMV or LS-CMV were photographed at 14 days post-inoculation. Lower panel, appearance of plants (from independent transformed lines) expressing transgenes encoding the Fny-CMV 1a and 2b protein under the control of the constitutive cauliflower mosaic virus 35S promoter. Non-transgenic (NT). Plants were five weeks old when photographed. The construction of transgenic plants is described in Section 2.2.2 Arabidopsis Accessions and Mutants. Scale bar represents 1 cm.

3.2.3 Determining the role of BAK1 in CMV-induced aphid resistance

The PRR co-receptors BAK1 and BKK1 have been implicated in antiviral defence in Arabidopsis, as Arabidopsis *bak1* mutants were shown to have increased susceptibility to three RNA viruses, while crude extracts of virus-infected leaf tissue also induced a typical PTI responses in a BAK1-dependent manner (Kørner et al., 2013) (discussed in Section 1.4.1). I carried out aphid performance assays to determine if BAK1 is involved in CMV-induced anti-aphid resistance. In two out of three experiments, the growth rate of aphids reared on infected *bak1-5* plants was not significantly different compared to the growth rate of aphids on uninfected *bak1-5* plants (Fig. 3.5A). Although in one experiment CMV-induced aphid resistance was still observed in *bak1-5* plants (Fig. 3.5C). This observation suggested that anti-aphid resistance was still induced by CMV in *bak1-5* mutants. However, this results is further discussed in Section 3.3.3. CMV-induced anti-aphid resistance was not observed in *bak1-5* plants when MRGR was measured, but in all experiments colony size was significantly reduced compared to mock inoculated *bak1-5* plants.

I repeated aphid performance assays using *bak1-5 bkk1* double mutant plants and observed that *M. persicae* MRGR was not significantly different compared to the growth rate of aphids on uninfected *bak1-5 bkk1* plants (Fig. 3.5C). This was observed in three experiments. Previous work carried out in our group demonstrated that CMV-induced aphid resistance still occurs in *bkk1* mutant plants (Groen et al., unpublished results). In total, my results, and those observed since, suggest that BAK1-mediated signalling plays an important role in CMV-induced anti-aphid resistance to *M. persicae*. However, BAK1 appears to only regulate CMV-induced signalling that affects aphid MRGR but not aphid colony growth, suggesting that two distinct resistance pathways that affect aphid performance are induced by CMV in Arabidopsis.

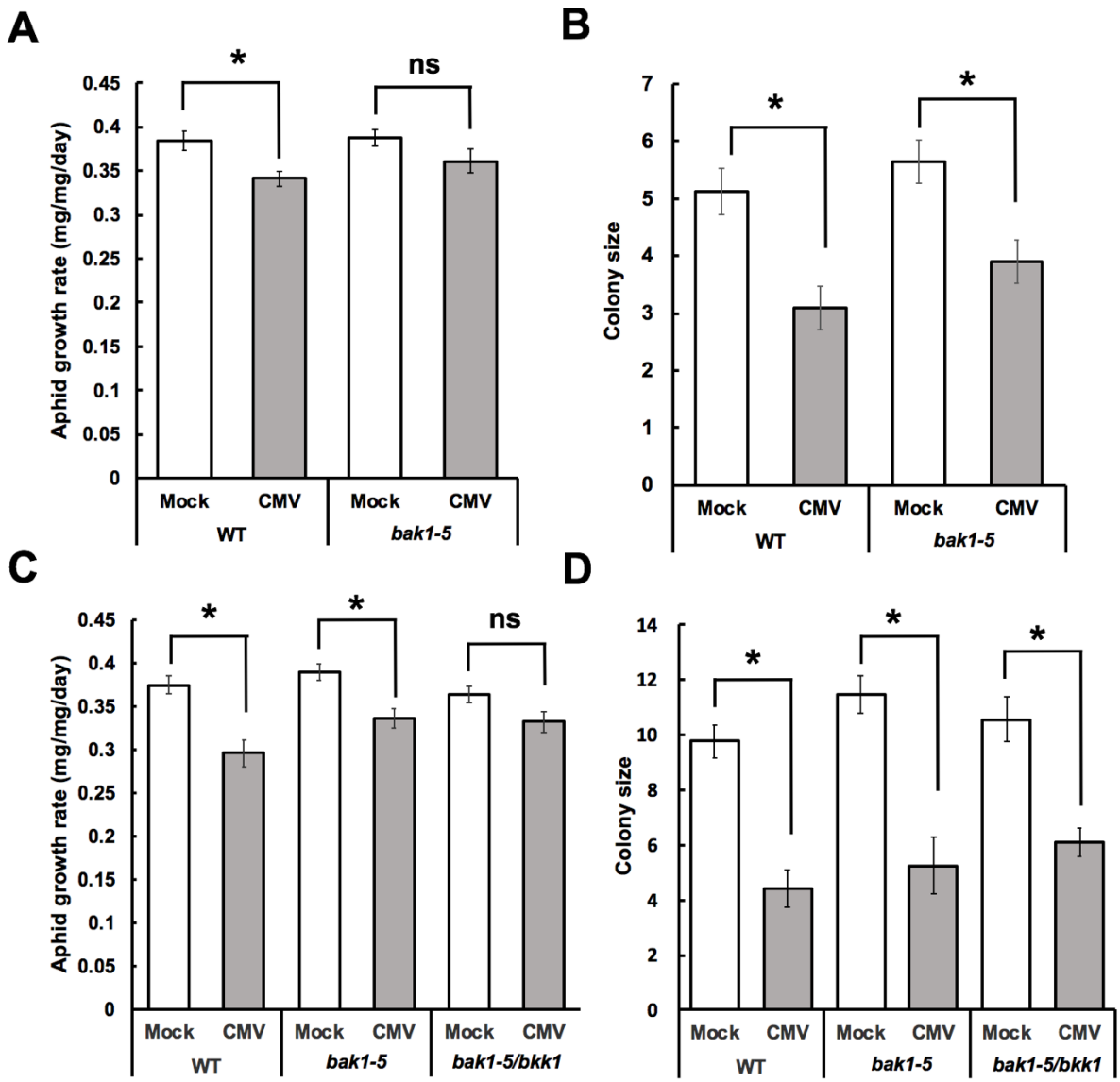

Figure 3.5. CMV infection appears to induce two distinct forms of resistance to *M. persicae*, only one of which may be BAK1-dependent.

The mean relative growth rate (MRGR) of individual aphids placed on WT Col-0, *bak1-5* (A) and *bak1-5 bkk1* (C). The colony size was recorded 10 days after infestation (B, D). Significant differences ($P < 0.05$, Student's t-test) are marked by an asterisk, non-significant is displayed as (ns). Error bars represent standard error of the mean calculated from the measurement of 16 aphids for A, and 20 aphids for C, and the mean number of aphids from 16 plants for B and 20 plants for D. Experiments A, B and C, D were carried out independently.

3.2.4 CMV-induced resistance affects specialist and generalist aphids differently

I found that the effects of a virus on host plant biochemistry can affect aphid species differentially. CMV-induced antixenosis (as indicated by decreased MRGR) in Arabidopsis depends on feeding deterrence mediated by the conversion of the most abundant indole glucosinolate, I3M, into the more effective deterrent 4MI3M, in a mechanism that is triggered by the 2a protein (Westwood et al., 2013a) (discussed in Section 1.6 Plant immunity triggered by CMV). Certain Brassicaceae specialist aphids are able to tolerate glucosinolates produced by host plants (Kazana et al., 2007). I set up aphid performance assays using the generalist aphid *M. persicae* and the Brassicaceae specialist aphids *B. brassicae* and *L. erysimi* to determine if CMV-induced anti-aphid resistance is effective against specialist aphids. In these experiments I included the *bak1-5* and *bak1-5 bkk1* mutants to observe if CMV-induced anti-aphid resistance affected colony growth of specialist aphids, as this would help determine which of the two resistance mechanisms discussed in Section 3.2.3 were relevant.

As previously observed, CMV infection caused a significant reduction in growth rate of *M. persicae* growth rate confined on these plants (Fig. 3.6A). In this experiment a significant reduction in *M. persicae* growth rate was observed in CMV-infected *bak1-5* plants, but not *bak1-5 bkk1* plants. CMV infection caused a significant reduction in *M. persicae* colony size in WT, *bak1-5* and *bak1-5 bkk1* mutants compared to mock inoculated control plants (Fig. 3.6B).

In experiments using the specialist aphid *B. brassicae* I observed no significant difference in the growth rate of aphids grown on CMV-infected compared to mock-inoculated plants, this was observed in WT, *bak1-5* and *bak1-5 bkk1* plants (Fig. 3.6C). Interestingly, I also observed a reduction in colony size of *B. brassicae* reared on CMV-infected plants compared to mock-inoculated plants in WT and mutant plants (Fig. 3.6D). In experiments using another specialist aphid, *L. erysimi,* I observed no significant different in the growth rate of aphids grown on CMV-infected compared to mock-inoculated plants. This was observed in WT, mutant *bak1-5* and

bak1-5 bkk1 plants (Fig. 3.6E). The colony sizes of *L. erysimi* reared on CMV-infected WT, *bak1-5* and *bak1-5 bkk1* plants were not significantly different to aphids reared on mock inoculated plants (Fig. 3.6F). These results suggests that specialist aphids are more tolerant of CMV-induced resistance, as the growth rate of both *B. brassica* and *L. erysimi* were unaffected on plants that were CMV-infected. However, in the case of *B. brassica* the production of nymphs was decreased on CMV-infected plants suggesting that aphid reproduction can be impacted even if the growth rate of individual aphids is unaffected. This supports my previous work which suggests there are two anti-aphid resistance mechanisms that are induced by CMV (summarised in Table 3.1).

Table 3.1. CMV-induced resistance consists of two resistance mechanisms.

		CMV-induced resistance	
		BAK1-dependent	**BAK1-independent**
	Aphid species	**MRGR**	**Reproduction**
Generalist	***M. persicae***	↓	↓
Specialist	***B. brassica***	ns	↓
	L. erysimi	ns	ns

CMV-induced resistance is able to induce two distinct pathways in Arabidopsis that affect generalist aphids (*Myzus persicae*) and specialist aphids (*Brevicoryne brassicae*, *Lipaphis erysimi*) differently. BAK1 is involved in the defence signalling that affects aphid MRGR. Whereas, BAK1-independent defence signalling appears to influence aphid reproduction. The involvement of BAK1-dependent and BAK1-independent pathways in resistance to the three aphid species test is summarised in the table above. Whether aphid performance was increased, decrease or was not significant changed is indicated by the direction of arrow, or ns for not significant.

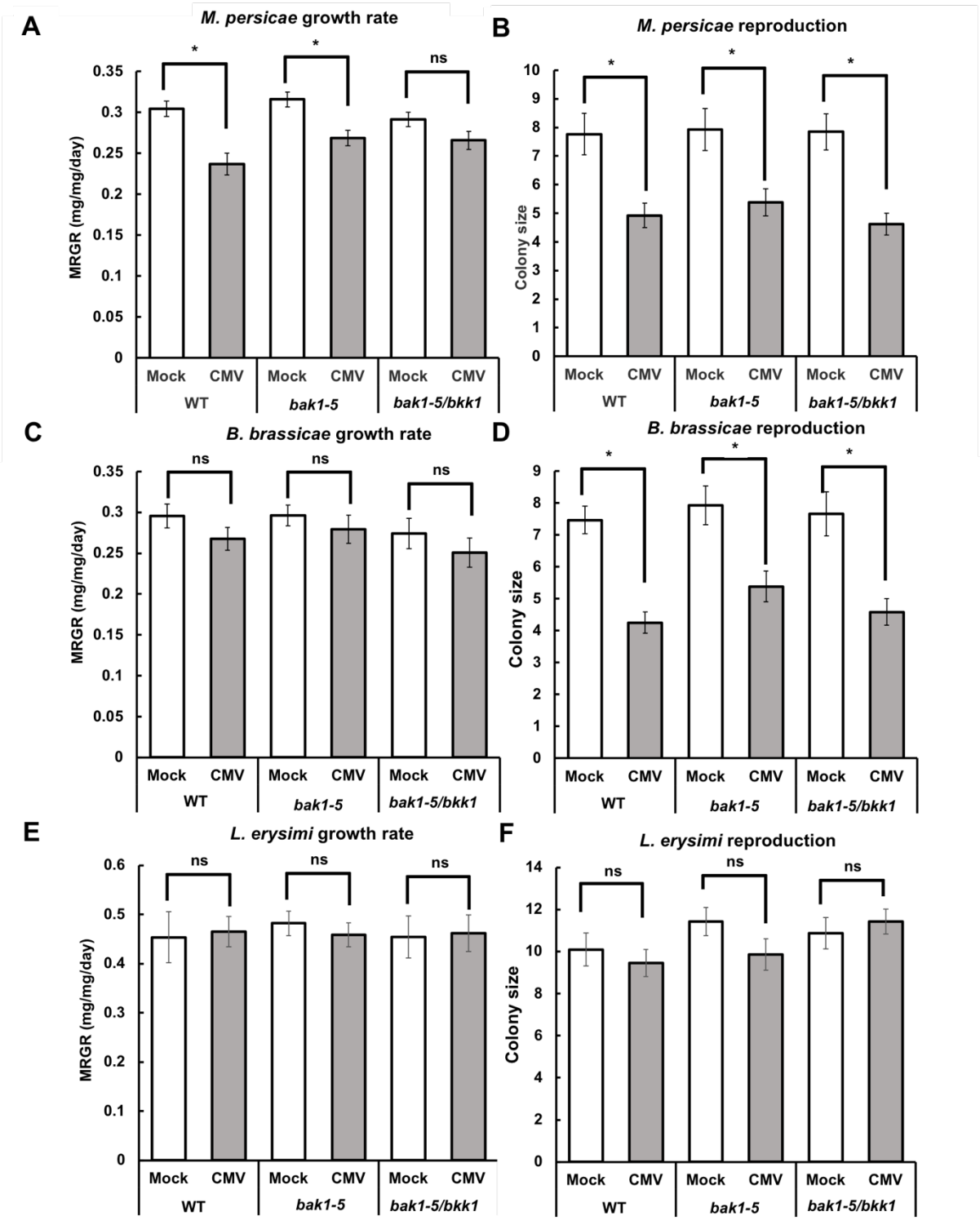

Figure 3.6. CMV-induced changes in specialist and generalist aphid performance on wild-type Arabidopsis, *bak1* and *bak1 bkk1* mutant plants.

The mean relative growth rate (MRGR) of individual aphids placed on WT Col-0, *bak1-5* and *bak1-5 bkk1* double mutants was recorded for *M. persicae* (A). *B. brassicae* (C) and *L. erysimi* (E). One-day-old nymphs were placed on Arabidopsis

mutants and allowed to feed for five days, after weighing the aphids were returned to the plant and colony size was then recorded at 10 days for *M. persicae* (B). *B. brassicae* (D) and *L. erysimi* (F). Significant differences between mock-inoculated and CMV-infected for each genotype ($P < 0.05$, Student's t-test) are marked by an asterisk, non-significant is displayed as (ns). Error bars represent standard error of the mean calculated from the measurement of 16 aphids for (A,C,E),and the mean number of aphids from 16 plants for (B,D,F).

3.2.5 Aphid performance is not affected in flg22-treated plants

BAK1 acts as a co-receptor for the receptor FLS2, and the pair activate immune signalling after perception of the 22-amino acid epitope of bacterial flagellin, flg22, a well-characterized MAMP (Chinchilla et al., 2007; Heese et al., 2007) (discussed in Section 1.4 Plant innate immunity). I previously determined that the 2a protein can induce aphid resistance in Arabidopsis. I carried out experiments to determine if the PTI defences induced by foliar application of flg22 cause resistance to aphids. As a control experiment, Arabidopsis plants were sprayed with water (mock treatment) or a solution of 1 µM flg22 1 day prior to a inoculation with virulent *Pseudomonas syringae* pv. tomato (Pst). As expected, control plants exhibited flg22-induced resistance to virulent Pst (Fig. 3.7). Arabidopsis WT Col-0, *bak1-5* and *bak1-5 bkk1* plants were sprayed with a foliar application of 1 µM flg22 one day prior to addition of a day-old nymph. I observed that the MRGR of *M. persicae* was not significantly different between mock and flg22-sprayed plants (Fig. 3.8A). This suggests that *M. persicae* is not affected by the PTI responses induced by flg22. The experiment was repeated using an increased concentration of flg22 solution (2 µM) but a similar result was observed (Fig. 3.8B).

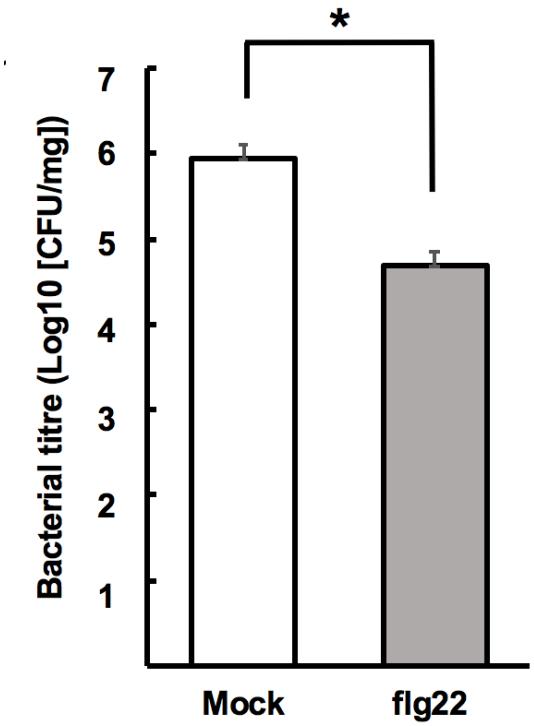

Figure 3.7. Foliar application of flg22 induces PTI in Arabidopsis.

Leaves of Arabidopsis plants were sprayed with a control treatment (water) or a 1 µM flg22 solution and 1 day later the same leaves were spray-inoculated with virulent *Pseudomonas syringae* pv. tomato (10^5 colony-forming units (CFU)/ml). Leaf tissue was sampled at 3 days post-inoculation and leaf extracts serially diluted to determine bacterial titres. There is a significant difference ($P < 0.05$, Student's t-test) between bacterial growth in control and flg22-treated plants. Error bars represent standard deviation of the mean calculated from the measurement of bacterial population from 5 plants for each treatment.

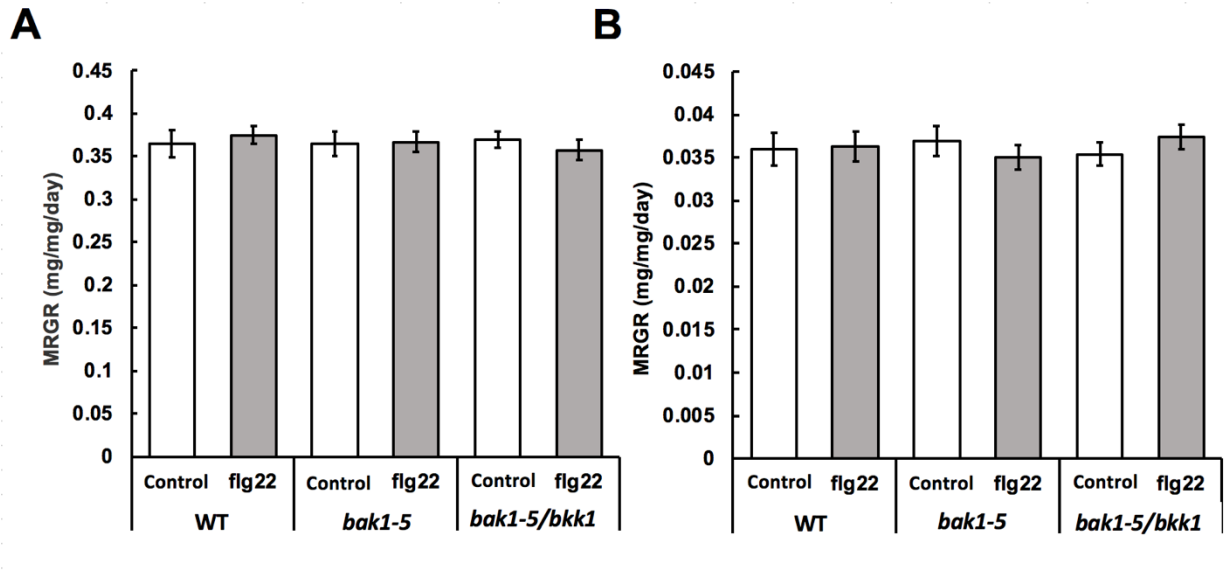

Figure 3.8. Aphid resistance is not induced by flg22 foliar application.

The mean relative growth rate (MRGR) of individual aphids placed on WT (Col-0) and on *bak1-5*, and *bak1-5 bkk1* double mutants, that had been sprayed one day prior with 1 µM (A) or 2 µM (B) of flg22 solution, or with water (Control). One-day-old nymphs were placed on Arabidopsis mutants and allowed to feed for five days. There was no significant difference between any of the treatments in both experiments (One-way ANOVA with post-hoc Tukey's tests). Error bars represent standard error of the mean, n=15 aphids for each treatment.

3.2.6 CMV infection can induce the BAK1-dependent root growth inhibition response

I prepared crude extracts of CMV-infected or mock-treated control Arabidopsis plants and compared their activities in a seedling growth-inhibition assay (Gómez-Gómez et al. 1999; Wang et al. 2010). Seedling root growth is highly sensitive to flg22. I used this assay to investigate if crude extracts of CMV-infected plants could activate the typical BAK1-dependent response of inhibited root growth after perception of PAMPs/DAMPs (Schwessinger et al., 2011). This was previously observed with three other positive-strand RNA viruses (Kørner et al., 2013) (Section 1.4.1).

I first set up an experiment using the application of flg22 to determine if CMV proteins or CMV-infected plant extract induce root growth inhibition (Fig. 3.9). Seedlings were germinated on MS medium and after one week were transferred to MS agar plates containing 10 nM or 1 µM flg22. After 3 days on flg22 containing plates seedling root growth was significantly reduced compared to seedlings grown on unamended agar plates (Fig. 3.9).

I transferred one week old Col-0 seedlings to MS agar plates containing crude extracts of CMV-infected or mock-inoculated plants and measured their root growth at 0, 3 and 5 days after transfer (Fig. 3.10). Mock-inoculated and CMV-infected extracts from WT Arabidopsis plants were purified and incorporated into the MS agar media at concentration of 0.01% (v/v) and 1% (v/v) (Kørner et al., 2013). The root growth of seedlings transferred to media containing CMV-extracts was significantly inhibited by both dilutions (Fig. 3.10).

Previous work in our lab demonstrated that crude extracts of CMV-infected *N. benthamiana* leaves inhibited root growth in both wild type and *fls2c* mutant seedlings (Groen et al., unpublished results). I wanted to investigate if BAK1 was involved in the root growth inhibition induced by CMV- infected Arabidopsis extracts. I set up a similar root growth assay using *bak1-5* and *bak1-5 bkk1* mutant seedlings (Fig. 3.11). The positive control treatment of flg22 caused root growth inhibition in

wild type seedlings, but not in the *bak1-5* or *bak1-5 bkk1* mutants as expected (Fig. 3.11). Treatment with CMV-infected Arabidopsis extracts induced root growth inhibition in WT seedlings, but *bak1-5* and *bak1-5 bkk1* mutant seedlings did not respond to CMV-infected plant extracts. These results confirmed that viral or plant components produced during CMV infection are able to induce a typical BAK1-dependent immune response.

To determine if root growth inhibition was due to plant- or virus-derived compounds I treated plants with purified CMV virions from infected *N. benthamiana* leaves (Section 2.3.2 Virus Preparation), or with plant extracts. Seedling root growth was significantly reduced when exposed to CMV-infected plant extract (Fig. 3.12). But amended MS media with highly purified CMV virions (100 ng/µl) did not induce root growth inhibition. This shows that the elicitor of root growth inhibition is produced as a results of infection but is not the CMV CP or RNA.

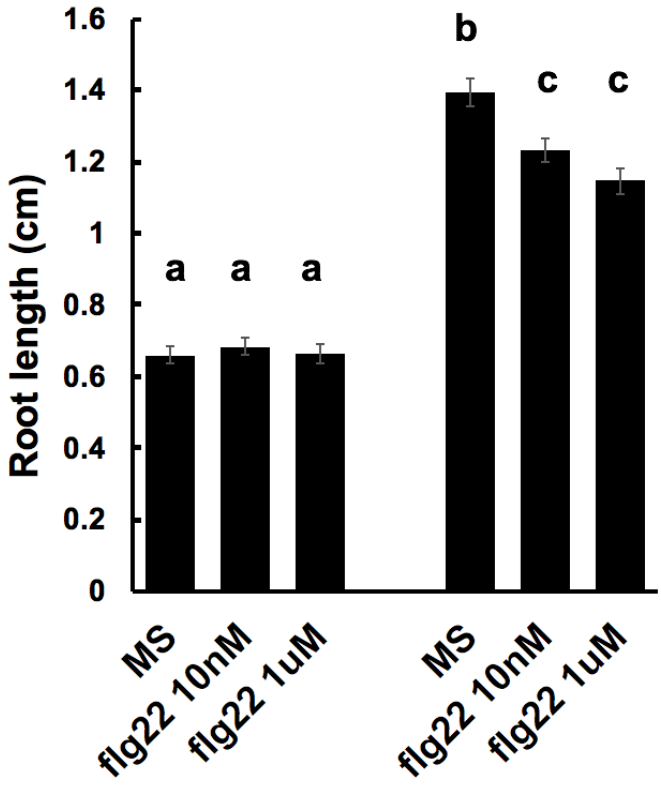

Figure 3.9. Arabidopsis root growth is inhibited by the application of PAMPs.

Arabidopsis WT seedlings were germinated on solid MS medium, after approximately one week seedlings were transferred to new MS plates containing 10 nM or 1 μM flg22. Root length was measured when seedlings were transferred to the treated plates and then 3 days later. Different letters indicate significant differences (One-way ANOVA with post-hoc Tukey's tests, $P < 0.05$). Twenty seedlings were used for each treatment group. These experiments were repeated three times with different sets of extracts and similar results were obtained.

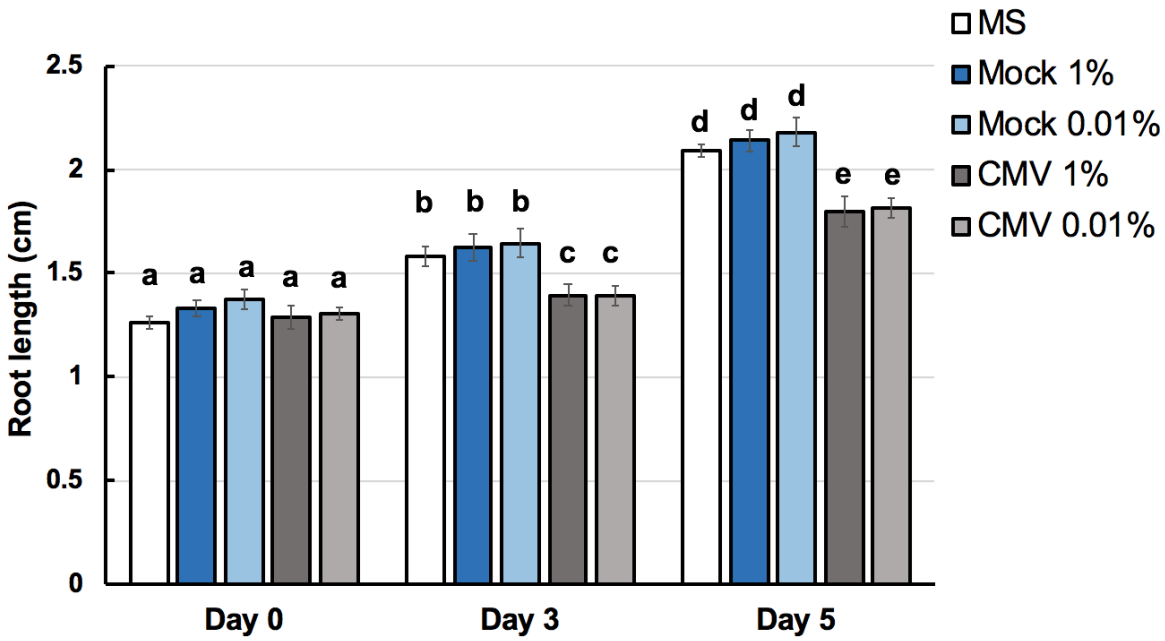

Figure 3.10. CMV-infected plant extract inhibit root growth inhibition in Arabidopsis seedlings.

Arabidopsis Col-0 seedlings were germinated on solid Murashige-Skoog (MS) medium, after one week seedlings were transferred to new MS plates containing extracts from mock- or CMV-infected plants at concentrations of 1% (v/v) or 0.01% (v/v). Root length was measured when seedlings were transferred to the treated plates (Day 0) and subsequently at 3 and 5 days after transfer. As I was only interested in differences in root growth at individual time points I carried out a one-way ANOVA to compare treatment groups at each time point. Significant differences between treatments at each time point were determined using post-hoc Tukey's test ($P < 0.05$), and significant differences indicated by different letters. Root growth of 18 and 22 seedlings was measured for each treatment. These experiments were repeated twice with different sets of extracts and similar results were obtained.

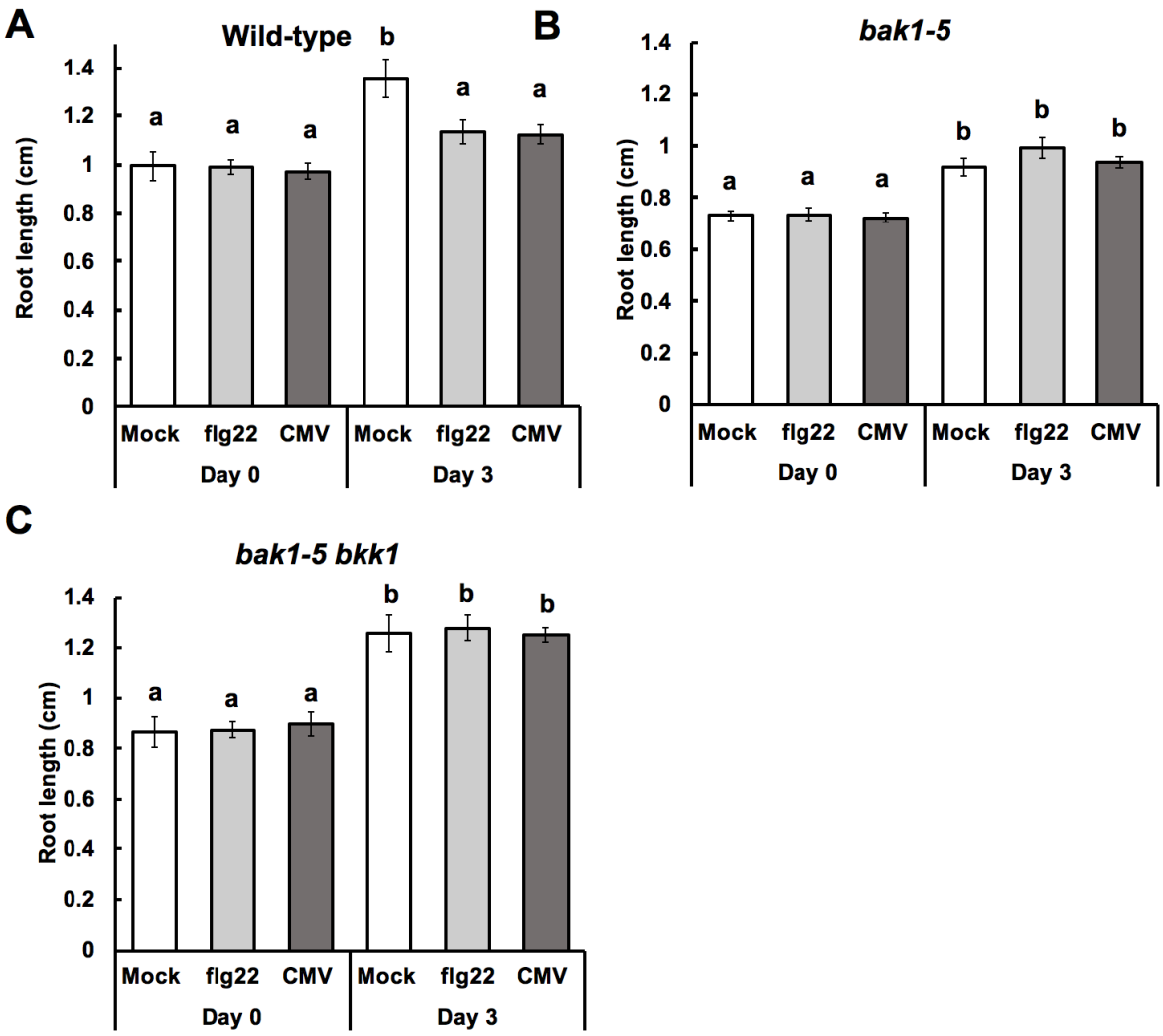

Figure 3.11. Crude extracts of CMV-infected Arabidopsis contain elicitors that induce BAK1-dependent PTI responses.

Arabidopsis wild-type (WT), *bak1-5* and *bak1-5 bkk1* seedlings were germinated on solid MS medium. After one week seedlings were transferred to new MS plates containing 1 µM flg22 or extracts from mock-inoculated (mock) or CMV-infected plants (1% v/v). Root length was measured when seedlings were transferred to the treated plates and subsequently at 3 days later. One-way ANOVA was used to compare treatment groups for each genotype (WT, *bak1-5, bak1-5 bkk1*). Significant differences between treatments for each genotype were determined using post-hoc Tukey's test ($P < 0.05$), and indicated by different letters. Root growth of between 15 and 20 seedlings was measured for each treatment.

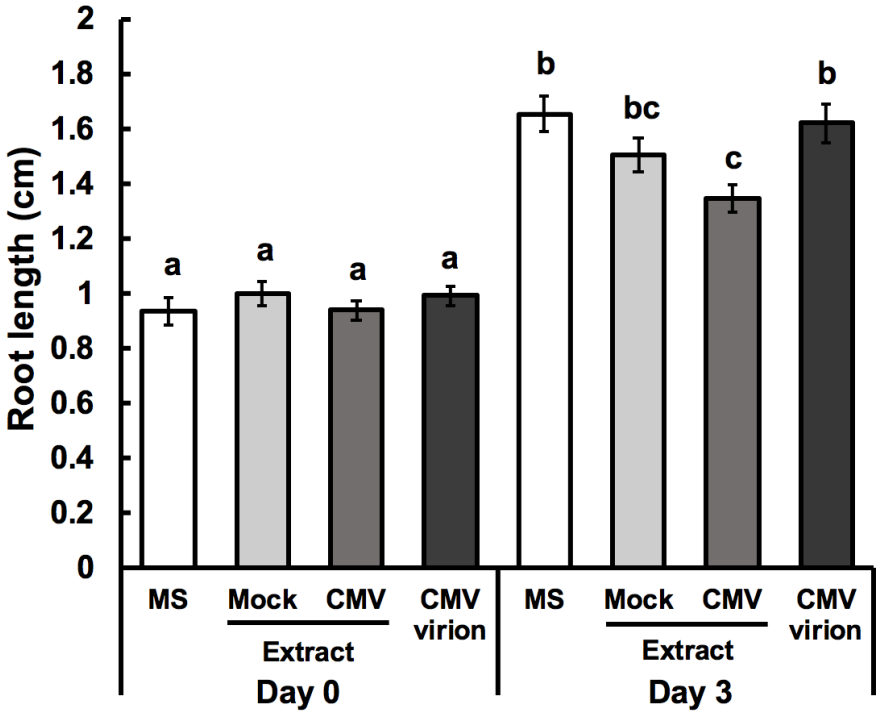

Figure 3.12. Root growth inhibition is triggered by CMV-infected plant extract and not by purified virions.

Arabidopsis WT seedlings were germinated on solid MS medium, after one week seedlings were transferred to new MS plates containing extracts from mock-inoculated and CMV-infected plants (1% v/v) or purified CMV virions (100 ng/µl). Root length was measured when seedlings were transferred to the treated plates and subsequently 3 days after transfer. Different letters indicate significant differences between treatments (One-way ANOVA with post-hoc Tukey's tests $P < 0.05$). Root growth of between 18 and 20 seedlings was measured for each treatment.

3.3 Discussion

3.3.1 The N-terminal domain of the Fny 2a protein is responsible for induction of antixenotic resistance to *M. persicae*

In this chapter, I built on previous work from our group that identified that CMV-induced anti-aphid resistance in Arabidopsis largely depends on the induction of antixenosis. This antixenosis is mediated by conversion of the indole glucosinolate, I3M, into the more effective aphid feeding deterrent 4MI3M by CYP81F2, in a mechanism that is triggered by the 2a protein (Westwood et al., 2013a). I further characterised the type of resistance induced by the 2a protein and identified the most likely regions in the 2a protein sequence responsible for inducing antixenosis.

The 2a protein sequence contains an RdRp domain located around residues 308-738 which was highly conserved between the two CMV strains, suggesting this region is unlikely to induce antixenosis. Residues 1-300 of the 2a protein contain regions of low similarity. At this point in my project I started to investigate the role of the 1a protein in suppression of 2b-induced antibiosis (discussed in Chapter 4 and 5), and a colleague took over my work on identifying which 2a protein region were responsible for inducing feeding deterrence.

This sequence analysis information I generated was used to generate a series of chimeric LS-CMV containing regions of Fny-RNA 2 (Rhee et al., in preparation). These chimeric viruses were used to inoculated Arabidopsis plants which were used in aphid performance assays. It was observed that residues 200-300 of the Fny 2a protein were crucial in inducing aphid resistance. There are 27 amino acid variations between the Fny and LS 2a protein sequence in the 200-300 region.

Work carried out by my colleague Dr Sun-Ju Rhee mapped each mutation and determined that the valine at position 237 in the Fny-CMV 2a protein sequence plays a role in the induction of antixenosis against aphids in CMV-infected *A. thaliana*. The replacement of isoleucine at this position in the LS-CMV 2a protein sequence with valine had a marked effect on aphid performance which was initially

surprising since both amino acids have hydrophobic side chains, making the $I_{237}V$ replacement conservative relative to some of the other sequence replacements.

It remains unknown how valine residue 237 of the Fny-CMV 2a protein might induce antixenosis against aphids in *A. thaliana*. The working hypothesis concluded from this research is that this residue may directly or indirectly facilitate an interaction between the Fny-CMV 2a protein with a host factor involved in either defensive signalling, or in the regulation of metabolism, leading to increased production of 4MI3M and/or other compounds that influence aphid feeding behaviour.

3.3.2 Determining the role of BAK1 in CMV-induced aphid resistance

Previous studies observed that mutants in BAK1 displayed increased susceptibility to three different RNA viruses, ORMV, TMV, and TCV (Korner et al., 2013). However, BAK1 is not only important for regulation of innate immunity but also involved in cell-death control and brassinosteroid (BR) signalling, a phytohormone important for plant growth (Li et al. 2002; Wang et al. 2008). My results show that certain host or viral factors are either directly or indirectly recognised by the PTI surveillance system in a BAK1-dependent manner.

To exclude the possibility that the increased susceptibility of *bak1-4* mutants (knockout mutants) to RNA viruses results from an impairment in BR signalling, I used the *bak1-5* mutant in aphid performance assays (Schwessinger et al. 2011). The *bak1-5* mutant contains a point mutation in a single amino acid that disrupts its role in defence responses. It is impaired in FLS2-dependent PTI signalling but it is not impaired in cell death control and in BR signalling (Roux et al., 2011; Schwessinger et al., 2011). I observed that *M. persicae* reared on CMV-infected *bak1-5* plants the MRGR, although slightly reduced, was not significantly different compared to aphids on control *bak1-5* plants (Fig. 3.6A).

Although aphid MRGR was not significantly reduced on infected *bak1-5* plants, aphids produced significantly less progeny on CMV-infected *bak1-5* plants

compared to aphids on control *bak1-5* plants (Fig. 3.6B). However, in one repeat of this experiment I observed that aphid MRGR was significantly reduced on CMV-infected *bak1-5* plants compared to control *bak1-5* plants (Fig. 3.6C). However, it is likely that the *bak1-5* seed stocks used in our lab at this time were contaminated with WT plants. Subsequent work in our group has since isolated pure *bak1-5* lines. These lines were then used to demonstrate that CMV-induced anti-aphid resistance is not observed in *bak1-5* plants (Groen et al., unpublished results).

Testing the role of BKK1 in the absence of BAK1 is normally hindered by the fact that the double *bak1 bkk1* mutants show constitutive activation of cell death (He et al., 2007). As I used the *bak1-5* allele, this mutation does not impaired in BR signalling and that does not confer deregulated cell death when combined with *bkk1* mutations (Schwessinger et al., 2011). We previously observed that CMV-induced anti-aphid resistance was still present in the *bak1-4* and *bkk1-1* mutants (Groen et al., unpublished results). Therefore, due to space and time limitations I did not include these mutants in my experiments. Instead I continued to focus on the *bak1-5* and *bak1-5 bkk1* mutant plants. The *bak1-5 bkk1* double mutant was impaired in CMV-induced aphid resistance (Fig. 3.6C).

My results discussed here and recent work from our group has led to the hypothesis that there are two parallel defensive signalling pathways induced by CMV in Arabidopsis which affects aphid performance. The first pathway appears to affect aphid growth rate (shorter term) which involves BAK1. The second pathway affects aphid fecundity (longer term) which involves JA signalling.

3.3.3 Aphid performance is not affected in flg22 treated plants

In transcriptome experiments CMV induced transcripts overlapped with typical PTI responses triggered by PAMPs (flg22, elf26, and chitin) (Westwood et al., 2013a). I induced a PTI response in Arabidopsis plants with application of flg22. There was no effect on aphid MRGR. This initially suggested that the PTI responses induced by CMV might not affect aphids. However, as BAK1 is required for the pathway that regulates defences that affect aphid MRGR it suggests the PTI response during

virus infection is either stronger, or that additional defences are required. In this work I did not investigate if flg22 application combined with virus infections leads to a potentiated defence response. Future work should investigate if flg22 application to virus-infected plants induces a stronger defence response when compared to control virus-infected plants. This may lead to a primed defence response and which may help in characterising if PTI is induced during CMV infection.

I observed that Arabidopsis root growth inhibition is triggered by a extracts from virus infected plants. This was also dependent on functional BAK1 signalling. This suggests BAK1 is able to perceive an extracellular viral PAMP or DAMPs produced as a consequence of infection. BAK1 is required for the establishment of PTI by ligand-induced heteromerization with surface-localised PRRs. Characterised PRRs that require BAK1 for signalling include FLS2, EFR, and PEPR1/PEPR2 (Chinchilla et al., 2007; Heese et al., 2007; Krol et al., 2010; Roux et al., 2011). We previously observed that CMV-infected plant extracts still induced PTI responses in *fls2* mutants plants (Groen et al., unpublished results). We have not tested whether *pepr1 pepr2* mutant plants respond to CMV-infected plant extracts. Previously it was observed that there was no difference in susceptibility of *pepr1 pepr2* double mutants to TCV infection, and AtPep signalling was not involved in resistance to TCV (Kørner et al., 2013). But in the case of CMV, BAK1 appears to not contribute against resistance to CMV. CMV replication in *bak1* and *bkk1* single and combinatorial mutants showed no alterations in CMV accumulation compared to wild type plants (Groen et al., unpublished results). Overall my results suggest that BAK1 is not involved in resistance to CMV, but is involved in perceiving CMV infection. Currently, we do not know if BAK1 is involved in directly recognising CMV, or indirectly by responding to DAMPs produced by viral infection. It would be interesting to explore the role of BAK1 in CMV recognition by using extracts from 2a-transgenic plants, or purified viral proteins. If root growth inhibition can be observed after application of purified viral proteins then it may suggest that CMV is recognized by a yet-unknown BAK1-dependent receptor.

Chapter 4. The CMV 1a protein interacts with the 2b protein and regulates the induction of antibiosis in Arabidopsis

4.1 Introduction

In Arabidopsis, CMV infection triggers antixenosis in a process mediated by the interplay of three viral proteins (1a, 2a and 2b) (Westwood et al., 2013a). The 2b protein influences host-aphid interactions in a number of host species (Westwood, 2013, 2014; Wu et al., 2017; Ziebell et al., 2011). In tobacco, the 2b-deficient mutant (CMVΔ2b) induces antibiosis resulting in increased aphid mortality (Ziebell et al., 2011). In tobacco, the 1a protein is the factor that triggers antibiosis, but during infection with wild-type CMV induction of antibiosis is counteracted by the 2b protein (Tungadi et al., 2020; Ziebell et al., 2011). The Fny-CMV 2b protein appears to have the opposite effect in Arabidopsis. Constitutive expression of the Fny-CMV 2b protein in transgenic Arabidopsis plants induces antibiosis and developmental abnormalities (Lewsey et al., 2007; Westwood et al., 2013a). In Arabidopsis, AGO1 negatively regulates antibiosis. Inhibition of AGO1 by the Fny-CMV 2b protein prevents AGO1 from targeting mRNAs, leading to the induction of antibiosis (Kettles et al., 2013; Westwood et al., 2013a).

Previous work in our group investigating 2b-induced antibiosis in Arabidopsis (Westwood et al., 2013a), led me to hypothesise that the 1a protein and 2b protein interact either directly or indirectly. I initially generated fluorescently tagged 1a, 2a and 2b proteins to observe changes in localisation resulting from interactions

between combinations of proteins. I subsequently generated BiFC constructs and carried out co-immunoprecipitation assays to confirm direct interactions.

4.2 Results

4.2.1 The CMV 1a protein inhibits 2b-induced resistance to aphid colony growth

Westwood and colleagues (2013) showed that the MRGR of aphids confined on *2b*-transgenic plants was significantly reduced, but antibiosis was not induced when aphids were reared on doubly transformed *1a/2b*-transgenic plants. I observed that another aphid performance indicator (aphid reproduction) was also negatively affected when aphids were confined on transgenic plants expressing the 2b protein (Fig. 4.1). Aphid colony growth on *2b*-transgenic plants was significantly decreased compared to colony growth on non-transgenic plants, but no reduction of colony growth occurred on *1a*-transgenic plants or on double *1a/2b*-transgenic plants (Fig. 4.1). This shows that 2b-induced antibiosis affects not only decreases the MRGR of individual aphids but also their ability to reproduce, and that the 1a protein is able to inhibit 2b-induced antibiosis.

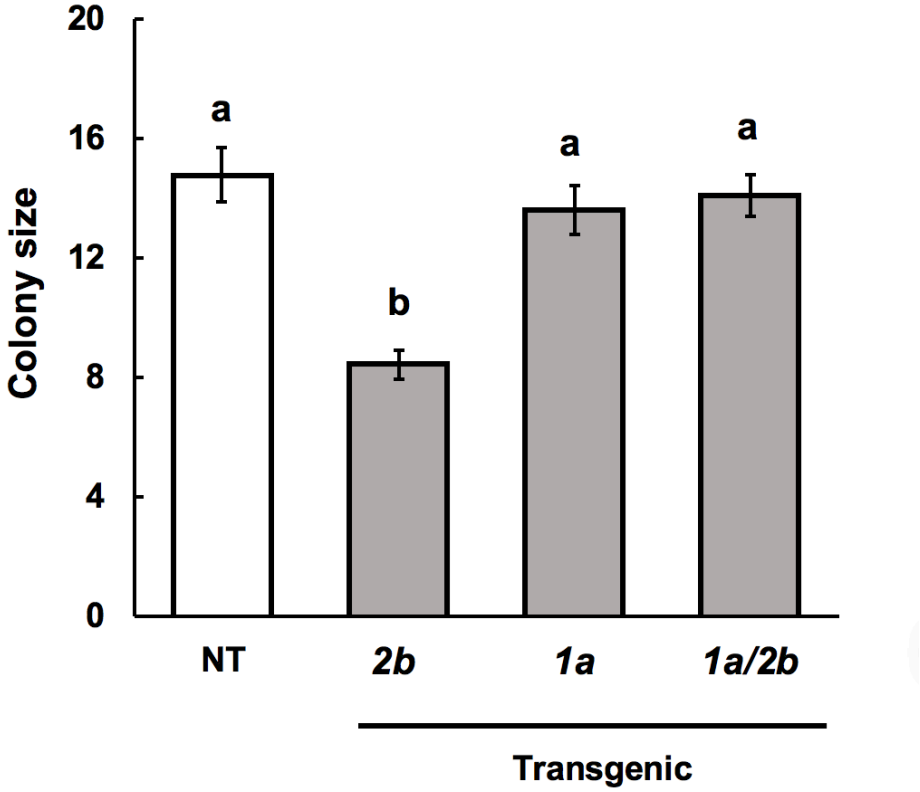

Figure 4.1. Aphid colony growth on transgenic Arabidopsis plants expressing the 1a and 2b proteins.

Individual one-day-old *M. persicae* nymphs were placed on plants and number of offspring (colony size) counted at 10 days post-infestation. Aphids were placed on plants that were: non-transgenic (NT) or transgenic plants expressing the CMV 2b protein, the CMV 1a protein or both. Different letters are assigned to significantly different groups (One-way ANOVA with *post-hoc* Tukey's tests, $P<0.05$). Error bars represent standard error of the mean, calculated from mean colony sizes from 16 plants per treatment.

4.2.2 Subcellular localisation of 1a, 2a and 2b CMV proteins

The aphid performance assays carried out on transgenic plants (Fig. 4.1), led me to investigate the possibility that the 1a protein and 2b protein proteins interact with each other either directly, or indirectly, for example by competing for binding to a cellular factor such as AGO1. To determine if a direct 1a-2b protein-protein interaction was likely, I studied the subcellular distribution of the 2b or 1a protein that were fused with either GFP or RFP (described in Section 2.5.6). Fusion proteins were expressed transiently in *N. benthamiana* leaves by agroinfiltration, and fluorescence was imaged by confocal laser scanning microscopy. The 2b-RFP protein was generated by fusing the 2b protein C terminus with RFP, and GFP-2b by fusion of GFP to the N terminus of the 2b protein. Consistent with previous investigations (González et al., 2010), 2b-RFP and GFP-2b were observed in the nucleus and cytoplasm (Fig. 4.2A,B).

Fluorescently tagged versions of the 1a protein were made with N-terminal fusions with either RFP (RFP-1a) or GFP (GFP-1a). Both RFP-1a and GFP-1a aggregated as punctate ‘specks’ (Fig. 4.2C,D). These specks consisted of individual foci that also clustered to form larger aggregations. Some of the 1a aggregates, as well as the smaller 1a foci appeared to associate close to the cell membrane (Fig. 4.2C, left panel). To determine if the 1a protein associated with intracellular membranes the styryl membrane-binding dye FM-4-64 was used to stain leaf tissue agroinfiltrated with GFP-1a. Despite the fact that in several experiments, GFP-1a foci were observed close to the cell membrane, there was no strong indication of co-localisation between the larger 1a protein aggregates and FM-4-64 dye (Fig. 4.2E). To determine if larger GFP-1a aggregations corresponded to ER-derived vesicles, leaves agroinfiltrated with GFP-1a were stained with the dye, ER-tracker (Fig. 4.2E). No co-localisation was observed between the GFP-1a and ER-tracker, indicating that the 1a protein aggregations are not localised to ER-derived vesicles.

The 2a protein was fused at its C-terminus to RFP (2a-RFP) or GFP (2a-GFP). Both 2a-RFP and 2a-GFP seemingly accumulated in the nucleus and cytoplasm (Fig. 4.3). This localisation pattern differed from previous reports, which did not detect 2a

in the nucleus (Cillo et al., 2002). When 2a-GFP was co-expressed with RFP-1a, RFP-1a still localised to ‘specks’ in the cytoplasm. The 2a-GFP signal still showed nuclear and cytoplasmic localisation, but also colocalised with 1a to cytoplasmic ‘specks’ (Fig. 4.3).

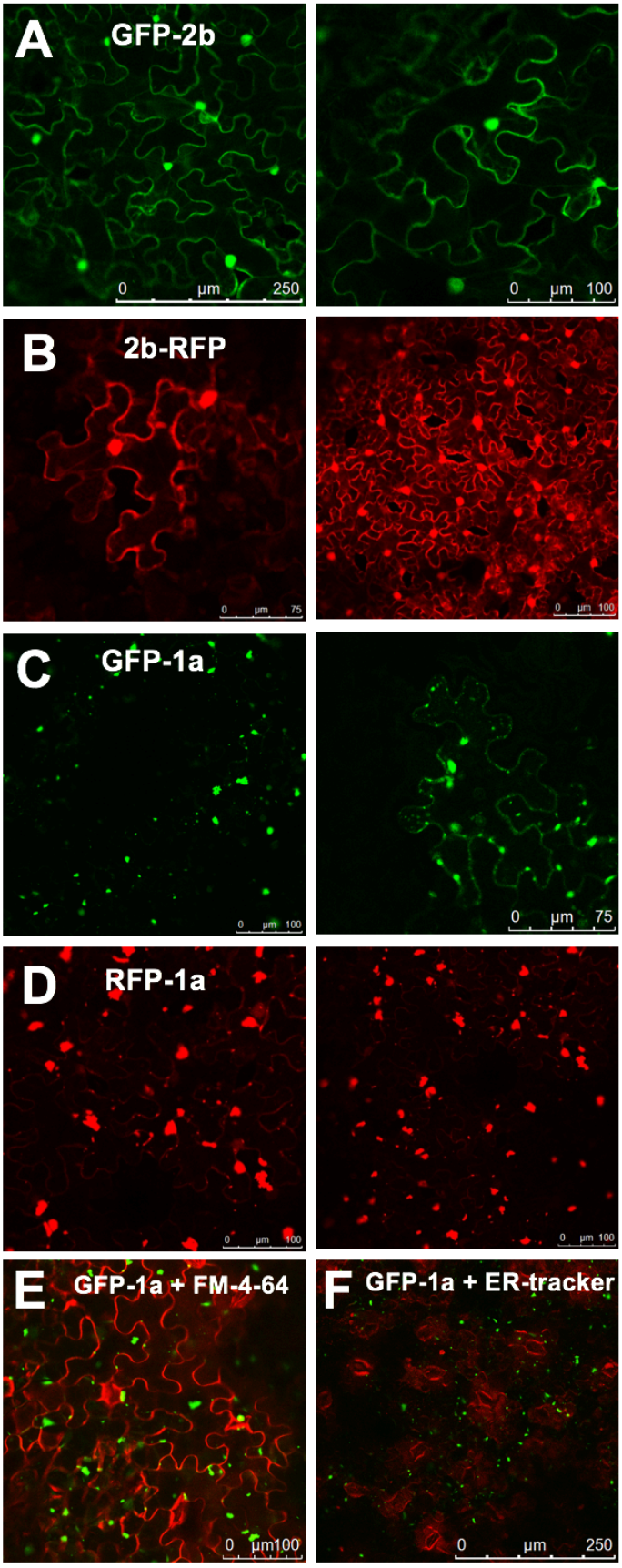
A
GFP-2b
0 µm 250
0 µm 100
B
2b-RFP
0 µm 75
0 µm 100
C
GFP-1a
0 µm 100
0 µm 75
D
RFP-1a
0 µm 100
0 µm 100
E
GFP-1a + FM-4-64
0 µm100
F
GFP-1a + ER-tracker
0 µm 250

Figure 4. 2. Subcellular localisation of the CMV 1a and 2b proteins**.**

The GFP- and RFP-1a protein fusions were expressed in *N. benthamiana* leaves by agroinfiltration and images recorded 3-4 days later by confocal laser scanning microscopy. Consistent with previous investigations of the Fny-CMV 2b protein (Du et al., 2014a; González et al., 2010), GFP-2b (A) and 2b-RFP (B) accumulated in the nuclei and cytoplasm. In contrast, GFP-1a (C) and RFP-1a (D) accumulated as punctate specks of varying size. At higher magnification (C, right panel) GFP-1a accumulation at the cell periphery could be observed. However, staining with a membrane-binding dye (FM-4-64) indicated that the larger GFP-1a aggregations did not co-localise with the cell membrane (E). Staining with ER-tracker (F) did not indicate co-localisation of GFP-1a with the endoplasmic reticulum network.

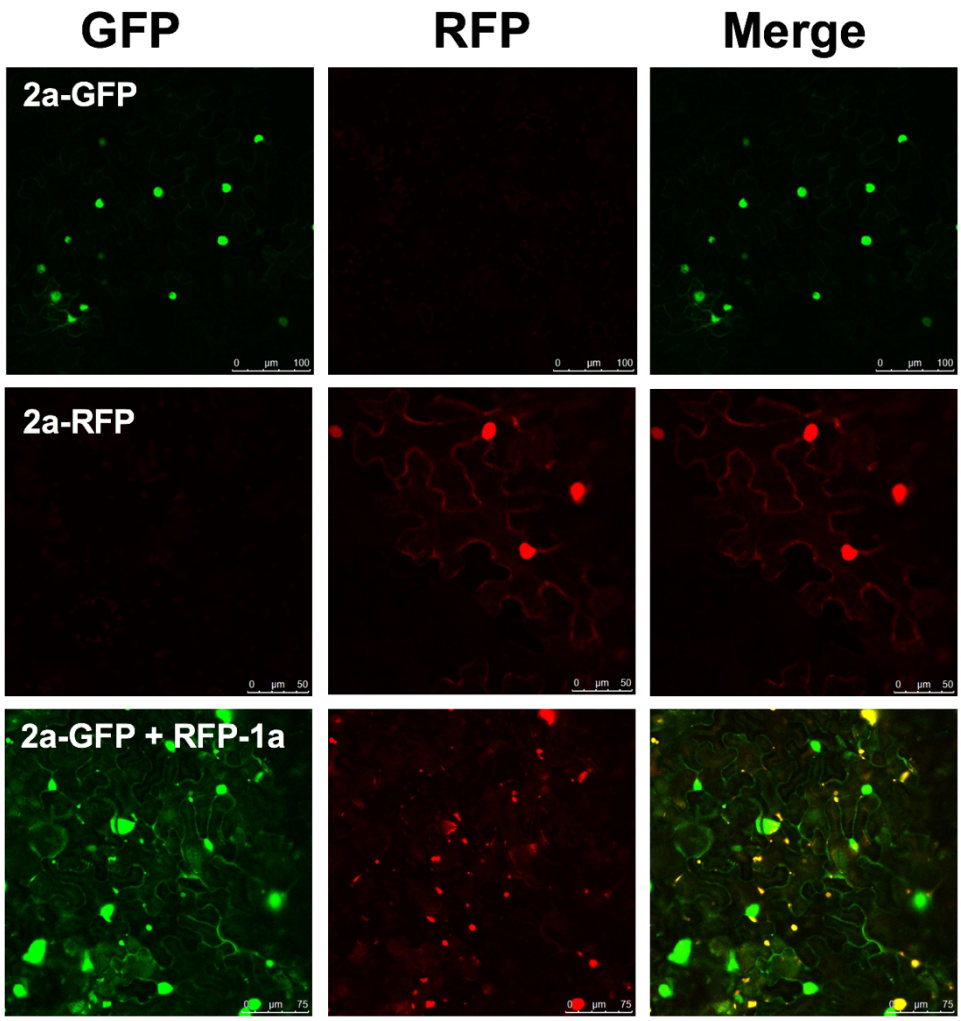

Figure 4.3. The 1a protein alters the localisation of the 2a protein observed using confocal microscopy.

Fluorescence derived from CMV 2a protein tagged at its C-terminus with GFP or RFP showed a similar pattern of localisation observed from GFP-2b or 2b-RFP (Fig. 4.2), localising to both the nucleus and cytoplasm. When 2a-GFP and RFP-1a were co-expressed (lower panel), the localisation of 2a-GFP was altered. Fluorescence originating from RFP-1a accumulates at ‘specks’ similar to those seen when the 1a protein was infiltrated by itself (Fig. 4.2). Fluorescence derived from 2a-GFP still localised to the nucleus and weekly to the cytoplasm but showed a change in localisation in the presence of 1a, which causes it to colocalise with 1a to the characteristic ‘specks’ reported earlier.

4.2.3 The 1a protein localises to P-bodies

The orthologous 1a protein of brome mosaic virus (BMV) associates with cytoplasmic processing bodies (P-bodies) (Beckham et al., 2007). I hypothesised that the CMV 1a protein may also associate with P-bodies, which would be consistent with the punctate distribution of the 1a protein (Fig. 4.2C,D). *A. tumefaciens* cells harbouring the RFP-1a construct were co-expressed with the P-body marker DCP1-GFP. When infiltrated individually, DCP1-RFP and DCP1-GFP formed punctate specks (Fig. 4.4A). When DCP1-GFP was co-expressed with RFP-1a the two proteins were observed to strongly co-localise (Fig. 4.4B). Thus, a large portion of RFP-1a protein appears to associate with P-bodies.

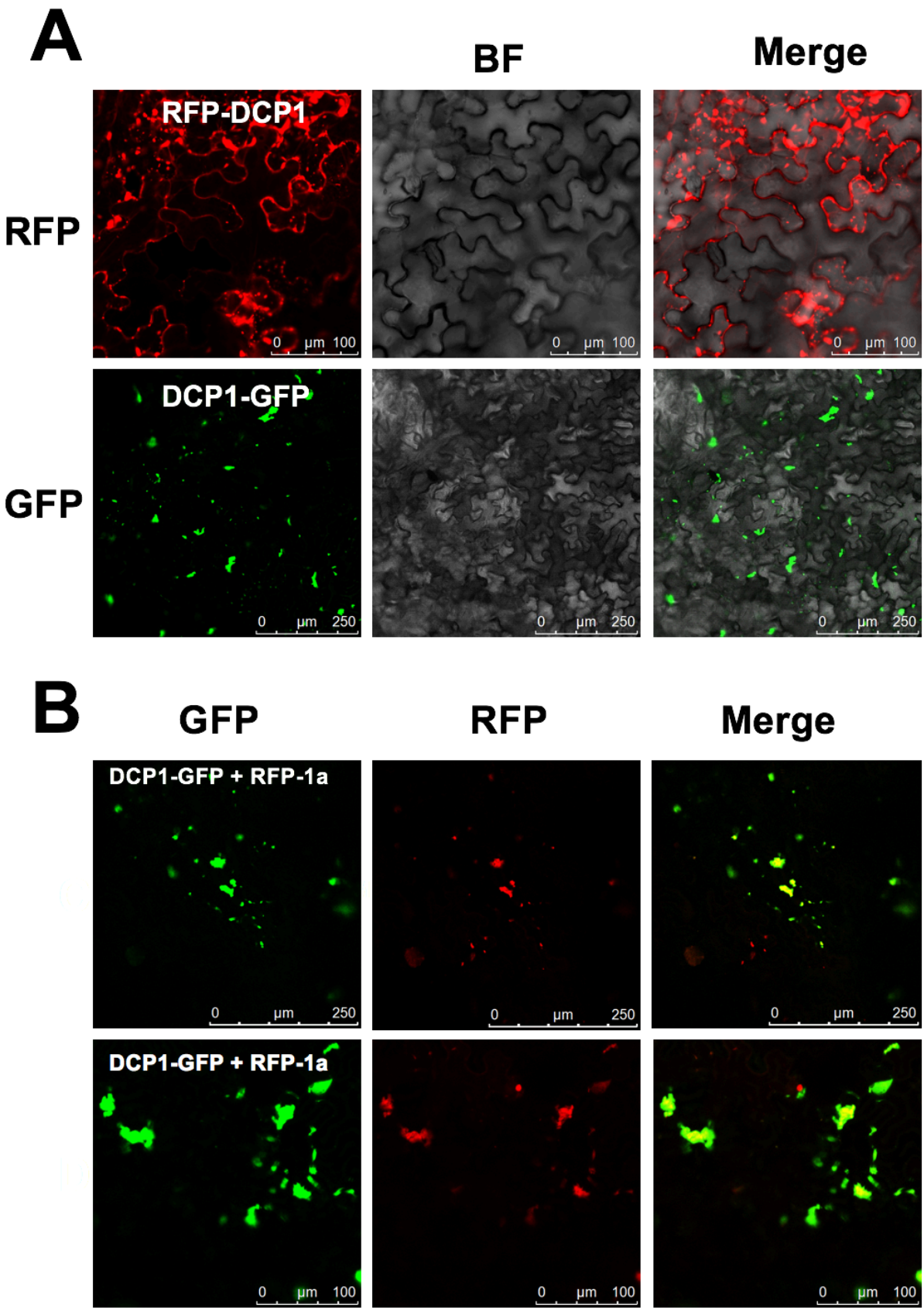
A
BF
Merge
RFP
RFP-DCP1
GFP
DCP1-GFP
0 µm 100
0 µm 250
B
GFP
RFP
Merge
DCP1-GFP + RFP-1a
DCP1-GFP + RFP-1a
0 µm 250
0 µm 100

Figure 4.4. The P-body marker DCP1 colocalises with the 1a protein.

Agroinfiltrated *N. benthamiana* leaves were imaged by confocal microscopy. A, Fluorescence from DCP1-GFP was observed as punctate specks with varying size. The localisation pattern of DCP1-GFP resembled that of GFP/RFP-1a. RFP-DCP1 fluorescence was brighter than DCP1-GFP and much more visible throughout the cell. RFP-DCP1 could be observed in small foci associated with the periphery of the cell, presumably P-bodies. B, When RFP-1a was co-expressed with DCP1-GFP strong co-localisation between DCP1 and the 1a protein was observed.

4.2.4 The 1a protein redistributes the 2b protein

To assess if the localisation of the 2b or 1a protein is altered when both viral proteins are present *in vivo*, 2b and 1a proteins with different fluorescent tags were co-expressed into *N. benthamiana* leaves. When agroinfiltrated singly, fluorescence due to GFP-2b or 2b-RFP proteins accumulated in the cytoplasm and nucleus (Fig. 4.5A,B). However, when co-expressed with 1a protein, the 2b proteins also co-localised to the fluorescent 'specks' (Fig. 4.5C,E) observed for GFP-1a protein localisation (Fig. 4.5D). When the RFP-1a construct was co-expressed with a construct encoding free, unfused GFP (35S:GFP), I did not observe re-localisation of free GFP to the sites where RFP-1a fluorescence accumulated (Fig. 4.6). Thus, 1a-2b co-localisation is specific and does not occur as a result of non-specific binding of GFP to the 1a protein.

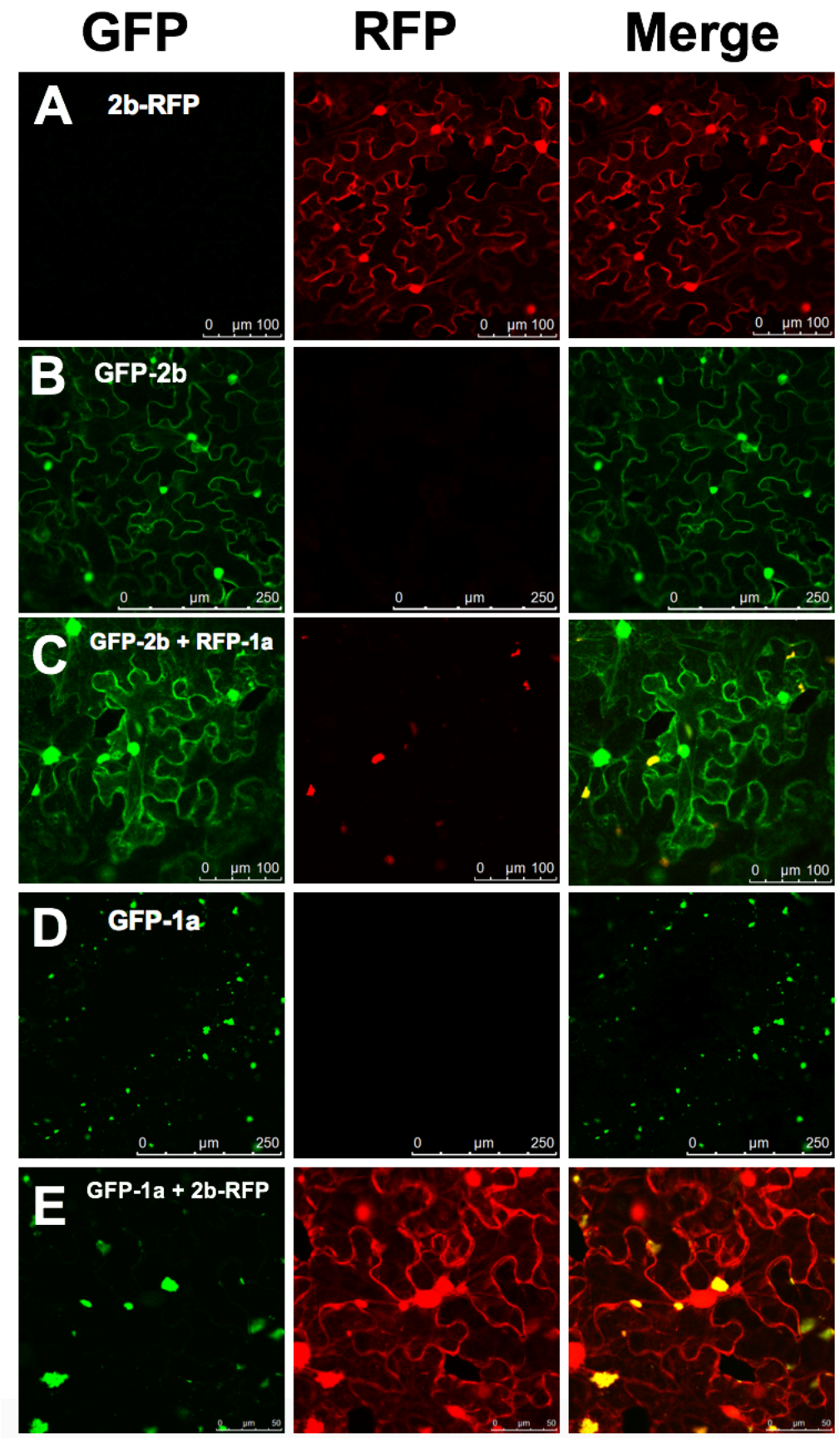
GFP
RFP
Merge
A
2b-RFP
B
GFP-2b
C
GFP-2b + RFP-1a
D
GFP-1a
E
GFP-1a + 2b-RFP
0 µm 100
0 µm 250
0 µm 50

Figure 4.5. The subcellular localisation of the 2b protein is altered by the 1a protein.

Agroinfiltrated tissue was observed using confocal microscopy. A, fluorescence derived from the 2b protein tagged at its N-terminus with GFP or C-terminus with RFP (B). C, fluorescence originating from RFP-1a proteins accumulates at small 'specks' throughout the cytoplasm and as larger aggregates. Fluorescence originating from the GFP-2b proteins accumulated at the nucleus and evenly throughout the cytoplasm, as seen in panel B, but a portion of the signal was observed to be present in the same cellular compartment as RFP-1a signal yielding a merged signal shown as yellow. D, 1a protein tagged at its N-terminus with GFP expressed alone appeared as aggregates and smaller foci. E, fluorescence derived from CMV 2b protein tagged at its C-terminus with RFP and 1a protein tagged at its N-terminus with GFP. The 2b-RFP protein can be observed in the nucleus and cytoplasm, but was additionally present in specks that strongly co-localise with GFP-1a. This pattern of 1a and 2b co-localisation is similar to C suggesting that the localisation of 1a and 2b proteins is not biased by the presence of either GFP or RFP sequences.

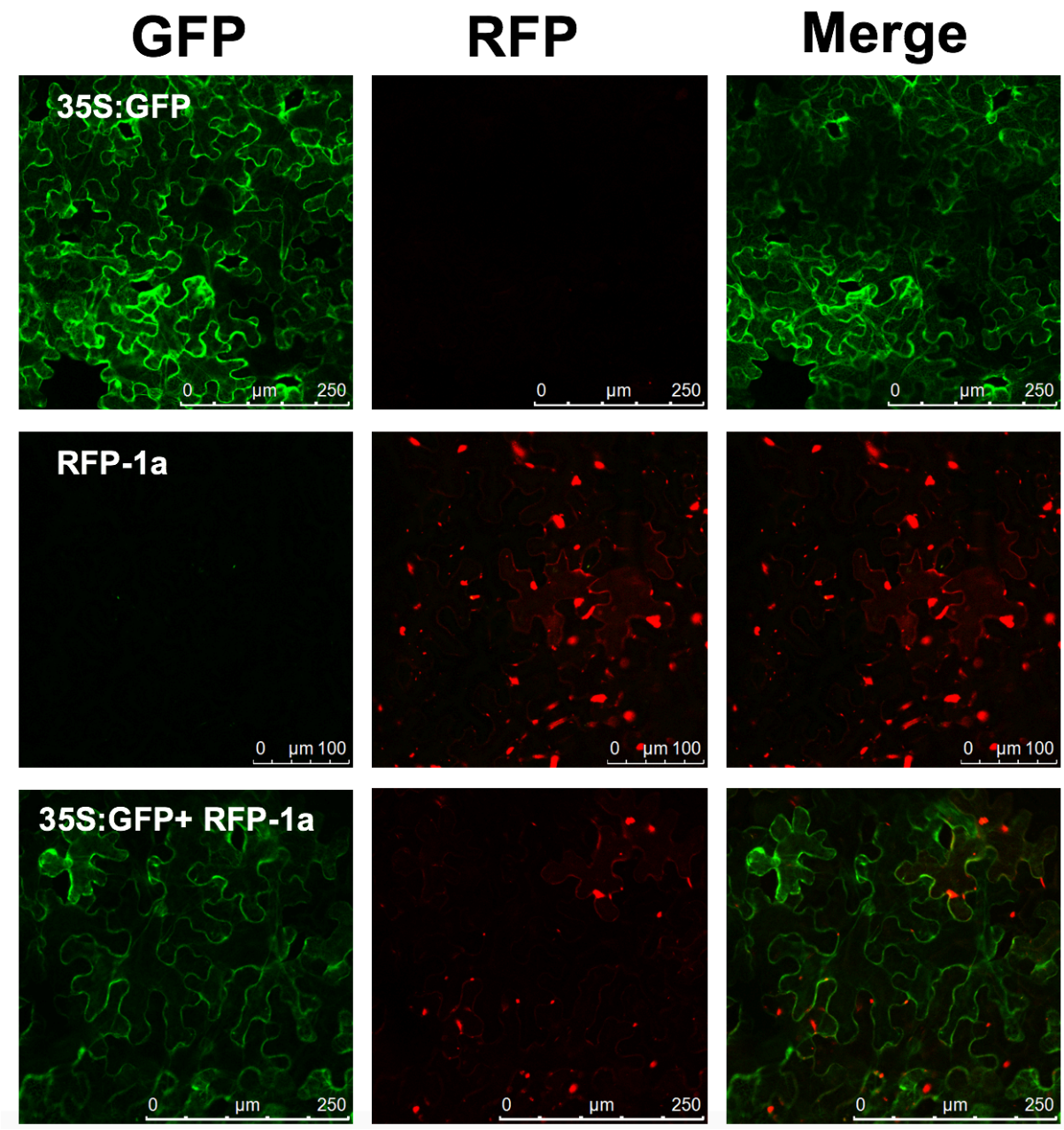

Figure 4.6. The 1a protein does not alter the localisation of GFP.

Agroinfiltrated tissue was observed by confocal microscopy. When expressed in *N. benthamiana* GFP accumulates in the cytoplasm. When RFP-1a and 35S:GFP were co-expressed I did not observe re-localisation of GFP to the sites where RFP-1a fluorescence accumulated. Thus, 1a-2b co-localisation is specific and does not occur as a result of non-specific binding of GFP to the 1a protein.

4.2.5 The 1a protein interacts directly with the 2b protein but not with AGO1 in bimolecular fluorescence complementation assays

To visualise potential protein-protein interactions *in vivo,* 2a, 2b, 1a and Arabidopsis AGO1 protein-coding sequences were fused with sequences encoding the yellow fluorescent protein (YFP) split into the N- and C-terminal portions (sYFPn and sYFPc, respectively) for bimolecular fluorescence complementation (BiFC) assays.

Using yeast two-hybrid assays and deletion mutants it was previously shown that the N-terminal regions of the CMV and BMV 1a proteins self-interact (O'Reilly et al., 1998). I confirmed self-interaction for the 1a protein (Fig. 4.7A), although the fluorescence intensity was not as great as the 2b-2b self-interaction (Fig. 4.8A). The 1a-2a protein interaction is required for formation of an active replicase complex (O'Reilly et al., 1998; Kim et al., 2002). I previously observed that the 1a and 2a proteins colocalise (Fig. 4.3). I confirmed the 1a-2a protein interaction by co-agroinfiltration of sYFP-1a and sYFP-2a constructs, which resulted in observable fluorescence that was localised to regularly sized small foci (Fig. 4.7B). For the 1a-2a protein interaction, fluorescence was distributed evenly around the cell periphery, likely following the tonoplast outline where the 1a and 2a proteins have previously been shown to localise by immunogold labelling (Cillo et al 2002). When sYFP-1a and sYFP-AGO1 were co-expressed no YFP fluorescence was observed, suggesting that the 1a protein and AGO1 do not directly interact.

Fluorescence derived from the reconstitution of the YFP fluorophore after sYFPn-2b and sYFPc-2b self-interaction localised to the nucleus and cytoplasm (Fig. 4.8A). This pattern of fluorescence was similar to that observed with GFP-2b and 2b-RFP (Fig. 4. 2A,B) and consistent with previous studies using sYFP-2b (González *et al*., 2010). The distribution of fluorescence for sYFP-2b changed following co-agroinfiltration of untagged 1a protein (Fig. 4.8B) with fluorescence still visible in the nucleus and cytoplasm, but was additionally present at the 'specks' previously observed with GFP/RFP-1a (Fig. 4.2C,D).

BiFC with sYFPn-1a with sYFPc-2b constructs were used to determine if the 1a and 2b proteins interact directly. Strong fluorescence was observed that localised as 'specks' (Fig. 4.8C), showing a similar pattern of fluorescence to that seen with GFP-1a and RFP-1a (Fig. 4.2C,D). The punctate specks observed for sYFPn-1a/sYFPc-2b interaction are hypothesised to be P-bodies. Fluorescence was not observed when the sYFP halves were swapped at the N-terminal of the 1a and 2b fusion proteins (sYFPc-1a/sYFPn-2b) (Fig. 4.8D), suggesting that the interaction of 2b with the 1a protein reconstitutes the YFP protein in certain conformations. The distribution of fluorescence occurring from the sYFPn-1a/sYFPc-2b interaction was distinct from the 1a-2a protein localisation pattern (Fig. 4.7B). This indicates that the interaction between the 1a and 2b proteins occurs in a different subcellular location than that of replicase complex formation on the tonoplast.

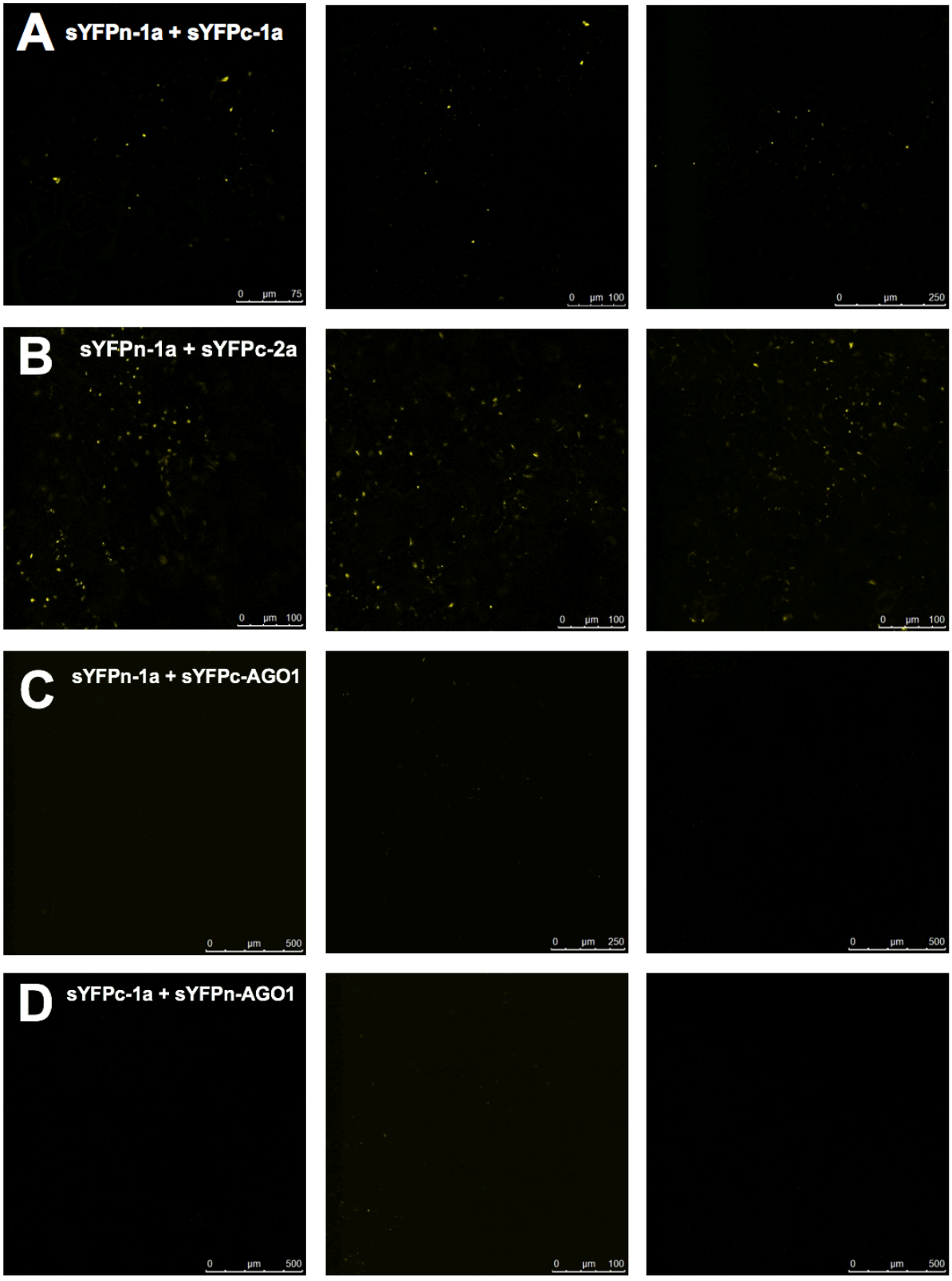
A
sYFPn-1a + sYFPc-1a
0 µm 75
0 µm 100
0 µm 250
B
sYFPn-1a + sYFPc-2a
0 µm 100
0 µm 100
0 µm 100
C
sYFPn-1a + sYFPc-AGO1
0 µm 500
0 µm 250
0 µm 500
D
sYFPc-1a + sYFPn-AGO1
0 µm 500
0 µm 100
0 µm 500

Figure 4. 7. The sYFP-1a protein interacts with itself and the 2a protein but not with AGO1 in BiFC assays.

Agroinfiltrated tissue was observed using confocal microscopy. A, when sYFPn-1a and sYFPc-1a where co-expressed I observed foci of faint fluorescence. B, I observed small foci of fluorescence when sYFPn-1a and sYFPc-2a where co-expressed, this was expected as these proteins form the viral replicase. C, D, when sYFP-1a and sYFP-AGO1 where co-expressed no fluorescence was observed suggesting that these proteins do not interact *in vivo*.

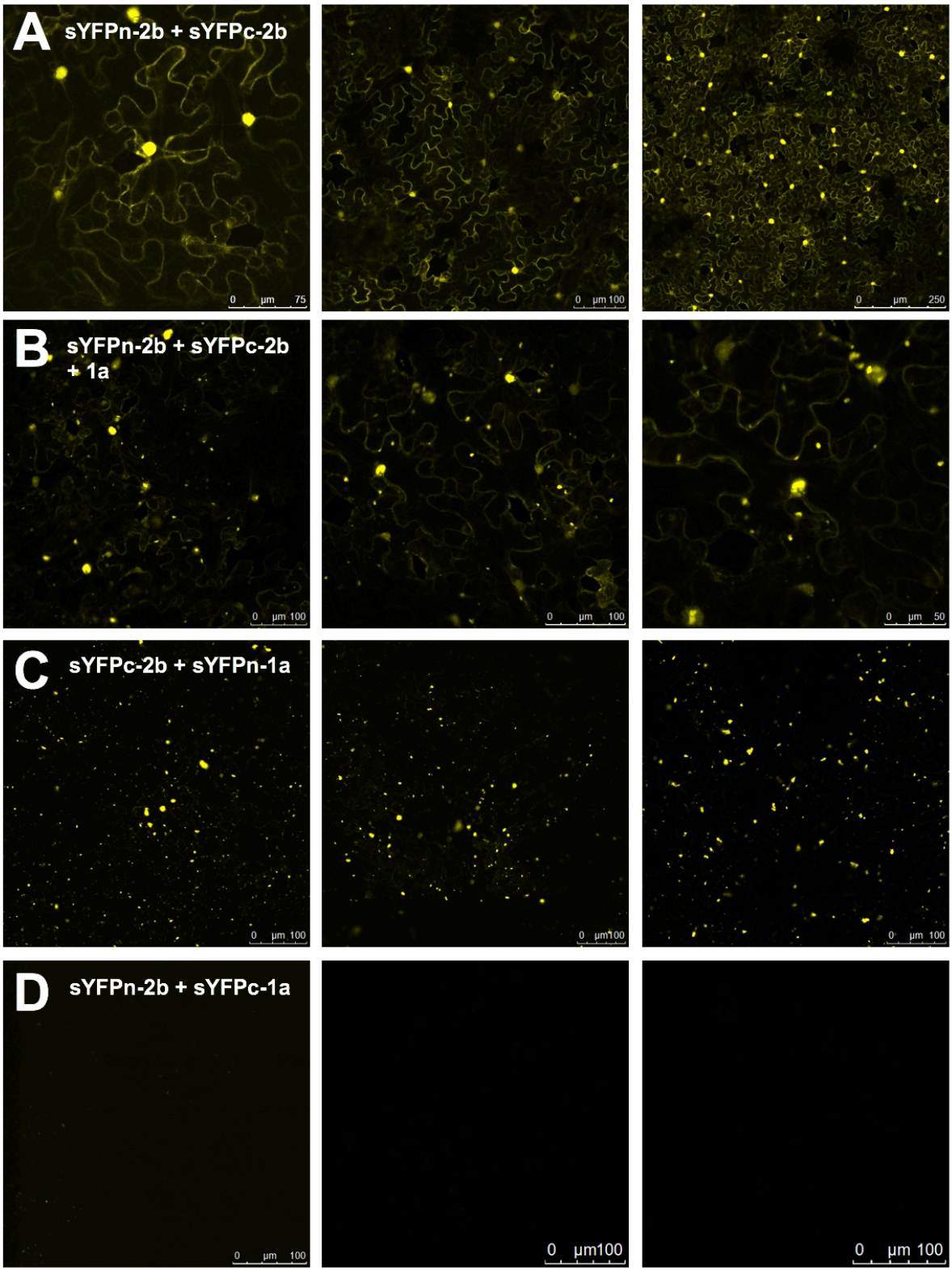

Figure 4.8. The 1a and 2b proteins interact with each other *in vivo*.

Agroinfiltrated tissue was observed using confocal microscopy. The 2b and 1a proteins were tagged at their N-termini with split yellow fluorescent protein (sYFP)

(sYFPn-2b, sYFPc-2b, sYFPn-1a and sYFPc-1a) to study protein-protein interactions *in vivo* by bimolecular fluorescence complementation. A, when sYFPn-2b and sYFPc-2b were co-expressed transiently in *N. benthamiana* leaves, the observed pattern of fluorescence showed mainly nuclear localisation, but also presence in the cytoplasm. B, when sYFPn-2b and sYFPc-2b were co-expressed with untagged 1a protein, the observed pattern of fluorescence, originating from the interaction of sYFP-2b proteins, still localised to the nucleus and diffusely in cytoplasm however, there was an additional pattern of fluorescence observed as specks within the cytoplasm. This suggests that the presence of 1a alters the localisation of interacting sYFP-2b pairs possibly causing them to co-localise with the 1a protein. C, when sYFPn-1a and sYFPc-2b were co-expressed, a strong fluorescent signal was observed, which localised to distinct punctate specks within the cytoplasm, this pattern of localisation was similar to that observed with GFP-1a and RFP-1a. D, no fluorescence was observed when the reciprocal sYFP were fused to the N-terminal of the 1a and 2b fusion proteins (sYFPc-1a/sYFPn-2b).

4.2.6 The 2b and 1a protein co-immunoprecipitate *in vivo*

The combination of co-localisation and BiFC data strongly suggested that the 1a protein and 2b protein directly interact *in vivo* and led me to hypothesise that this interaction might limit the ability of the 2b protein to interact with AGO1. To further confirm the interaction between 2b and 1a protein, I transiently expressed GFP-2b together with RFP-1a, or control proteins in *N. benthamiana*. Three days after agroinfiltration, GFP-2b proteins were immunoprecipitated using GFP-affinity beads and purified proteins were analysed by western immunoblot analysis using antibodies raised against GFP or RFP (Fig. 4.9). I found that RFP-1a co-immunoprecipitated with GFP-2b, but not with the GFP-affinity beads alone. GFP was used as a negative control to exclude the possibility that the 1a protein interacts non-specifically with GFP. The multiple bands detected for GFP-2b in panel A were commonly observed throughout multiple experiments. This appeared to be a property of the 2b protein as I also observed this with 2b-RFP. There appears to be three bands detected of lower molecular weight than would be expected for GFP-2b.It is most likely that these bands are detected partially digested GFP-2b. After IP with anti-GFP a single band was always observed. This suggests that the IP was unable to bind to the multiple bands observed in the total cell lysate.

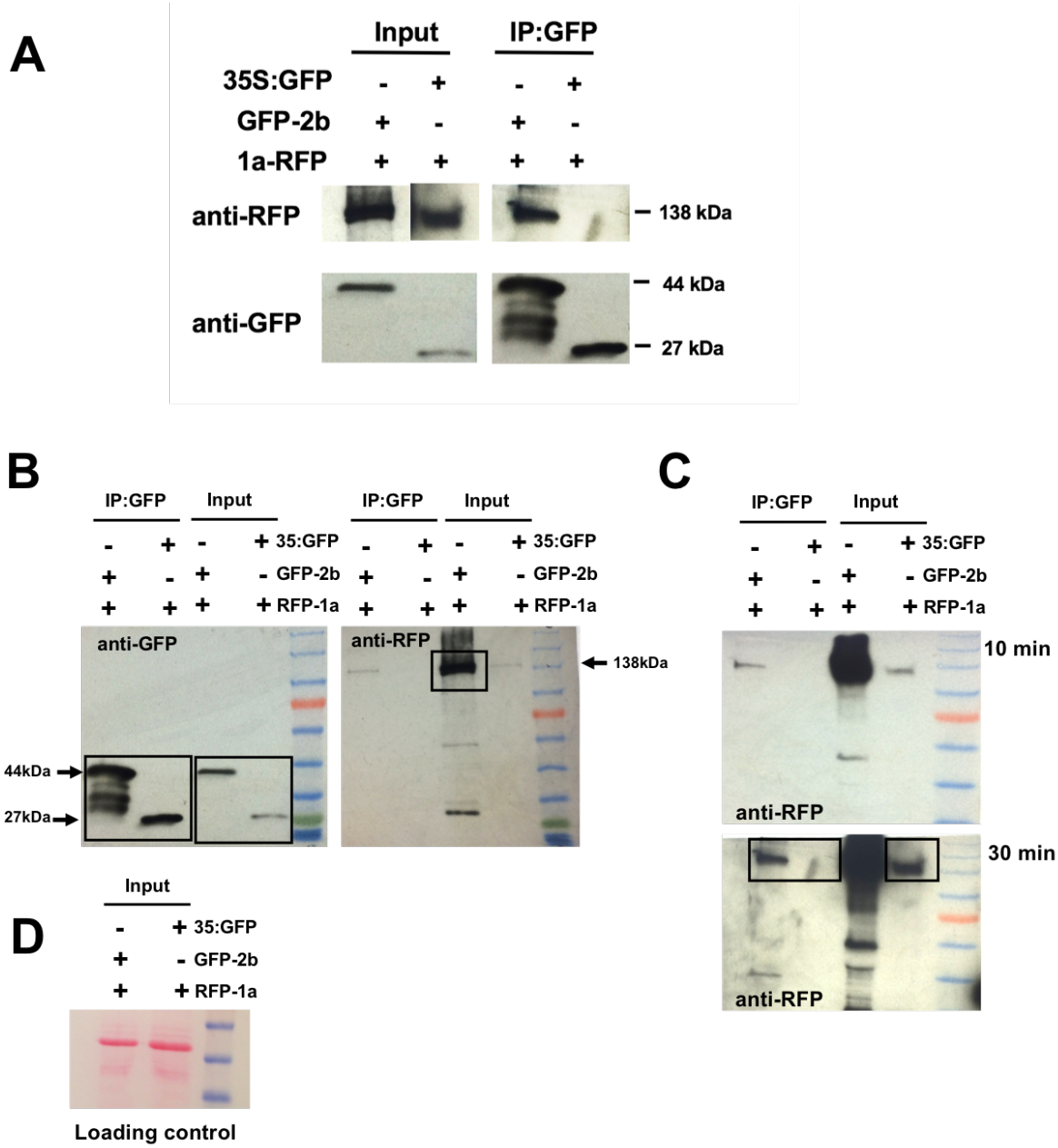

Figure 4.9. Co-immunoprecipitation of the 1a and 2b protein *in vivo*.

Total proteins from *N. benthamiana* leaves were subjected to immunoprecipitation with GFP-Trap beads followed by immunoblot analysis with anti-GFP antibodies to detect GFP-2b or 35S:GFP and anti-RFP antibodies to detect RFP-1a. RFP-1a could be detected in both input samples with a corresponding band of approximately 138kDa. After Immunoprecipitation with GFP-pull down RFP-1a could only be detected when co-expressed with GFP-2b, and was not detected with expressed with 35S:GFP. A, Imaged bands displayed are from the same blot but exposed to X-ray film for different time periods for clarity. The original blot is shown below the

composite image (B, C). C, as the band corresponding to RFP-1a in the IP:GFP sample was relatively faint the blot was exposed for 10 and 30 minutes to ensure RFP-1a wasn't carried through when co-expressed with GFP. Black rectangles indicate bands used to form the composite blot. D, the loading control is shown for the input sample stained with Ponceau stain .

4.3 Discussion

4.3.1 Subcellular localisation of 1a, 2a and 2b proteins

In this chapter, I characterised the subcellular localisation of the 1a protein by confocal imaging. This led me to confirm a novel interaction between the 1a protein and the 2b VSR. These results link viral protein subcellular localisation to the biological phenotypes that I observed in aphid performance assays. The ability of the 1a protein to interact with the 2b protein appears to be the molecular basis of the suppression of 2b-induced antibiosis during Fny-CMV infection.

The pattern of fluorescence I observed with tagged 2a protein differed from other published data, which has not reported the presence of 2a in the nucleus during CMV infection. Previous studies observed the CMV replicase complex at the vacuolar membrane (tonoplast) in tobacco and cucumber using immunogold labelling and cellular fractionation (Cillo et al., 2002; Gal-On et al., 2000). The 2a protein was observed in cytoplasmic and membrane-associated fractions (Gal-On et al., 2000). However, the constructs I used contained the 35S promoter and consequently expressed at high levels. It is conceivable that the nucleus was acting as a sink for over-accumulating viral proteins. GFP translocates to the nucleus, even when expressed as homotetramer fusion, suggesting it can diffuse through the nuclear pore (Seibel et al., 2007). My results confirmed the 1a and 2a protein interact (Fig. 4.7), and that the 1a protein relocates a portion of the 2a protein to specks that may be replicase complexes (Fig. 4.3).

The CMV 1a protein has only previously been reported in the tonoplast, but this evidence comes from fractionation studies and, to my knowledge, imaging of fluorescent-tagged CMV 1a proteins has not previously been reported in the literature. When expressed transiently in *N. benthamiana* I observed a distinct subcellular localisation pattern for the 1a protein of punctate ‘specks’ throughout the cytoplasm. I confirmed that the CMV 1a protein does not localise to ER-derived vesicular replication structures, that have been reported for the orthologous BMV 1a protein (Bamunusinghe et al., 2011). The subcellular localisation of the larger 1a protein aggregations do not appear to be associated with the tonoplast, when tissue

was stained with the styryl membrane-binding dye FM-4-64 (Bolte et al., 2004). The localisation of these larger specks are discussed below). 1a protein fluorescence was also observed at the cell periphery, at small granular dots. These smaller structures appear to be localised at the membrane, at the time of study I did not have suitable tonoplast markers, suitable markers would bind TIPs, a known target of the 1a protein (Hunter et al., 2007).

I showed that the 1a protein colocalises to DCP1 (Fig. 4.4). DCP1 is a member of the Arabidopsis decapping complex (Xu et al., 2006), and commonly used as a marker for P-bodies. The decapping complex is involved in P-body formation and translational repression (Xu and Chua 2009) (described further in Section 6.3). This suggests that a portion of the 1a replication protein associates with P-bodies. I initially hypothesised that by re-localising the 2b protein to P-bodies, the 1a protein may limit the ability of the 2b protein to interact with AGO1 in the cytoplasm and nucleus and inhibit its miRNA-directed slicing activity, which is explored further in Chapter 5. It is unlikely that the CMV replication complex interacts with P-bodies, as is the case for BMV, as they are spatially separated. However, it appears that the 1a protein may have an additional function at P-bodies as I observed them in close proximity. My results suggest that the 1a protein is able to relocate a fraction of 2b protein to P-bodies, potentially linking the RNA silencing and RNA decay pathways.

4.3.2 The 1a protein directly interacts with the 2b protein

I observed that when the 2b and 1a protein were co-expressed there was strong colocalisation. The 1a protein also altered the subcellular localisation of the 2b protein to punctate specks. Similar specks were also observed in BiFC experiments with 1a and 2b proteins suggesting that these proteins directly interact. This suspected direct interaction was confirmed using a third assay (co-immunoprecipitation). In total, these results demonstrate that the Fny-CMV 1a protein can directly bind to the 2b protein *in vivo.*

The direct interaction between the 1a and 2b protein explains the observed re-localisation of 2b protein into 'specks' in the presence of 1a (Fig. 4.5C,E). It appears that the 1a protein recruits the 2b protein, and is able to alter its function. The 1a protein is able to recruit the 2a protein to the tonoplast membrane in order to form the replicase complex. Although the 1a protein altered the localisation of the 2b protein, the 2b protein was still observed in the nucleus and cytoplasm. The interaction of the 1a protein with 2b and the 2b proteins subsequent re-localisation appears not to have any effect on the ability of 2b to self-interact (Fig. 4.8B). Cucumoviral 2b proteins tetramers show preference for binding short dsRNA (Chen et al., 2008; Rashid et al., 2008), this suggests that the 1a protein does not interfere with 2b activity in the cytoplasm. In BiFC assays the 2b protein was only observed to interact with the 1a protein in specific conformations. I did not observe any YFP fluorescence when sYFPc-1a and sYFPn-2b were co-expressed. Both the sYFPc-1a and sYFPn-2b constructs were shown to be functional in BiFC assays which suggests that structural arrangement of the 2b and 1a protein in this case, did not lead to reconstitution of the YFP fluorophore.

The direct interaction between the 2b and 1a protein is able to abolish developmental abnormalities and the induction of antibiosis typically observed when the 2b protein is transgenically expressed in Arabidopsis (Westwood et al., 2013a). This suggests that the 1a protein is able to directly interact with the 2b protein, and this interaction prevents phenotypes associated with disruption of the miRNA pathway (Fig. 3.4). I hypothesised that this is due to the 1a protein limiting the ability of the 2b protein from interacting with AGO1 (this is explored further in Chapter 5). The 1a protein does not directly interact with AGO1, but the 1a protein may play a role in modulating some aspect of AGO1 activity within P-bodies.

Work from our group has shown that aphids reared on tobacco plants infected with Fny-CMV exhibit increased feeding from the phloem, resulting in increased survival and reproduction (Ziebell et al., 2011). Although *M. persicae* survival and reproduction was increased on tobacco plants infected with Fny-CMV, antibiosis was induced in plants infected with Fny-CMVΔ2b (Ziebell et al., 2011). In contrast to Arabidopsis, the 2b proteins appears to inhibit the induction of antibiosis by the Fny-CMV RNA 1 and/or the 1a protein in tobacco (Tungadi et al., 2020). The

induction of antibiosis in Arabidopsis is due to AGO1 inhibition by the 2b protein, and consequent misregulation of mRNA targets (Westwood et al., 2013a). As it is the 1a protein that triggers antibiosis in tobacco, it is not known what host factors or signalling pathways the 1a protein inhibits. It is unlikely that the 1a protein inhibits the tobacco AGO1 activity.

Chapter 5. The 1a protein competes with AGO1 for binding to the 2b protein, but without inhibiting 2b RNA silencing suppressor activity.

5.1 Introduction

The 2b protein influences host-aphid interactions (Westwood, 2013, 2014; Wu et al., 2017; Ziebell et al., 2011). In tobacco, the mutant CMVΔ2b induces antibiosis that increases aphid mortality (Ziebell et al., 2011). In tobacco the 1a protein is the factor that triggers antibiosis, but during infection with wild-type CMV induction of antibiosis (which is deleterious to aphid-mediated transmission) is counteracted by the 2b protein (Tungadi et al., 2020; Ziebell et al., 2011). Interestingly, the Fny-CMV 2b protein appears to have the opposite effect in Arabidopsis. Constitutive expression of the Fny-CMV 2b protein in transgenic Arabidopsis plants induces antibiosis (Westwood et al., 2013a). Since Arabidopsis AGO1 negatively regulates antibiosis, it was concluded that 2b-induced antibiosis results from the interaction of the Fny-CMV 2b protein with AGO1 (Kettles et al., 2013; Westwood et al., 2013ab).

Co-expression of the CMV 1a and 2b proteins in transgenic plants inhibited aphid resistance and also ameliorated the 2b-induced developmental abnormalities that occur in *2b*-transgenic Arabidopsis plants (Lewsey et al. 2007; Westwood et al., 2013a). This suggested that the CMV 1a protein negatively regulates the ability of

the 2b protein to inhibit AGO1 activity (Westwood et al., 2013a). However, Westwood et al. (2013) were not able to determine the effect of 1a protein was due to a direct 1a-2b interaction or if the 1a protein had an indirect effect e.g. through binding a host factors such as AGO1.

5.2 Results

5.2.1 The CMV 1a and 2b proteins colocalise with host components of the RNA silencing and RNA decay pathways

In Chapter 4 I established that the 1a protein directly interacts with the 2b protein. In Chapter 4 I also demonstrated that the 1a protein colocalises with DCP1, a protein involved in mRNA decay at P-bodies. The 1a and 2b proteins were shown to interact at specks, which appeared similar to the localisation pattern observed for DCP1-GFP. In this chapter I further investigated the localisation of viral and host proteins, to determine if localisation of viral proteins to the P-body is required for the regulation of antibiosis.

I hypothesised that the 1a-2b interaction might limit the ability of 2b to interact with AGO1. I used a BiFC assay with sYFP-AGO1 and sYFP-2b to observe if the localisation of YFP fluorescence was altered by the 1a protein. When sYFPn-AGO1 and sYFPc-2b were co-expressed I observed that they interacted in the cytoplasm and nucleus (Fig. 5.1), a similar pattern was previously reported for the AGO1-2b interaction (Gonzalez et al., 2010). When the combination of sYFPn-AGO1, sYFPc-2b and RFP-1a were co-expressed I observed that the 1a protein altered the localisation of the AGO1-2b interaction. YFP fluorescence derived from the AGO1-2b interaction could be observed localising with the 1a protein at specks. These specks displayed a typical localisation pattern observed previously for the 1a protein (Fig. 4.2). This suggests that the 1a protein is not only able to alter the subcellular localisation of the 2b protein, but is also able to relocate 2b when it bound to AGO1. Colocalisation between AGO1, and the 1a and 2b proteins was only observed at sites were the 1a protein was present. The 1a protein did not inhibit AGO1 from

interacting with the 2b, in BiFC assays, protein in the cytoplasm or nucleus (Fig. 5.1).

Using agroinfiltration I co-expressed AGO1-GFP and 2b-RFP in *N. benthamiana* and observed strong colocalisation between AGO1 and 2b (Fig. 5.2). Interaction between 2b and AGO1 was previously observed in the nucleus and in cytoplasmic foci when coexpressed in *N. benthamiana* (Zhang et al., 2006). I observed that AGO1-GFP and 2b-RFP colocalised in cytoplasmic foci, although in these coinfiltration experiments I did not observe nuclear colocalisation. The pattern of fluorescence I observed when AGO1-GFP and 2b-RFP were co-expressed was different to that observed for 2b-AGO1 interaction in BiFC assays (Fig. 5.3).

When DCP1-RFP and AGO1-GFP were co-expressed I observed strong colocalisation at cytoplasmic foci (Fig. 5.2). Colocalisation between DCP1 and AGO1 was mostly observed at similar foci/aggregations, and several smaller DCP1-RFP foci were observed not localising to AGO1-GFP. This suggests that AGO1 may not be present in P-bodies in all cases. When expressed by itself AGO1-GFP did not localise to the nucleus (Fig. 5.3A). However, the cytoplasmic fraction of AGO1 was previously reported to associate with P-bodies (Pomeranz et al., 2010). I observed AGO1 in the nucleus and cytoplasm when co-expressed with 2b in BiFC assays (Fig. 5.3B). When sYFPn-AGO1 was co-expressed with sYFPc-LS2b no YFP fluorescence was observed. Arabidopsis AGO1 does not interact with 2b proteins encoded by Subgroup II CMV strains, such as LS- and Q-CMV (Lewsey et al., 2007; Zhang et al., 2006).

When DCP1-GFP and 2b-RFP were co-expressed there was no colocalisation. The 2b protein was observed in the nucleus and cytoplasm but DCP1 did not alter its localisation (Fig. 5.4A). DCP1 occurred in aggregates within the cell, often close to the cell membrane. When DCP1 and 2b were co-expressed with a construct expressing an untagged 1a protein, I observed that the localisation of the 2b protein changed, resulting in colocalisation of DCP1 with 2b (Fig. 5.4A). It appears that addition of the 1a protein causes the 2b protein to relocate to colocalise with DCP1 in specks that were assumed to be P-bodies.

In order to confirm if the 1a and 2b proteins were both present in P-bodies I co-expressed sYFPn-1a, sYFPc-2b and DCP1-RFP. I observed YFP fluorescence as specks, similar to those I previously characterised for the 1a-2b protein interaction (Fig. 4.8). These specks colocalised to foci of DCP1-RFP fluorescence suggesting that all three proteins are in close association within P-bodies (Fig. 5.4B).

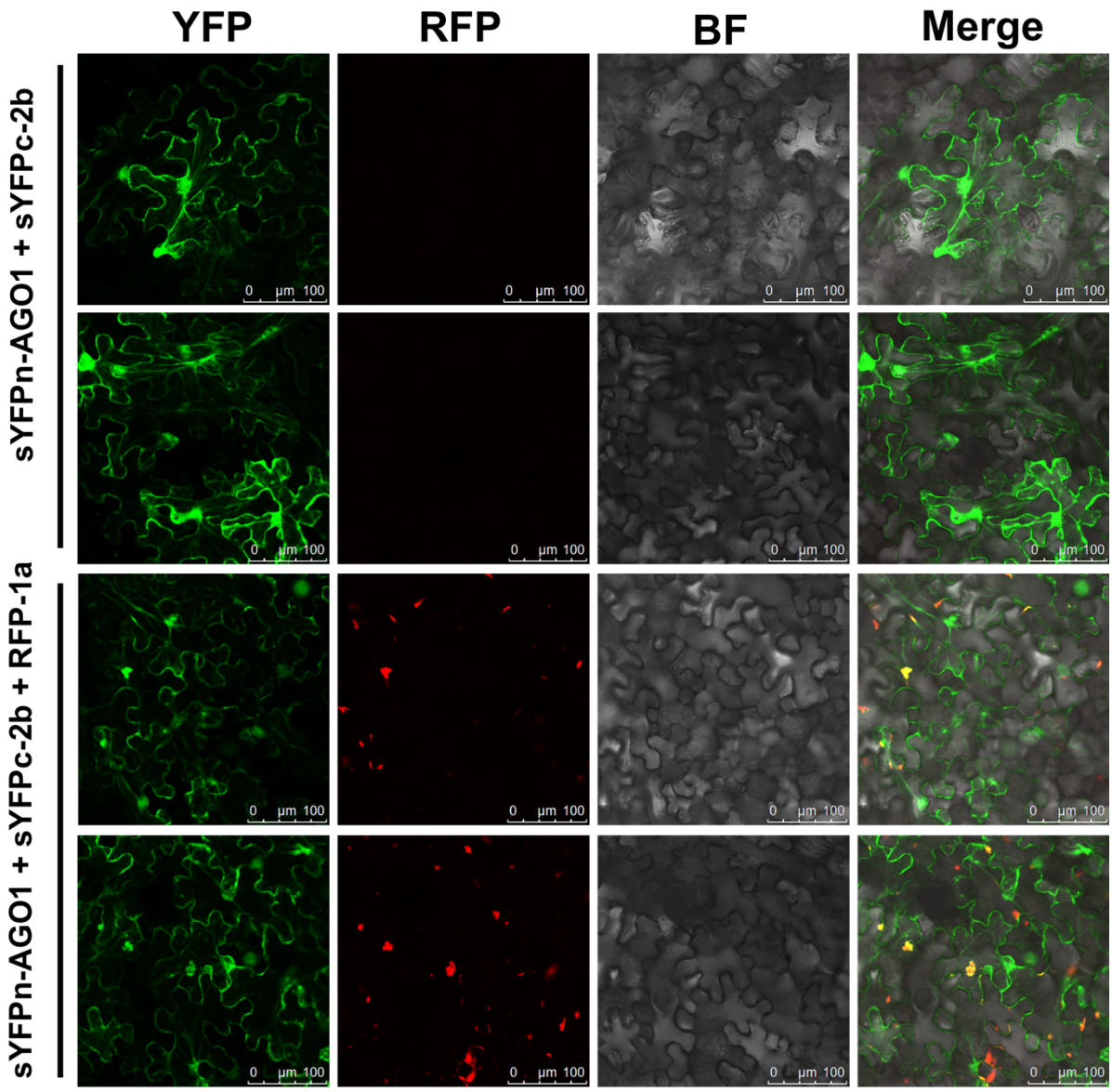

Figure 5.1. The 1a protein colocalises with AGO1 and the 2b protein.

When sYFPn-AGO1 and sYFPc-2b were co-expressed by agroinfiltration, fluorescence was observed in the cytoplasm and nucleus, as has been previous reported for the AGO1-2b interaction (Gonzalez et al., 2010). When nYFP-AGO1 and cYFP-2b were co-expressed with RFP-1a I observed that the 1a protein colocalised with fluorescence generated from AGO1-2b interaction, suggesting that all three proteins colocalise. YFP fluorescence is false-coloured as green so that colocalisation could be observed as yellow in the merged image. Merged images superimposed with optical bright field (BF) image are shown on the right.

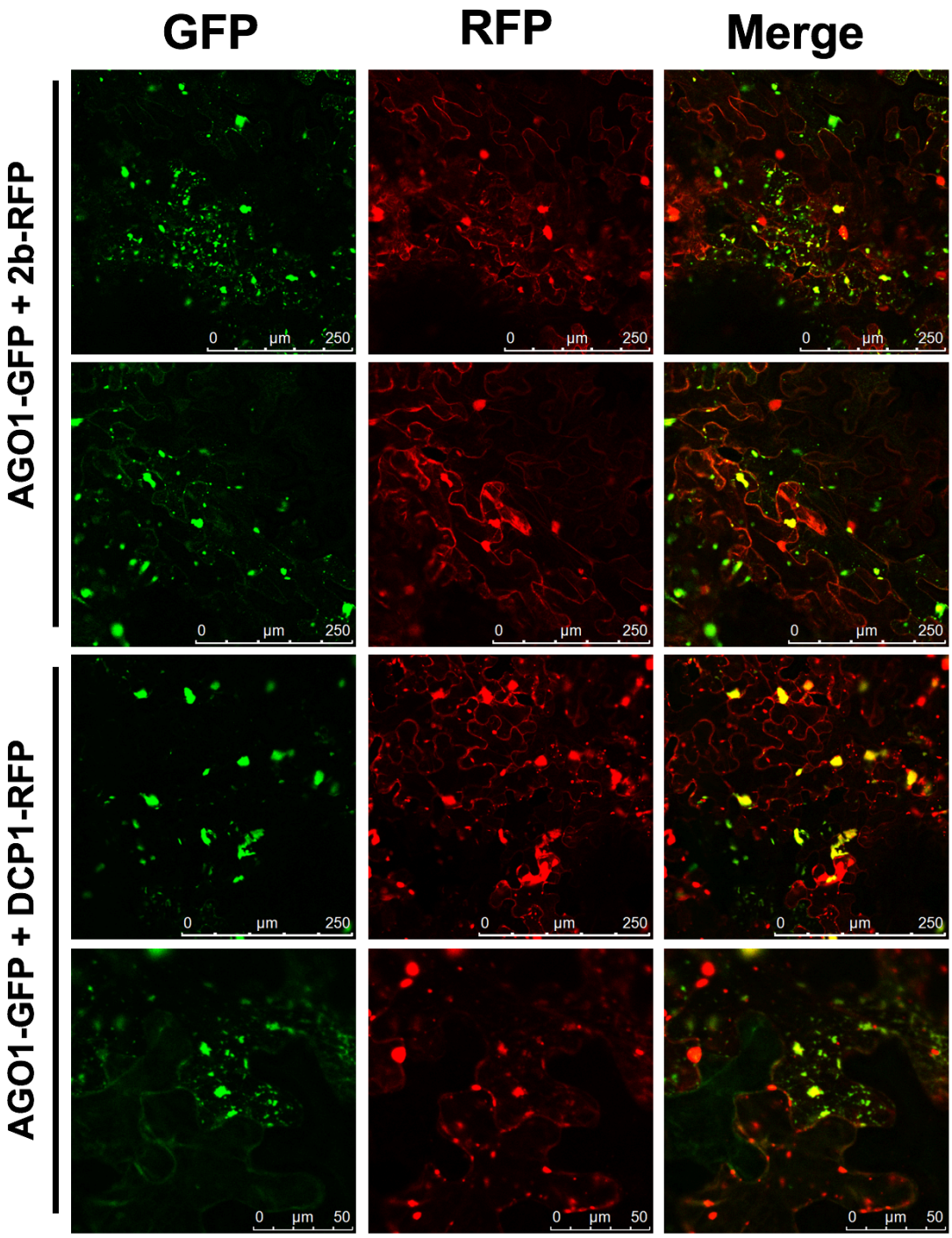

Figure 5.2. AGO1 colocalises with DCP1 and the 2b protein.

When AGO1-GFP and 2b-RFP were co-expressed by agroinfiltration (upper panels), fluorescence derived from AGO1-GFP was observed in the cytoplasm and in specks throughout the cell, in a similar pattern as observed when AGO1-GFP was expressed by itself (Fig. 5.3A). The localisation of 2b-RFP was altered by the presence of AGO1-GFP, 2b-RFP was observed in the cytoplasm and nucleus as previously reported (Fig. 4.2), but also colocalised with AGO1-GFP at specks. Co-

expression of AGO1-GFP and DCP1-RFP (lower panels), resulted in areas of colocalisation presumed to be P-bodies.

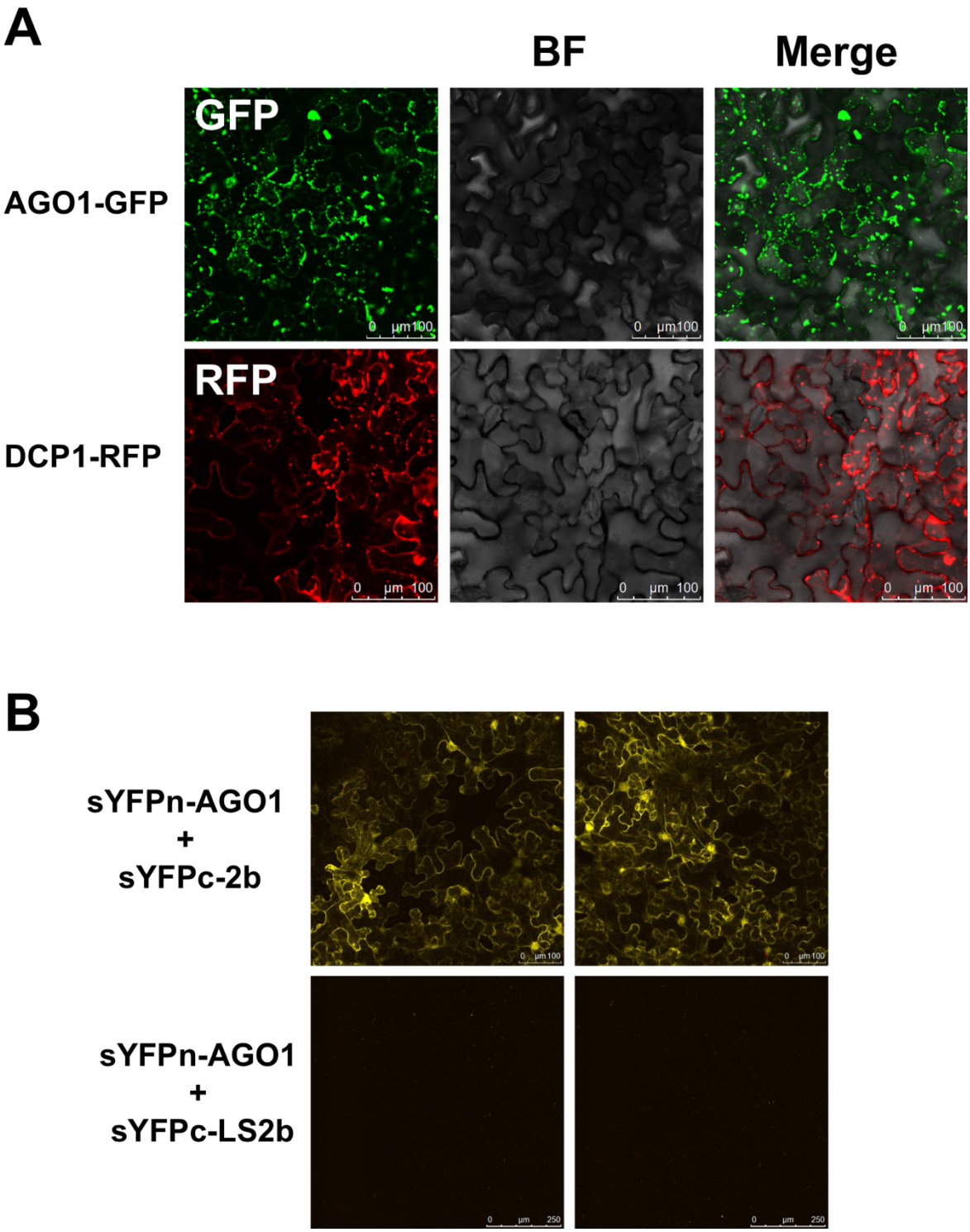

Figure 5.3. The Fny-CMV, but not the LS-CMV, 2b protein interacts with Arabidopsis AGO1.

A, AGO1-GFP and DCP1-RFP were expressed individually, fluorescence from AGO1-GFP was observed as punctate specks with varying size throughout the

cytoplasm. When DCP1-RFP was infiltrated I observed a similar pattern of localisation. Although foci of DCP1-RFP were observed more often at the cell periphery. Merged images superimposed with optical bright field (BF) image are shown on the right. B, when sYFPn-AGO1 and sYFPc-2b were co-expressed I observed YFP fluorescence in the nucleus and cytoplasm. When sYFPn-AGO1 was co-expressed with a sYFPc construct containing the LS-2b sequence no YFP fluorescence was observed.

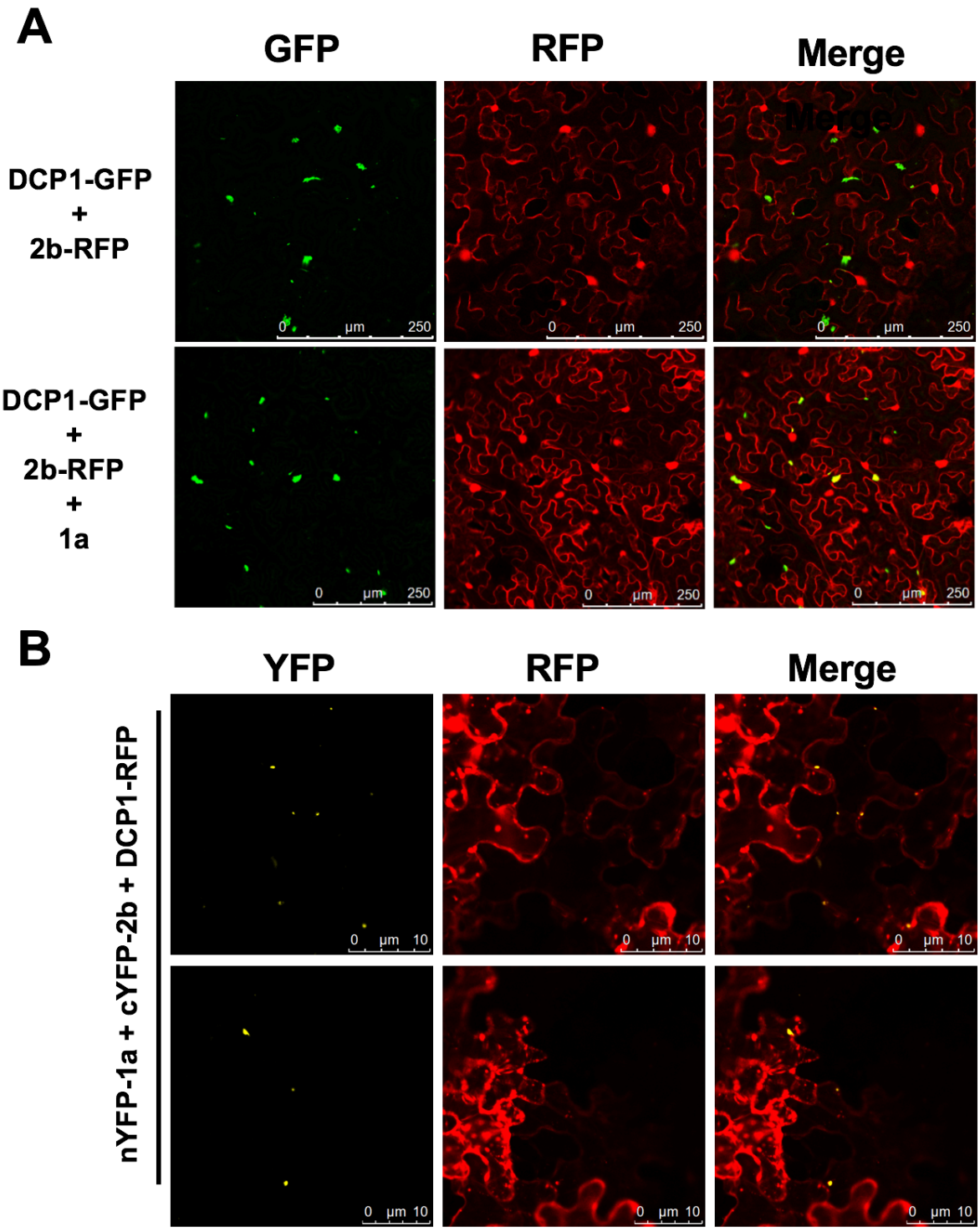

Figure 5.4. The 1a protein recruits the 2b protein to P-bodies.

A, when the P-body marker DCP1-GFP was co-expressed with 2b-RFP no colocalisation was observed (A, upper panel). When DCP1-GFP and 2b-RFP where co-expressed with an untagged 1a protein, DCP1-GFP and 2b-RFP were observed to colocalise suggesting that the presence of the 1a protein is required to recruit the 2b protein to P-bodies. B, sYFPn-1a, sYFPc-2b with DCP1-RFP were co-expressed. YFP fluorescence was observed for the sYFPn-1a/sYFPc-2b interaction. When the YFP signal was merged with the DCP1-RFP signal, the 1a-2b protein YFP signal was observed to colocalise with the P-body marker.

5.2.2 The 1a protein inhibits 2b protein AGO1 binding

I tested the ability of AGO1 to interact directly with the CMV 1a protein in a co-immunoprecipitation assay (Fig. 5.5). AGO1-GFP was unable to bind the RFP-1a protein *in vivo*. AGO1-GFP was detected as a smear in the input sample (panel A). This may be due to sample degradation from freeze thaw cycles of the cell lysate. Additionally, P19 was used as a silencing suppressor in this experiment to enhance protein expression. The Tombusvirus p19 VSR causes over-accumulation of miR168, which results in downregulation of AGO1 protein level (Varallyay et al., 2010). I carried out several experiments with increasing concentrations of P19 relative to AGO1 in transient expression assays and observed increased AGO1 degradation at higher concentrations of P19. However, after IP treatment with anti-GFP a single band of expected size (150kDa) was observed. Due to time constraints I was unable to repeat this experiment with a specific AGO1 antibody. However, in future work we aim to obtain the AGO1 and AGO2 antibodies for this theme of research.

The lack of interaction between AGO1 and 1a is consistent with BiFC results for AGO1 and 1a, that indicated that the 1a protein and AGO1 do not interact directly (Fig. 4.7). To further investigate the ability of the 1a protein to inhibit the 2b-AGO1 interaction, I carried out a competitive binding experiment. Increasing amounts of *A. tumefaciens* harbouring a T-DNA construct encoding the 1a protein was co-expressed with cells harbouring T-DNA vectors encoding 2b-RFP and AGO1-GFP, and the ability of AGO1 to co-immunoprecipitate the 2b was quantified using densitometric analysis (Fig. 5.6). I observed that when the 1a protein was expressed, AGO1 co-immunoprecipitated a smaller proportion of the 2b protein. This supports the idea that the 1a protein competes with AGO1 for interaction with the 2b protein. To further confirm if the presence of the 1a protein altered the AGO1-2b protein interaction, sYFP-tagged 2b and AGO1 constructs were co-expressed. I observed that addition of the 1a protein significantly reduced the intensity of fluorescence due to reconstitution of the YFP fluorophore caused by the sYFPn-2b and sYFPc-AGO1 interaction (Fig. 5.7).

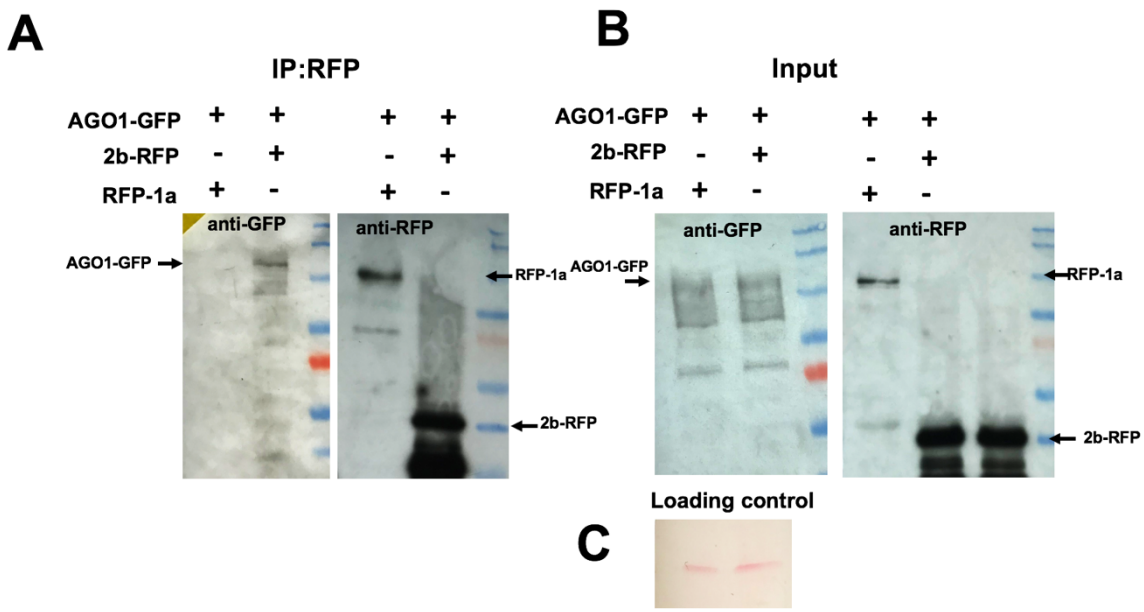

Figure 5.5. AGO1 does not interact with the 1a protein *in vivo*.

Total proteins extracted from agroinfiltrated *N. benthamiana* leaves were subjected to immunoprecipitation with RFP-Trap beads followed by immunoblot analysis with anti-GFP antibodies to detect AGO1-GFP and anti-RFP antibodies to detect RFP-1a or 2b-RFP. AGO1-GFP could be detected in both input samples with a corresponding band of approximately 140kDa. After immunoprecipitation with RFP-Trap AGO1-GFP could only be detected when co-expressed with 2b-RFP, and was not detected when expressed with RFP-1a. RFP-1a and 2b-RFP were both detected after immunoprecipitation with RFP-Trap beads. The loading control is shown for the input sample stained with Ponceau stain.

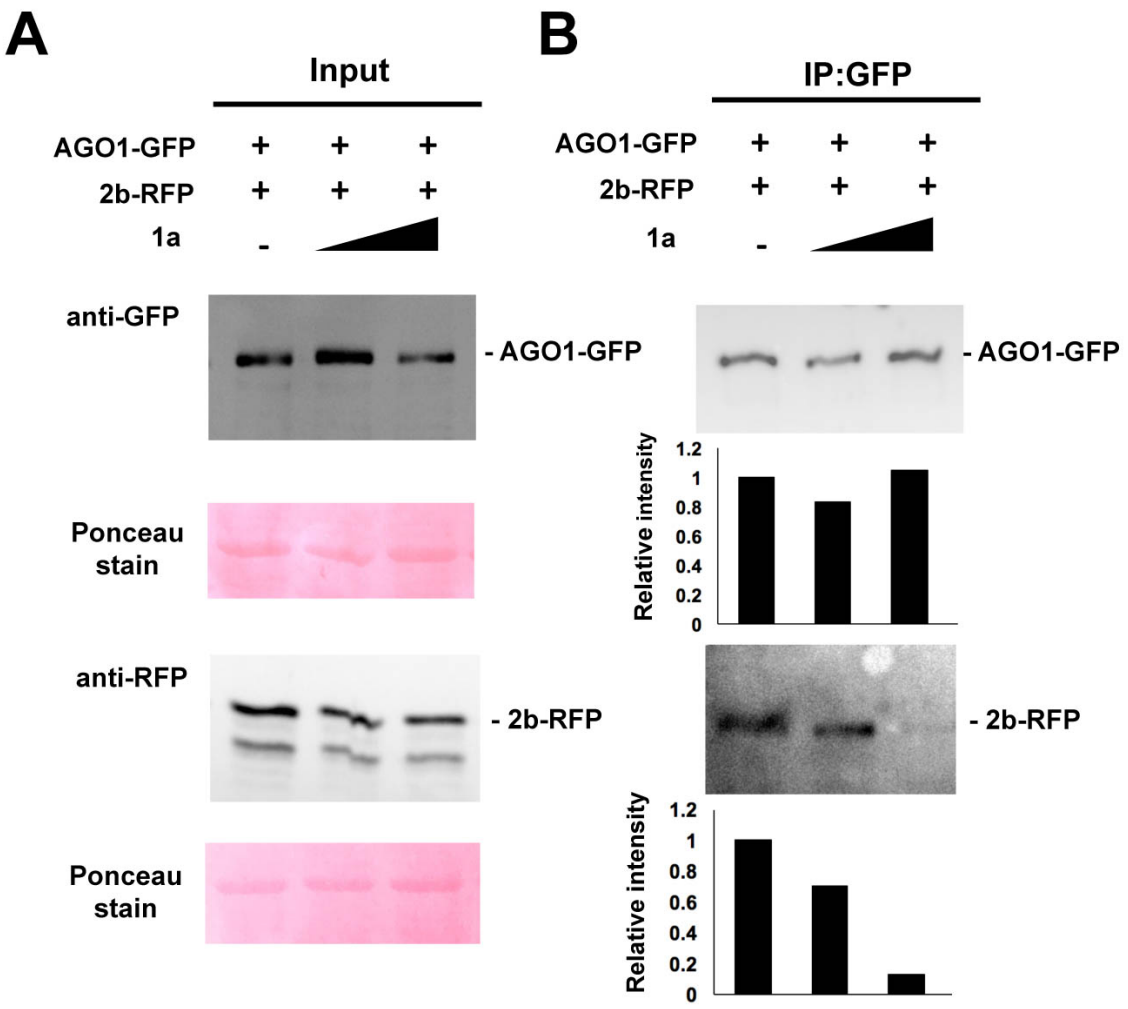

Figure 5.6. The CMV 1a protein inhibits the 2b protein from binding to AGO1.

A, representative western blots of AGO1-GFP and 2b-RFP extracted from *N. benthamiana* after transient expression. A suspension of infiltration buffer and empty Agrobacterium cells was used to dilute samples to ensure the ratio of 2b : AGO1 remained constant as increasing amounts of 1a was added. The final OD_{600} of each treatment was 1, while the relative OD_{600} of *A. tumefaciens* harbouring T-DNA constructs encoding AGO1-GFP and 2b-RFP was 0.25 in all three treatments. The relative OD_{600} of *A. tumefaciens* harbouring T-DNA constructs encoding the 1a protein was 0.25 and 0.5, which corresponded to a ratio of AGO1-GFP : 2b-RFP : 1a of 1:1:1 and 1:1:2, respectively. Total proteins were extracted and 10 ug of protein in sample buffer was loaded per well. Bottom panel shows loading control (Ponceau stain). B, representative Co-IP experiments with proteins expressed by co-agroinfiltration revealed an inhibitory effect of the CMV 1a protein on AGO1-2b

interaction. The immune complexes were formed by pre-incubation with anti-GFP beads (IP AGO1-GFP) and revealed with RFP antibody (bottom panel). Densitometric analysis was performed using a GeneGnome XRQ (Syngene) and analysed using GeneTools analysis software.

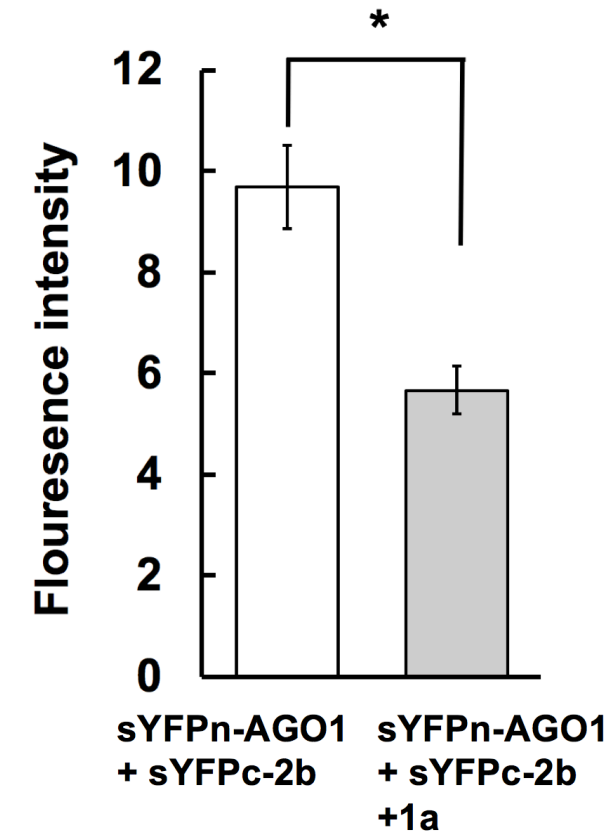

Figure 5.7. The 1a protein prevents 2b and AGO1 from interaction in BiFC assays.

A. tumefaciens harbouring T-DNA constructs encoding sYFPn-AGO1 and sYFPc-2b were co-expressed into *N. benthamiana* leaves at a final OD_{600} of 0.9. Untransformed *A. tumefaciens* cells resuspended in infiltration buffer were diluted to OD_{600} so that the final OD_{600} of each construct was 0.3. The RFP-1a construct was co-expressed with sYFPn-AGO1 and sYFPc-2b at a ratio of 1:1:1 with a total OD_{600} of 0.9. The intensity of YFP fluorescence for each image was calculated using the Lecia Application Suite X (LAS X). Measurements were collected from 5 individual plants, that were each infiltrated at 5 patches giving a total of 25 images for each treatment. The asterisk indicates a significant difference (Student's t-test, $P<0.05$). Error bars represent standard error of the mean.

5.2.2 The 1a protein alters 2b protein localisation but does not affect 2b silencing suppressor activity

To determine if the 1a protein inhibits 2b protein VSR activity a transiently expressed GFP reporter gene was agroinfiltrated into patches of *N. benthamiana* leaves alone or together with constructs expressing the 1a or 2b proteins (Fig. 5.8). Following agroinfiltration, transient accumulation of free GFP fluorescence was imaged and quantified at 4, 8 and 16 days post infiltration. Agroinfiltration of a GFP construct on its own resulted in low intensity fluorescence, which decayed within a week (Fig. 5.8B). When free GFP and CMV 2b constructs were co-expressed, both the intensity and duration of the fluorescence signal were increased, with GFP fluorescence visible until at least 16 days post-infiltration. P19 is the tombusvirus VSR (Vargason et al., 2003) and when a P19 construct was co-expressed this also increased the duration and intensity of the GFP signal (Fig. 5.8B). Co-agroinfiltration of 2b or P19 with free GFP did not alter the subcellular localisation of the GFP signal (Fig. 5.8B).

Co-expression of 1a and free GFP had no effect on the observed levels of GFP fluorescence (Fig. 5.8), which confirmed that the 1a protein does not possess VSR activity or compromise GFP stability. Since the 1a protein binds to the 2b protein, it was suspected that the presence of 1a might interfere with the VSR activity of 2b. However, co-agroinfiltration of constructs encoding 1a, 2b and free GFP did not alter the intensity or duration of fluorescence, or corresponding GFP protein levels (Fig. 5.8C). The 1a protein had no effect on the VSR activity of P19. Thus, the 1a protein does not inhibit the VSR activity of the 2b protein and has no general anti-VSR properties.

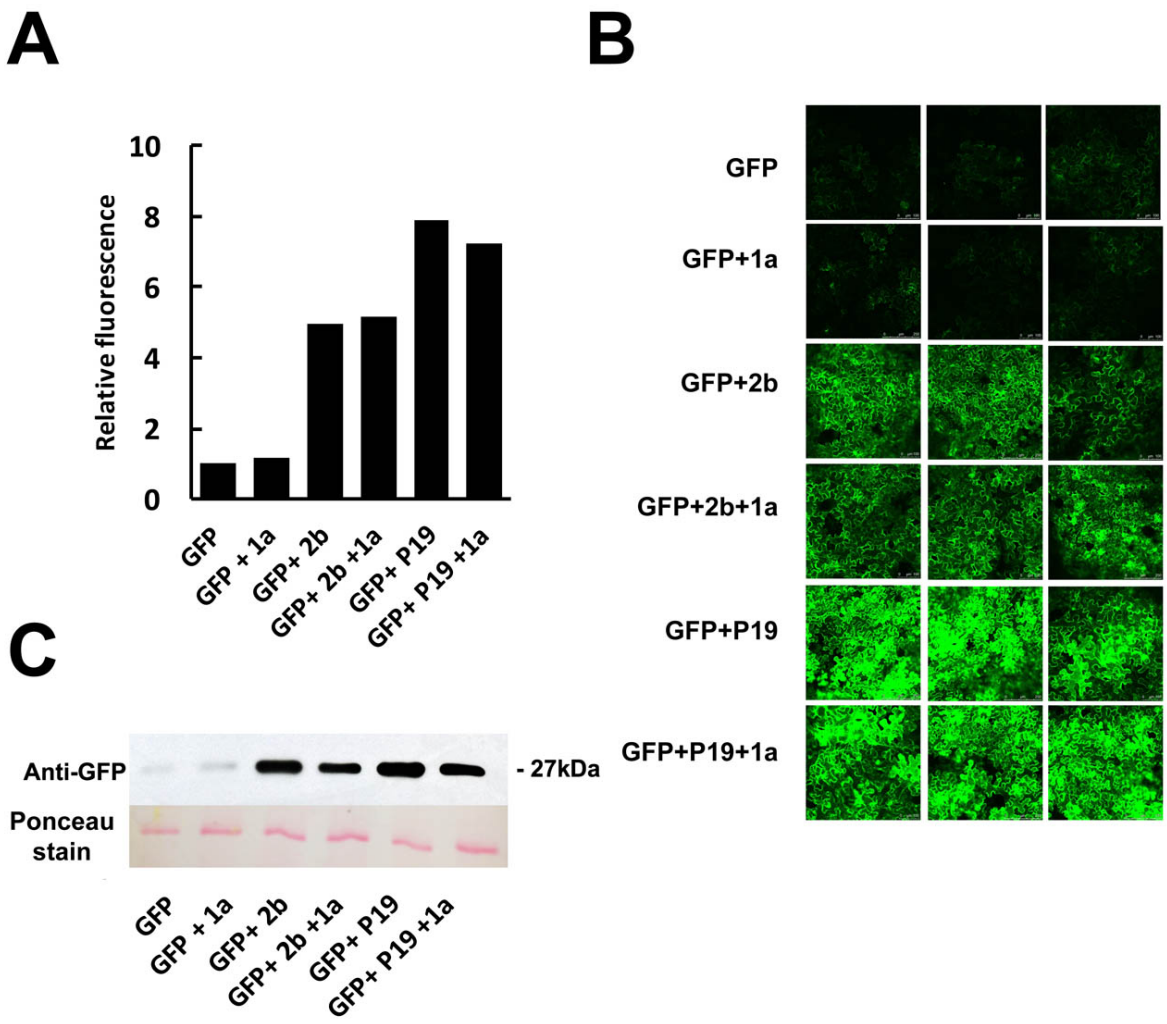

Figure 5.8. CMV 1a protein does not affect 2b RNA silencing suppressor activity.

Green fluorescent protein (GFP) was expressed transiently, using a 35S promoter, in *N. benthamiana*. A, the relative intensity of fluorescence for each treatment 16 days after infiltration was calculated. GFP intensity was quantified, by imageJ, as the integrated density (IntDen) of each image. Number of independent leaves imaged for each treatment, n = 15. B, Typical confocal images of GFP fluorescence in the presence of 1a, 2b or P19, as indicated. When GFP was co-expressed with CMV 2b protein or the P19 protein the intensity and duration of fluorescence was increased due to their VSR activity. Co-expression of CMV 1a protein had no effect on any of the three treatments. Number of independent leaves imaged for each treatment, n = 15. C, leaf disks where harvested 16 days after infiltration for

immunoblot analysis. GFP protein accumulation was confirmed using anti-GFP antibodies.

5.3 Discussion

5.3.1 Viral proteins colocalise with host components of the RNA silencing and RNA decay pathways

In this chapter, I further characterised the subcellular localisation of the 1a and 2b protein by confocal imaging. In Chapter 4 I observed that the 1a protein localised to P-bodies. Using confocal imaging I observed that the 1a protein is able to relocate 2b proteins to P-bodies, potentially linking RNA silencing and RNA decay pathways in CMV infection.

The 2b protein only localises to P-bodies, when 1a protein is present (Fig. 5.4A). This suggests the ability of the 1a protein to modify 2b subcellular localisation is an important aspect of this interaction. However, I observed that the interaction of 2b-AGO1 in nucleus/cytoplasm, although reduced, still occurred when 1a was co-expressed in BiFC assays. Although the 2b protein primarily inhibits RNA silencing by sequestering siRNAs, inhibition of AGO1 slicer activity by the 2b protein is likely important for the infection process. When 2b-RFP and AGO1-GFP were co-expressed I observed the formation of cytoplasmic foci, but was unable to confirm these were P-bodies (Fig. 5.2).

I considered that the 1a protein may play a role in preventing 2b from interacting with AGO1 in P-bodies, but while maintaining 2b inhibition of AGO1 in the cytoplasm/nucleus. This may explain why the 1a protein does not completely inhibit the 2b-AGO1 interaction in BiFC assays (Fig. 5.7). By preventing 2b-inhibition of AGO1 in P-bodies it appears that AGO1 can resume normal miRNA processing. This also highlights that AGO1 function within P-bodies is important in antiviral defence and the induction of antibiosis. I do not currently know what exact AGO1 activity is restored in P-bodies by the 1a protein, but it most likely relies on

preventing the 2b protein from inhibiting AGO1 slicer activity specifically in this cellular compartment (discussed further in Section 6.3).

Arabidopsis decapping mutants have increased levels of potential targets of miRNAs, suggesting that there is a link between decapping and AGO1 activity (Motomura et al., 2012). Recently it was shown that the CaMV multifunctional viral translation transactivator/viroplasmin (TAV) protein functions as a suppressor of nonsense-mediated mRNA decay (Lukhovitskaya and Ryabova, 2019). TAV was shown to interact specifically with VARICOSE (VCS) at the decapping complex, and co-localised with components of the decapping complex. At the time of study I was unable to establish if the 1a protein directly interacts with P-body components.

However, it seems more likely that it is due to the action of the 1a protein sequestering the 2b protein to P-bodies that is important in preventing inhibition of AGO1. I did not confirm whether the 2b protein is able to interact with P-body components when it is relocated to P-bodies. I initially hypothesised that by re-localizing the 2b protein to P-bodies, the 1a protein may limit the ability of the 2b protein to interact with AGO1 in the cytoplasm and nucleus and inhibit AGO1's miRNA-directed slicing activity, this is discussed in Section 5.3.2. Alternatively, the 1a protein may inhibit antibiosis by preventing 2b-inhibition of AGO1 slicer activity in P-bodies.

5.3.2 The CMV 1a replication protein and 2b VSR interact directly to modulate AGO1 activity

I have shown that the CMV 1a replication protein has, in addition to its previously documented functions in virus replication and pathogenesis (Palukaitis, 2019; Seo et al., 2019), the ability to modulate the association of the 2b VSR with one of its host targets, AGO1. AGO1 is a key target of VSRs encoded by several viruses and inhibition of AGO1 activity for some viruses can provide an effective means of diminishing antiviral RNA silencing (Csorba et al., 2009). It was once thought that

cucumoviral 2b VSRs inhibit antiviral RNA silencing by binding to AGO1 (Zhang et al., 2006) until subsequent work showed that 2b's VSR activity is primarily dependent upon its ability to titrate double-stranded siRNAs (Chen et al., 2008; González et al., 2010, 2012; Goto et al., 2007; Rashid et al., 2008). In any case, inhibiting AGO1 activity may be a counterproductive means of inhibiting antiviral RNA silencing. For example, in Arabidopsis, AGO1 regulates *AGO2* mRNA levels using miR403 and de-repression of AGO2 accumulation by the 2b protein triggers the establishment of another layer of antiviral silencing (Harvey et al., 2011). The CMV 1a protein may play an important role in preventing the 2b protein from triggering this additional line of host defence. In tobacco, it appears that the 1a protein is the factor that triggers aphid resistance, and this is countered by the 2b protein (Tungadi et al., 2020; Ziebell et al., 2011). In both plant hosts, the 1a and 2b proteins have antagonistic roles in conditioning CMV-induced effects on aphid-plant interactions suggesting the interplay of the 1a and 2b proteins determines the outcome (induction of aphid resistance or aphid susceptibility) of CMV infection on plant-aphid interactions in different hosts. This reinforces previous work showing that the effects of viral proteins on plant-aphid interactions are complex and combinatorial (Tungadi et al., 2020; Westwood et al., 2013a, 2014).

In *2b*-transgenic Arabidopsis plants the 2b protein induces stunting of shoots and roots, and developmental abnormalities, including floral deformation (Lewsey et al., 2007). These effects occur in part through inhibition of AGO1 activity (in particular, inhibition of mRNA slicing directed by miR159) and also through effects that the 2b protein has within the host cell nucleus (Du et al., 2014a,b; Lewsey et al., 2007, 2009). The symptom-like phenotypes of *2b*-transgenic plants can be exaggerated compared with the symptoms seen in CMV-infected, non-transgenic plants (Fig. 3.4) (Lewsey et al., 2007). I think it likely that by binding the 2b protein and ameliorating these 2b-induced phenotypes, the 1a protein may limit the virulence of CMV and moderate the deleterious effects of virus infection on the host. This would be beneficial for CMV since excessive damage to the host plant may decrease virus yield or decrease the ability of susceptible hosts to reproduce, favouring the emergence of resistant individuals in the host population, an effect modelled in Groen et al. (2016).

Modulating 2b activity would benefit aphid-mediated CMV transmission. In Arabidopsis, AGO1 negatively regulates antibiosis against aphids (Kettles et al., 2013; Westwood et al., 2013ab), and 2b-induced inhibition of AGO1 activity, as seen in *2b*-transgenic plants, is deleterious to aphids and would compromise their ability to vector the virus. My results confirm that 1a prevents induction of antibiosis by the 2b protein in Arabidopsis and suggests a mechanism by which direct interaction between 1a and 2b, will regulate the extent of 2b-mediated inhibition of AGO1 (Fig. 5.6).

5.3.3 The interaction of 1a and 2b does not inhibit 2b VSR activity

The 2b protein performs its VSR role primarily in the cytoplasm (González et al., 2012). Increasing the nuclear and nucleolar enrichment of Fny-2b compromises its VSR activity but enhances CMV virulence, accelerating the appearance of disease symptoms in Arabidopsis plants (Du et al., 2014a). Similar to CMV 2b, other VSRs, including the potyviral HC-Pro and tombusviral P19, bind sRNAs (Kasschau and Carrington, 1998; Lakatos et al., 2006; Ye et al., 2003) and are most effective as inhibitors of antiviral RNA silencing when present in the cytoplasm (Riedel et al., 1998; Uhrig et al., 2004). For example, translocation of P19 into the nucleus by host ALY proteins greatly impairs its VSR activity demonstrating that binding sRNAs by P19 occurs in the cytoplasm (Canto et al., 2006). Other host proteins can inhibit VSR activity. For example, the tobacco rgsCAM protein binds to VSRs of several viruses, including the CMV 2b protein, and inhibits and destabilizes them (Nakahara et al. 2012). However, to my knowledge the inhibition of one of the 2b protein's effects on the RNA silencing pathway (i.e. inhibition of AGO1 activity) is the first documented instance of regulation of a VSR by another viral protein.

Although the 1a protein directly interacts with the 2b protein and alters its localisation and inhibits the AGO1-2b protein interaction, it has no effect on 2b VSR activity. The results are consistent with our previous work showing that 2b-mediated inhibition of antiviral RNA silencing and 2b-mediated inhibition of AGO1-mediated,

miRNA-directed mRNA cleavage are separate 2b functions and determined by different functional domains within the 2b protein (Gonzalez et al. 2010, 2012). My data suggests that re-localisation to P-bodies by the 1a protein does not diminish the ability of 2b to inhibit RNA silencing and that the 1a protein is able to inhibit the induction of 2b-induced antibiosis against aphids and ameliorate 2b-mediated disruption of plant development without disrupting the ability of the 2b protein to perform its vital counterdefence role.

Chapter 6. General Discussion

6.1 CMV-induced inhibition of aphid growth and reproduction in Arabidopsis are mediated via two parallel defensive signalling pathways

It was previously established that anti-aphid resistance induced by CMV infection in Arabidopsis depends on the 2a protein triggering feeding deterrence, which is mediated by the conversion of the most abundant indole glucosinolate, I3M, into the feeding deterrent 4MI3M (Westwood et al., 2013a). My findings are fully in line with what is known about the regulation of I3M and 4MI3M production from the literature but also indicate that BAK1 is involved in CMV-mediated aphid resistance in Arabidopsis. Using a combination of *bak1-5* mutant plants and generalist and specialist aphids I determined that CMV-induced aphid resistance in Arabidopsis is mediated via two parallel defensive signalling pathways. The first defence signalling pathway involves BAK1-dependent signalling and decreases aphid MRGR. This is also in line with the work by Prince at al. (2014) who found that BAK1 contributes to PTI against aphids in Arabidopsis. It was previously found that an aphid effector *M. persicae* candidate effector10 suppresses the flg22-mediated ROS burst (Bos et al., 2010), which also requires BAK1 (Chinchilla et al., 2007; Heese et al., 2007). I discovered a second BAK1-independent signalling pathway that reduces aphid reproduction. The signalling pathways induced by CMV infection leading to reduced aphid MRGR and reproduction are summarised in a model (Fig. 6.1).

BAK1 and BKK1 have overlapping function in regulating PTI defences. BKK1 plays a major regulatory role in the FLS2-, EFR-, and PEPR1/2-dependent signalling pathways in addition to BAK1 (Roux et al., 2011). Early and late responses to flg22 and elf18 are dramatically reduced in the double mutant *bak1-5 bkk1-1*. Additionally, responses to the DAMP Pep1 are severely impaired in the *bak1-5 bkk1-1* mutant, consistent with the BAK1 dependence of Pep1-triggered responses (Krol et al., 2010). It is possible that DAMPs produced as a consequence of CMV infection are

not perceived in *bak1-5* or *bak1-5 bkk1* mutant plants and this leads to an attenuated immune response. I observed that root growth inhibition triggered by plant extracts from CMV-infected plants is abolished in *bak1-5* and *bak1-5 bkk1-1* mutant plants. This suggests that BAK1 may have a role in the perception of CMV directly or indirectly sensing CMV-induced DAMPs. It is likely that *M. persicae* is sensitive to BAK1-regulated PTI-responses induced by CMV, although my results show these defence responses only decrease the MRGR of individual aphids and not aphid reproduction.

Previous work in our group observed that CMV-induces transcripts that overlapped with those induced by three PAMPs (flg22, elf26, and chitin) (Westwood et al., 2013a). It is not known if the PTI response triggered by CMV is due to the interaction of viral proteins with host factors or occurs as a general response to CMV infection. Transgenic plants expressing the 2a protein could be used in transcriptome experiments to differentiate between 2a-induced defence signalling and antixenosis. Knowledge of which signalling pathways are induced by the 2a protein may also help determine which host proteins it interacts with. The immune response triggered by the 2a protein appears to not inhibit CMV replication (Westwood et al., 2013a; Rhee et al., in preparation). Similarly, *bak1-5* plants do not show enhanced susceptibility to CMV infection (Groen et al., 2020). This is opposed to the role of BAK1 in other pathosystems, which was shown to confer resistance to several RNA viruses (Kørner et al., 2013). This suggests that BAK1 is activated in response to CMV infection but is not required for resistance to CMV. The activation of BAK1 by CMV infection may be important in fine tuning defence responses in Arabidopsis that lead to feeding deterrence.

My results from aphid colony growth experiments suggest that BAK1-independent defences were induced by CMV infection that reduced generalist and specialist aphid reproduction. Recent work from our group discovered that JA signalling is required for the defence pathway that affects aphid colony growth (Groen et al., 2020). CMV-induced resistance affecting both MRGR and aphid colony was abolished in the absence of functional JA biosynthesis (*dde2*) and JA-insensitive (*coi1*) mutants (Casteel et al., 2015; Groen et al., 2020). JA is also known to promote the accumulation of indole-glucosinolates, camalexin and the non-protein amino

acid Nδ-acetylornithine (Zhou et al., 1999; Mikkelsen et al., 2003; Adio et al., 2011). It is likely that JA is able to regulate the build-up camalexin and of I3M, the precursor of 4MI3M in a BAK1-independent manner during CMV-mediated aphid resistance in Arabidopsis. We have yet to quantify the expression of *CYP81F2* or total levels of 4M13M in *bak1-5* mutants infected with CMV. If *CYP81F2* is not induced in CMV-infected *bak1-5* mutant plants, it suggests that additional defences, such as camalexin, are responsible for the reduction in colony size observed on these plants.

Camalexin is able to confer resistance to the Brassicaceae specialist aphid *B. brassicae* (Kuśnierczyk et al., 2008), which is less sensitive to indole glucosinolates than *M. persicae*. Infestation of Arabidopsis with *B. brassicae* increased the expression of *CYP79B2*, *CYP79B3*, and *PAD3* causing an increase in the concentration of camalexin (Kuśnierczyk et al., 2008; Mewis et al., 2012). We previously observed that CMV-induced anti-aphid resistance was still present in *pad3* mutants, when aphid performance was measured as MRGR (Westwood et al., 2013a). Camalexin accumulation is increased in the *dcl1-9* and *ago1-25* mutants, as well as in *2b*-transgenic Arabidopsis (Kettles et al., 2013; Westwood et al., 2013a), in which the miRNA pathway is disrupted (Lewsey et al., 2007; Zhang et al., 2006). My results show that the MRGR of *B. brassicae* was unaffected on CMV infected plants (Fig. 3.6), in a BAK1-independent manner. This suggests that camalexin levels induced during CMV infection do not negatively affect the MRGR of this specialist aphid. This may be due to the fact that a single aphid may not be sufficient to induce camalexin production, whereas colony growth assays may lead to increases in camalexin. And that aphid colony growth on CMV-infected plants may lead to the induction of multiple signalling pathways.

My results highlight the importance of multiple measurements of aphid performance. As results from aphid colony growth experiments may be confounded by the effects of aphid infestation, and induction of additional signalling pathways that may have crosstalk with virus induced defences. More experiments are needed to fully elucidate the mechanisms behind BAK1-independent signalling induced by CMV-induced resistance to *M. persicae*.

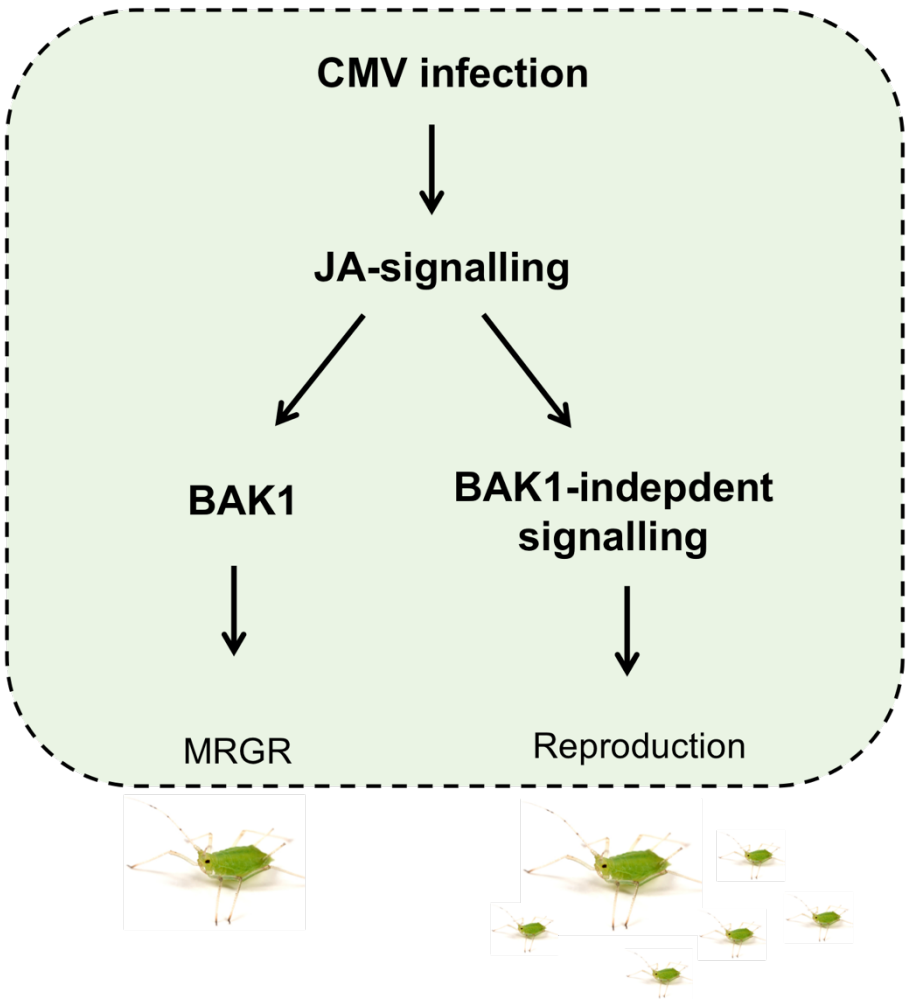

Figure 6.1. CMV-induced resistance is able to induce two distinct pathways in Arabidopsis that affect *Myzus persicae* performance.

Arabidopsis plants infected with Fny-CMV induce a form of resistance (antixenosis) based on the production of an aphid feeding deterrent, 4MI3M, through activation of defensive signalling. JA biosynthesis is required for the defence pathways that affect aphid MRGR and aphid colony growth (Groen et al., 2020). BAK1 is required for the perception of CMV infection and the induction of defence signalling that negatively affects aphid MRGR. Whereas, BAK1-independent defence signalling negatively regulates aphid reproduction.

6.2 The CMV 1a protein interacts directly with the 2b protein and prevents the induction of antibiosis in Arabidopsis

In Chapter 4 I showed that the 1a protein directly interacts with the 2b protein. At the start of the work it was not certain if the 1a protein modulated the 2b protein's activity by direct interaction, or indirectly through a host factor (Westwood et al., 2013a). The symptom-like phenotypes of *2b*-transgenic plants are more severe than symptoms seen in CMV-infected, non-transgenic plants (Lewsey et al., 2009). CMV-induced developmental symptoms are conditioned partly through the ability of the 2b protein to inhibit AGO1 activity (Du et al., 2014b; Lewsey et al, 2007, 2009; Zhang et al., 2006). In *2b*-transgenic Arabidopsis plants the 2b protein induces stunting of shoots and roots, and floral deformation (Lewsey et al., 2007). These effects occur in part through inhibition of AGO1 activity (in particular, inhibition of mRNA slicing directed by miR159) and also through effects that the 2b protein has within the host cell nucleus (Du et al., 2014a,b; Lewsey et al., 2007, 2009). This suggests that 1a protein negatively regulates the inhibition of AGO1 by the 2b protein, which may ameliorate the potential damage caused by CMV to its hosts, and in Arabidopsis would prevent the induction of a secondary layer of resistance mediated by AGO2, which provides a secondary antiviral mechanism that is important when the primary AGO1-mediated layer is not active (Harvey et al., 2011). AGO2 was shown to be upregulated during CMV infection and *ago2* mutants are hyper-susceptible to CMV (Harvey et al., 2011), and AGO2 have been shown to loaded with CMV siRNAs (Zhang et al., 2006). This suggests that AGO2 provides an additional layer of anti-viral resistance during CMV infection. However, inhibition of AGO2 activity does not lead to antibiosis or reduced aphid performance. Mutants in *ago2*, *ago4*, or *ago7* mutants do not reduce aphid performance (Kettles et al., 2013). This suggests that impaired miRNA processing is responsible for negatively affecting aphid reproduction via inhibition of AGO1 by the 2b protein. The localisation of AGO2 is less characterised compared to AGO1, and AGO2 has not been reported in cellular bodies, as seen in human cells. The 2b protein was also shown to interact with AGO4 from Arabidopsis (Hamera et al., 2012), but not reported to interact with AGO2.

As the antiviral role for AGO2 is normally hidden in the presence of active AGO1, because the latter regulates the expression of AGO2 via the production of miR403 (Allen et al., 2005). However, during infection with CMV stains that inhibit AGO1, such as Fny-CMV, AGO2 is expressed at higher levels and then surfaces as an antiviral defence protein. The increased expression of AGO2 during CMV infection presumably contributes to viral resistance but also does not influence aphid feeding behaviour.

Future work is required to fully understand the dynamics of how AGO1 and AGO2 interact with viral proteins, and how this influences aphid behaviour. The novel interaction between 2a and 1a proteins has the potential to limit AGO1 inhibition which will consequently affect the level of AGO2 during infection. Future work in our lab will further investigate the importance of AGO2 in this CMV-aphid-Arabidopsis interaction. We aim to carry out future experiments quantifying *AGO2* expression levels in transgenic 2b and 1a/2b plants. If *AGO2* expression levels are reduced to normal levels in transgenic 1a/2b plants it suggests that the 1a protein is able to modify AGO1 miRNA binding activity. Similarly, as AGO2 localisation is less characterised compared to AGO1 it would be interesting to investigate if the localisation of AGO2 changes in the presence of CMV proteins, especially the 2b protein.

The 1a protein also prevents the induction of antibiosis allowing 2a-induced deterrence (which benefits virus transmission) to predominate (Fig. 6.2) (Westwood et al., 2013a). The effect of 1a on the 2b protein, however, does not affect its ability to suppress RNA silencing and so is also beneficial to the virus. The VSRs of several viruses target AGO1 in order to prevent antiviral silencing (discussed in Section 1.5.2 Viral suppressors of RNA silencing). However, disruption of antiviral silencing, via AGO1 inhibition, can also interfere with the miRNA signalling pathway. For example, the polerovirus P0 protein targets AGO1 for destruction (Pazhouhandeh et al., 2006; Baumberger et al., 2007; Bortolamiol et al., 2007), and the potyvirus HC-Pro binds to miRNA biosynthetic intermediates (Kasschau et al., 2003; Chapman et al., 2004; Lakatos et al., 2006). For viruses that do not require aphids for transmission, inhibiting AGO1 is an effective strategy for preventing antiviral silencing. However, the 2b-AGO1 interaction could be viewed as a booby trap, since

for CMV the induction of antibiosis results in poor aphid performance. In order to avoid disrupting the miRNA pathway, CMV subverts RNA silencing primarily through sequestration of siRNAs (Gonzalez et al., 2012). Furthermore, inhibiting AGO1 activity may be a counterproductive means of inhibiting antiviral RNA silencing. In Arabidopsis, AGO1 regulates AGO2 mRNA levels using miR403 and de-repression of AGO2 accumulation by the 2b protein triggers the establishment of another layer of antiviral silencing (Harvey et al., 2011). Thus, the interaction between the 1a replication protein and the 2b VSR represents a novel form of regulation by which a virus is able to modulate its ability to induce symptoms, suppress host resistance while simultaneously modifying interactions between its host and its insect vectors.

6.3 The 1a protein relocates the 2b protein to P-bodies

In Chapters 4 and 5 I confirmed that the 1a protein localised to P-bodies, and that the 1a protein is able to relocate the 2b protein to this cellular compartment. I observed that the 2b and 1a protein as well as AGO1 colocalised to P-bodies. This suggests that the spatial distribution of the 2b protein, dictated by the 1a protein, may play an important role in preventing the induction of antibiosis without compromising 2b VSR activity.

The RNA decay pathway is essential in maintaining mRNA quantity and quality control. RNA decay or exonucleolytic RNA turnover is a 5'–3' and 3'–5' exoribonuclease-dependent, ubiquitous mechanism by which mRNA molecules are enzymatically degraded (Zhang et al., 2017). It is initiated by removal of the 3'-poly(A) tails followed by exosome complex-mediated 3'–5' cleavage or decapping and subsequent exoribonuclease (XRN)-mediated 5'–3' decay (Souret et al., 2004). Deadenylation is catalysed by a conserved poly(A)-specific ribonuclease and the conserved carbon catabolite repressor 4 complex (Liang et al., 2009). Removal of the 5' cap is catalysed by the combined action of several conserved decapping proteins (DCP) (Zhang et al., 2017). In Arabidopsis, the decapping complex is

comprised of DCP1, DCP2, DCP5 and VCS (Xu et al., 2006), which are also involved in P-body formation and translational repression (Xu et al., 2009).

P-bodies are cytoplasmic ribonucleoprotein foci implicated in miRNA-directed RNA slicing and mRNA storage, and their formation is increased by induction of RNA silencing (Eulalio et al., 2007; Kulkarni et al., 2010). I observed that a P-body decapping protein, DCP1, co-localised with the 1a protein, indicating that a fraction of the 1a protein associates with P-bodies. I have not confirmed whether the 1a protein and DCP1 directly interact, if DCP1 and the 1a protein are in close proximity, or if the 1a protein interacts with other P-body components.

Viruses have mechanisms to protect their RNA molecules from the host surveillance machinery. TMV is able to activate RNA decay pathways to down-regulate RNA silencing and modulate symptom development (Conti et al., 2017). Recently, it was shown that turnip mosaic virus (TuMV) infection is able to disrupt the RNA decay pathway (Li and Wang, 2018). The TuMV HC-Pro VSR is able to interact and inhibit XRN4 slicing activity while VPg (a genome-linked viral protein) is able to disrupt the interaction between DCP1 and DCP2 by targeting DCP2 to the nucleus. Similarly the CMV CP was shown to play a role in the binding of viral RNAs, and was shown to interact with the RDR6/SGS3 complex (Zhang et al., 2017). It was proposed that the ability of the CP to bind RNAs protects viral RNA intermediates from RNA decay, which increases the substrate concentration of RDR/SGS3 complex and subsequently improves host antiviral silencing (Zhang et al., 2017). AGO7 was shown to accumulate with SGS3 and RDR6 in cytoplasmic siRNA bodies that are distinct from P-bodies. siRNA bodies are formed upon stress-induced translational repression. AGO7 congregates with miR390 and SGS3 in membranes and its targeting to the nucleus prevents its accumulation in siRNA bodies and ta-siRNA formation.

In human cells the interaction between AGO proteins and the P-body-associated GW182 (TNRC6A) is critical to gene silencing (Lazzaretti et al., 2009). GW182 co-localises with proteins of decapping in cytoplasmic foci, which were initially known as GW-bodies (Eystathioy et al., 2003). Plant P-bodies share many conserved proteins with yeast and human P-bodies indicating that plant P-bodies execute

similar functions, i.e. translational repression and decapping. Human AGO1 and AGO2 co-localize to DCP1 and are well known markers (Liu et al., 2005). AGO2 has not been identified in cytoplasmic foci in plants, but is far less characterised compared to AGO1.

These results are the first to my knowledge to demonstrate a link between CMV, P-bodies and the RNA decay pathway. I was unable to establish if the 1a protein directly interacts with DCP1, or other P-body components. Several recent publications have documented that viral proteins interact with components of the RNA decay pathway, such as DCP2 and VCS (Li and Wang, 2018; Lukhovitskaya and Ryabova, 2019). However, without knowing which P-body component the 1a protein interacts with it is hard to assume if it is involved in disrupting RNA decay. It is more likely that the 1a protein is only present at P-bodies as a function of its role in limiting the 2b-AGO1 interaction.

My results suggest that P-bodies are an important during CMV infection, which the 1a protein can modify to allow the degradation of mRNA transcripts, when miRNA-directed slicing of RNA targets is disrupted by the 2b protein. If AGO1 slicer activity is restored by the 1a protein in P-bodies, it suggests that target mRNAs may be processed, or stored within P-bodies. It is unlikely that AGO1 slicer activity is completely blocked by the 2b protein during CMV infection. Unlike in animals, there is minimal evidence of miRNA-mediated mRNA decay independent of slicer activity in plants (Arribas-Hernández et al., 2016). This suggests that the 1a protein may restore AGO1's role in miRNA-directed mRNA cleavage or RNA decay within P-bodies. Although the exact process that regulates the AGO1-dependent degradation of mRNA targets during CMV infection will require further investigation.

Further studies should make use of BiFC assays to determine if the 1a protein interacts directly with DCP1, or other P-body proteins. If the 1a protein was found to interact with a P-body component this would represent a novel interaction between a viral replicase protein and a host P-body component. Although even if the 1a protein interacts with a host component involved in RNA decay/miRNA processing, it is unlikely to inhibit its function. As transgenic plants expressing the 1a protein do not show any developmental phenotypes or induce antibiosis it

suggests that the 1a protein itself does not disrupt miRNA biogenesis or the downstream activity of miRNA-directed slicing of mRNA targets (Fig. 3.3, Fig. 3.4). It would also be interesting to explore if the LS-CMV 1a protein localises to P-bodies. As the LS-CMV 2b protein does not interact with AGO1, or trigger antibiosis in Arabidopsis, it would be interesting to observe if the LS-CMV 1a protein is able to co-localise with DCP1. If it does not localise with DCP1, this would support our hypothesis that the Fny-CMV 1a protein localises to P-bodies to prevent the induction of antibiosis during infection.

6.4 The 1a protein is a key regulator of 2a-induced antixenosis and 2b-induced antibiosis

In both Arabidopsis and tobacco, the 1a and 2b proteins appear to have antagonistic roles in conditioning CMV-induced effects on aphid–plant interactions. In Arabidopsis, AGO1 negatively regulates antibiosis against aphids (Kettles et al., 2013; Westwood et al., 2013a) and the inhibition of AGO1 by the Fny 2b protein induces antibiosis (Westwood et al., 2013a). It was initially hypothesised by Westwood et al. (2013a) that direct or indirect interactions between viral gene products might tune host anti-aphid defence responses. In tobacco, the 1a protein has the ability to trigger antibiosis against aphids, but this is counteracted by the 2b protein (Tungadi et al 2019; Ziebell et al., 2011). My results confirmed a direct interaction between the 2b and 1a protein. I additionally showed that the 1a protein competes with AGO1 for interaction with the 2b protein. This suggests that interaction between the 1a and 2b proteins determines whether antixenosis or antibiosis is the dominant form of CMV-induced aphid resistance in different hosts (Tungadi et al., 2020; Westwood et al., 2013a).

During early infection replication is prioritised and as a result the majority of 1a protein is coupled to the 2a protein at tonoplast replicase complexes, which is required for efficient replication of viral RNAs. However, the 2b RNA silencing suppressor protein of CMV inhibits antiviral silencing primarily by binding of virus-

derived siRNAS (González et al., 2012), allowing viral gene products including the 1a and 2a replicase proteins, to accumulate. During the initial infection, before cytoplasmic 2a is able to induce antixenosis, 2b-induced inhibition of AGO1 may result in antibiosis being the dominant form of resistance. As virus infection progresses, an increasing amount of the 2a protein becomes phosphorylated (Kim et al., 2002), preventing replicase formation. Disassociation of the replicase complex allows the 1a protein to carry out other functions. An increasing amount of the 1a protein may be free to localise to P-bodies that have formed as a result of antiviral silencing (Eulalio et al., 2007). The movement of the 1a protein to the P-body is required for the relocation of the 2b protein to P-bodies.

My results suggest that the 1a protein competitively binds to the 2b protein preventing its interaction with AGO1. But it appears that in P-bodies the close proximity of 1a-2b-AGO1 may be an important aspect of this interaction. The outcome of the 2b-AGO1 interaction appears to be dependent on which cellular compartment they are located. It is possible that the 1a protein restores AGO1 slicer activity by competing with AGO1 for interaction with the 2b protein exclusively in P-bodies. This is supported by the observation that 2b-AGO1 interaction still occurred in the cytoplasm when 1a was present. An increase in the amount of free 2a protein in the cytoplasm and concomitant build-up of 1a protein in P-bodies is likely to prevent 2b-induced suppression of AGO1 slicer activity. As the 1a protein does not interact with AGO1 directly, and does not disrupt the miRNA pathway, its presence at P-bodies is most likely related to its ability to relocate the 2b protein. The spatial separation of AGO1 when it is in complex with the 2b protein appears to permit 2b's inhibition of AGO1 slicer activity in the cytoplasm, while maintaining AGO1 slicer activity within P-bodies. This is in agreement with my observation that the 1a protein has no effect on 2b VSR activity.

Therefore, the 1a protein represents a key regulator of antibiosis and antixenosis. As the relative proportion of 1a protein binding to the 2a, or 2b protein likely determines which pathway is induced. The 1a protein could be observed as a suppressor of antibiosis, this is partly due to its ability to interact with the 2b protein. Complete, inhibition of the 2b-AGO1 interaction would likely not be beneficial for virus replication, as it is important that RNA-silencing is maintained. However, the

1a protein can bypass complete inhibition of 2b protein activity by spatially separating this interaction to P-bodies.

The ability for CMV to induce antibiosis and antixenosis in Arabidopsis may have biological significance. Early aphid infestation of a host plant may result in the host plant being killed before virus replication has had time to produce inoculum, or lead to aphid overcrowding causing the departure of winged aphids before sufficient inoculum has built up. Similarly, the early build of aphid vectors may trigger additional host defences or signalling pathways that may negatively affect viral replication. It is unknown if these two distinct forms of resistance are mutually exclusive, or form a continuum depending on the dynamic of viral proteins in the cell. The interplay of the 1a, 2b and 2a proteins allows this CMV to overcome RNA silencing-mediated resistance, while avoiding the induction of antibiosis, and inducing the synthesis of a feeding deterrent, 4MI3M, through activation of defensive signalling.

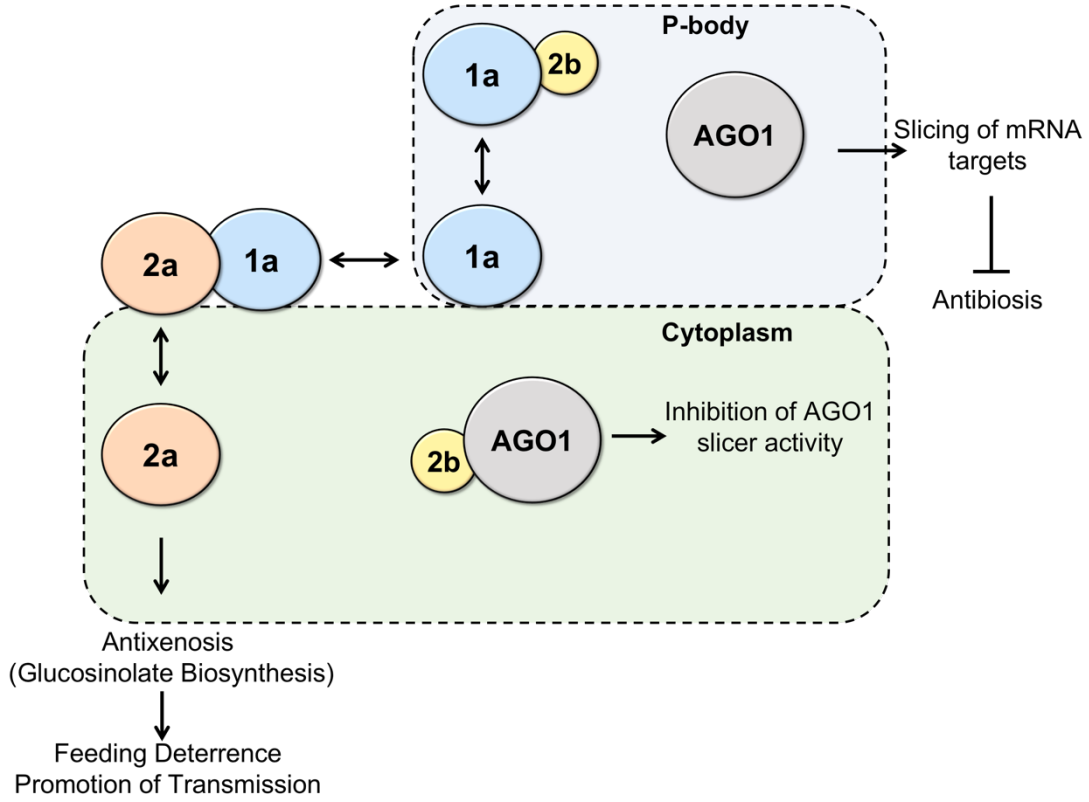

Figure 6.2. The interaction of the CMV 1a and 2b protein regulates the ability of AGO1 to induce strong aphid resistance.

The 2b RNA silencing suppressor protein of CMV inhibits antiviral silencing through binding of virus-derived siRNAs (González et al., 2012), allowing viral gene products including the 1a and 2a replicase proteins, to accumulate. The 2b protein can also bind to and inhibit AGO1 slicer activity, AGO1 also negatively regulates induction of a toxicity-based resistance to aphids (antibiosis). The 1a replicase protein is able to bind to the 2b protein in processing bodies (P-bodies) and moderates the inhibition of AGO1 by the 2b protein. The 1a-2b protein interaction occurs in the P-body and restores AGO1 activity, which normalises miRNA-directed slicing of mRNA targets during CMV infection preventing the induction of antibiosis. Phosphorylation of the 2a protein causes disassociation of the viral replicase complex. The 2a protein is then able to induce defence signalling, which results in feeding deterrence, which is thought likely to increase aphid dispersal and thus enhance transmission of non-persistently aphid-transmitted viruses like CMV (Westwood et al., 2013a).

6.5 Future avenues of work

6.5.1 Identifying 2a-interacting host proteins that trigger antixenosis

The 2a protein induces anti-aphid resistance when transgenically expressed in Arabidopsis (Westwood et al., 2013a). Currently, we do not know which host factors interact with the 2a protein to initiate immune signalling. Early in my project I generated infectious clones of Fny-CMV and LS-CMV RNA 2 containing a FLAG tag at the N terminal. I was able to immunoprecipitate the 2a protein and detect the 2a protein with anti-FLAG antibodies when purified from infected *N. benthamiana* and Arabidopsis plants.

Due to time constraints and focusing on other aspects of my project I was unable to progress with this research theme. My original aim was to immunoprecipitate the 2a protein from Arabidopsis plants infected with Fny-CMV and LS-CMV and identify potential interacting proteins. Proteins that interact with the Fny-2a and LS-2a proteins are unlikely to be responsible for triggering anti-aphid resistance since this is specific to the Fny-2a protein. Comparing the sequences of the 2a protein the N-terminal region was identified as the most likely region causing antixenosis induction. In future work this region could be expressed transiently in *N. benthamiana* and used as bait to characterise interacting proteins.

6.5.2 Identifying regions of the 2b protein that bind to the 1a protein

In Chapter 4 I demonstrated that the 1a and 2b proteins interact. Future work investigating this interaction will likely provide insights into the exact nature of this interaction. I initially observed that the 1a protein is able to supress 2b-inhibition of AGO1 activity in transgenic Arabidopsis plants. This suggests that this interaction in Arabidopsis is relevant during CMV infection. I carried out all further interaction work using transient expression of viral fusion proteins in *N. benthamiana*. It would be worth re-confirming the 1a-2b interaction *in planta* during CMV infection by co-immunoprecipitation. This would help understand the dynamics of when this protein

interaction occurs during infection, and if it is correlated to changes in expression of marker genes associated with antibiosis or antixenosis.

Current work in our group aims to identify which regions of the 2b protein are required for the interaction with the 1a protein. The C-terminal domain of the 2b protein encompasses 16 amino acid residues that have been shown to negatively regulate symptom induction and severity in three different host species (Lewsey et al., 2007). This effect was assumed to be due to increased inhibition of AGO1 activity by the mutant 2b$\Delta^{95\text{-}110}$ protein. In light of my observation that the 2b and 1a proteins interact, it is possible that increased symptoms associated with CMV 2b$\Delta^{95\text{-}110}$ infection are due to a loss of interaction with the 1a protein. It is likely that that a mutant 2b protein with a loss of 1a interaction would have exaggerated disease symptoms, compared to the wildtype 2b protein, and antibiosis would be induced.

Bibliography

Adio, A. M., Casteel, C. L., De Vos, M., Kim, J. H., Joshi, V., Li, B., Juéry, C., Daron, J., Kliebenstein, D. J., and Jander, G. (2011). Biosynthesis and defensive function of Nδ-acetylornithine, a jasmonate-induced Arabidopsis metabolite. The Plant Cell, 23(9), 3303-3318.

Agius, C., Eamens, A. L., Millar, A. A., Watson, J. M., and Wang, M. B. (2012). RNA silencing and antiviral defense in plants. Methods in Molecular Biology (Clifton, N.J.), 894, 17-38.

Allan, A. C., Lapidot, M., Culver, J. N., and Fluhr, R. (2001). An early tobacco mosaic virus-induced oxidative burst in tobacco indicates extracellular perception of the virus coat protein. Plant Physiology, 126, 97-108.

Allen, E., Xie, Z., Gustafson, A. M., and Carrington, J. C. (2005). MicroRNA-directed phasing during trans-acting siRNA biogenesis in plants. Cell, 121, 207-221.

Anderson, P. K., Cunningham, A. A., Patel, N. G., Morales, F. J., Epstein, P. R., and Daszak, P. (2004). Emerging infectious diseases of plants: pathogen pollution, climate change and agrotechnology drivers. Trends in Ecology and Evolution, 19(10), 535-544.

Antolín-Llovera, M., Ried, M. K., Binder, A., and Parniske, M. (2012). Receptor kinase signaling pathways in plant-microbe interactions. Annual Review of Phytopathology, 50, 451-473.

Antolín-Llovera, M., Ried, M. K., and Parniske, M. (2014). Cleavage of the SYMBIOSIS RECEPTOR-LIKE KINASE ectodomain promotes complex formation with Nod Factor Receptor 5. Current Biology, 24, 422-427.

Arribas-Hernández, L., Kielpinski, L. J., and Brodersen, P. (2016). mRNA Decay of Most Arabidopsis miRNA Targets Requires Slicer Activity of AGO1. Plant physiology, 171(4), 2620-2632.

Balaji, S., Bhat, A. I., and Eapen, S. J. (2008). A phylogenetic reexamination of Cucumber mosaic virus isolates based on 1a, 2a, 3a and 3b proteins. Indian Journal of Virology, 19(1), 17-25.

Bamunusinghe, D., Seo, J. K., and Rao, A. L. (2011). Subcellular localisation and rearrangement of endoplasmic reticulum by *Brome mosaic virus* capsid protein. Journal of Virology, 85, 2953-2963.

Baulcombe, D. (2004). RNA silencing in plants. Nature, 431, 356-363.

Baumberger, N., and Baulcombe, D. C. (2005). Arabidopsis ARGONAUTE1 is an RNA slicer that selectively recruits microRNAs and short interfering RNAs. Proceedings of the National Academy of Sciences of the United States of America, 102, 11928-11933.

Baumberger, N., Tsai, C. H., Lie, M., Havecker, E., and Baulcombe, D. C. (2007). The Polerovirus silencing suppressor P0 targets ARGONAUTE proteins for degradation. Current Biology, 17, 1609-1614.

Beckham, C., Light, H., Nissan, T,. Ahlquist, P., Parker, R., and Noueiry, A. (2007). Interactions between brome mosaic virus RNAs and cytoplasmic processing bodies. Journal of Virology, 81, 9759-9768.

Beclin, C., Berthome, R., Palauqui, J.C., Tepfer, M., and Vaucheret, H. (1998). Infection of tobacco or Arabidopsis plants by CMV counteracts systemic post-transcriptional silencing of nonviral (trans)genes. Virology, 252, 313-317.

Blanc, S. (2007). A protein key to plant virus transmission at the tip of the insect vector stylet. Proceedings of the National Academy of Sciences of the United States of America, 104, 17959-17964.

Blevins, T., Rajeswaran, R., Shivaprasad, P. V., Beknazariants, D., Si-Ammour, A., Park, H. S., Vazquez, F., Robertson, D., Meins, F., Jr, Hohn, T., and Pooggin, M. M. (2006). Four plant Dicers mediate viral small RNA biogenesis and DNA virus induced silencing. Nucleic Acids Research, 34(21), 6233-6246.

Boccard, F., and Baulcombe, D. (1993). Mutational analysis of cis-acting sequences and gene function in RNA3 of cucumber mosaic virus. Virology, 193, 563-578.

Boller, T., and Felix, G. (2009). A renaissance of elicitors: perception of microbe-associated molecular patterns and danger signals by pattern-recognition receptors. Annual Review of Plant Biology, 60, 379-406.

Bolte, S., Talbot, C., Boutte, Y., Catrice, O., Read, N.D. and Satiat-Jeunemaitre, B. (2004). FM-dyes as experimental probes for dissecting vesicle trafficking in living plant cells. Journal of Microscopy, 214, 159-173.

Bortolamiol, D., Pazhouhandeh, M., Marrocco, K., Genschik, P., and Ziegler-Graff, V. (2007). The Polerovirus F box protein P0 targets ARGONAUTE1 to suppress RNA silencing. Current Biology, 17(18), 1615-1621.

Bos, J. I. B., Prince, D., Pitino, M., Maffei, M. E., Win, J., and Hogenhout, S. A. (2010) A functional genomics approach identifies candidate effectors from the aphid species *Myzus persicae* (green peach aphid). PLoS Genetics, 6, e1001216.

Bouché, N., Lauressergues, D., Gasciolli, V., and Vaucheret, H. (2006). An antagonistic function for Arabidopsis DCL2 in development and a new function for DCL4 in generating viral siRNAs. The EMBO Journal, 25(14), 3347-3356.

Bracha-Drori, K., Shichrur, K., Katz, A., Oliva, M., Angelovici, R., Yalovsky, S., and Ohad. N. (2004). Detection of protein-protein interactions in plants using bimolecular fluorescence complementation. The Plant Journal, 40, 419-427.

Bradford, M. M. (1976). A rapid and sensitive method for the quantitation of microgram quantities of protein utilizing the principle of protein-dye binding. Analytical Biochemistry, 72, 248-254.

Brault, V., Uzest, M., Monsion, B., Jacquot, E., and Blanc, S. (2010). Aphids as transport devices for plant viruses. Comptes Rendus-Biologies, 333, 524-538.

Calil, I. P., and Fontes, E. (2017). Plant immunity against viruses: antiviral immune receptors in focus. Annals of Botany, 119(5), 711-723.

Canto, T., Prior, D. A. M., Hellwald, K. H., Oparka, K. J., and Palukaitis, P. (1997). Characterization of cucumber mosaic virus: 4. Movement protein and coat protein are both essential for cell-to-cell movement of cucumber mosaic virus. Virology, 237, 237-248.

Canto, T., Uhrig, J. F., Swanson, M., Wright, K. M., and MacFarlane, S. A. (2006). Translocation of tomato bushy stunt virus P19 protein into the nucleus by ALY proteins compromises its silencing suppressor activity. Journal of Virology, 80, 9064-9072.

Canto, T. and Palukaitis, P. (2001). A cucumber mosaic virus (CMV) RNA 1 transgene mediates suppression of the homologous viral RNA 1 constitutively and prevents CMV entry into the phloem. Journal of Virology, 75, 9114-9120.

Carbonell, A., Fahlgren, N., Garcia-Ruiz, H., Gilbert, K. B., Montgomery, T. A., Nguyen, T., Cuperus, J. T., and Carrington, J.C (2012). Functional analysis of three Arabidopsis ARGONAUTES using slicer-defective mutants. Plant Cell, 24:3613–3629.

Carmo-Sousa, M., Moreno, A., Garzo, E., and Fereres, A. (2014). A non-persistently transmitted-virus induces a pull-push strategy in its aphid vector to optimize transmission and spread. Virus Research, 186, 38-46.

Carr, J. P., and Murphy, A. A., In: Palukaitis P, García-Arenal F, editors. Cucumber Mosaic Virus. St Paul MN: APS Press; (2019). pp. 47-58.

Carr, J. P., Donnelly, R., Tungadi, T., Murphy, A. M., Jiang, S., Bravo-Cazar, A., Yoon, J. Y., Cunniffe, N. J., Glover, B. J., and Gilligan, C. A. (2018). Viral Manipulation of Plant Stress Responses and Host Interactions With Insects. Advances in Virus Research, 102, 177-197.

Carrère, I., Tepfer, M., and Jacquemond, M. (1999). Recombinants of cucumber mosaic virus (CMV): determinants of host range and symptomatology. Archives of Virology, 144(2), 365-379.

Carvalho, C. M., Santos, A. A., Pires, S. R., Rocha, C. S., Saraiva, D. I., Machado, J. P., Mattos, E. C., Fietto, L. G., and Fontes, E. P. (2008). Regulated nuclear trafficking of rpL10A mediated by NIK1 represents a defense strategy of plant cells against virus. PLoS Pathogens, 4(12), e1000247.

Casteel, C. L., M. De Alwis, A., Bak, H., Steven, A., and Jander, G. 2015. Disruption of ethylene responses by Turnip mosaic virus mediates suppression of plant defense against the aphid vector, *Myzus persicae*. Plant Physiology. 169,209-218.

Chakrabarty, R., Banerjee, R., Chung, S. M., Farman, M., Citovsky, V., Hogenhout, S. A., Tzfira, T., and Goodin, M. (2007). pSITE vectors for stable integration or transient expression of autofluorescent protein fusions in plants: probing *Nicotiana benthamiana*-virus interactions. Molecular Plant-Microbe Interactions, 20, 740-750.

Chapman, E. J., Prokhnevsky, A. I., Gopinath, K., Dolja, V. V., and Carrington, J. C. (2004). Viral RNA silencing suppressors inhibit the microRNA pathway at an intermediate step. Genes and Development, 18, 1179-1186.

Chaturvedi, S., Seo, J. K. and Rao, A. L. (2016). Functionality of host proteins in *Cucumber mosaic virus* replication: GAPDH is obligatory to promote interaction between replication-associated proteins. Virology, 494, 47-55.

Chen, H. Y., Yang, J., Lin, C., and Yuan, A. (2008). Structural basis for RNA-silencing suppression by *Tomato aspermy virus* protein 2b. The EMBO Journal, 9, 754-760.

Chen, B., and Francki, R. I. B. (1990). Cucumovirus transmission by the aphid *Myzus persicae* is determined solely by the viral coat protein. Journal of General, 71, 939-944.

Chinchilla, D., Shan, L., He, P., de Vries, S., and Kemmerling, B. (2009). One for all: the receptor-associated kinase BAK1. Trends in Plant Science, 14, 535-541.

Chinchilla, D., Zipfel, C., Robatzek, S., Kemmerling, B., Nürnberger, T., Jones, J. D., Felix, G., and Boller, T. (2007). A flagellin-induced complex of the receptor FLS2 and BAK1 initiates plant defence. Nature, 448(7152), 497-500.

Cillo, F., Mascia, T., Pasciuto, M. M. and Gallitelli, D. (2009). Differential effects of mild and severe cucumber mosaic virus strains in the perturbation of MicroRNA-regulated gene expression in tomato map to the 3′ sequence of RNA 2. Molecular Plant-Microbe Interactions, 22, 1239-1249.

Cillo, F., Roberts, I. M., and Palukaitis, P. (2002). *In situ* localization and tissue distribution of the replication-associated proteins of *Cucumber mosaic virus* in tobacco and cucumber. Journal of Virology, 76, 10654-10664.

Clay, N. K., Adio, A. M., Denoux, C., Jander, G., and Ausubel, F. M. (2009). Glucosinolate metabolites required for an Arabidopsis innate immune response. Science, 323(5910), 95-101.

Clough, S. J., and Bent, A. F. (1998). Floral dip: a simplified method for Agrobacterium-mediated transformation of *Arabidopsis thaliana* . The Plant Journal, 16, 735-743.

Cole, R. A. (1997). The relative importance of glucosinolates and amino acids to the development of two aphid pests *Brevicoryne brassicae* and *Myzus persicae* on wild and cultivated brassica species. Entomologia Experimentalis et Applicata, 85, 121-133.

Conti, G., Zavallo, D., Venturuzzi, A. L., Rodriguez, M. C., Crespi, M., and Asurmendi, S. (2017). TMV induces RNA decay pathways to modulate gene silencing and disease symptoms. The Plant Journal. 89, 73-84.

Csorba, T., Pantaleo, V., and Burgyán, J. (2009). RNA silencing: an antiviral mechanism. Advances in Virus Research, 75, 35-71.

Culver, J. N., and Padmanabhan, M. S. (2007). Virus-induced disease: altering host physiology one interaction at a time. Annual Review of Phytopathology, 45, 221-243.

Cuperus, J. T., Fahlgren, N., and Carrington, J. C. (2011). Evolution and functional diversification of MIRNA genes. The Plant Cell, 23, 431-442.

Curtis, M. D., and Grossniklaus, U. (2003). A gateway cloning vector set for high-throughput functional analysis of genes *in planta*. Plant Physiology, 133, 462-469.

den Boon, J. A., and Ahlquist, P. (2010). Organelle-like membrane compartmentalization of positive-strand RNA virus replication factories. Annual Review of Microbiology, 64, 241-256.

Deshoux, M., Monsion, B., and Uzest, M. (2018). Insect cuticular proteins and their role in transmission of phytoviruses. Current Opinion in Virology, 33, 137-143.

Devonshire, A. L., Foster, G. M., and Sawicki, R. M. (1977). Peach-potato aphid, *Myzus persicae* (Sulz.), resistant to organophosphorus and carbamate insecticides on potatoes in Scotland. Plant Pathology, 26, 60-62.

Diaz-Pendon, J. A., Li, F., Li, W. X., and Ding, S. W. (2007). Suppression of antiviral silencing by cucumber mosaic virus 2b protein in Arabidopsis is associated with drastically reduced accumulation of three classes of viral small interfering RNAs. The Plant Cell, 19(6), 2053-2063.

Ding, S. W., Anderson, B. J., Haase, H. R. and Symons, R. H. (1994). New overlapping gene encoded by the cucumber mosaic virus genome. Virology, 198, 593-601.

Ding, S. W., Shi, B. J., Li, W. X. and Symons, R. H. (1996). An interspecies hybrid RNA virus is significantly more virulent than either parental virus. Proceedings of the National Academy of Sciences of the United States of America, 93, 7470-7474.

Ding, S. W. (2010). RNA-based antiviral immunity. Nature Reviews Immunology, 10, 632-644.

Dodds, P. N., and Rathjen, J. P. (2010). Plant immunity: towards an integrated view of plant-pathogen interactions. Nature Reviews Genetics, 11, 539-548.

Dombrecht, B., Xue, G. P., Sprague, S. J., Kirkegaard, J. A., Ross, J. J., Reid, J. B., Fitt, G. P., Sewelam, N., Schenk, P. M., Manners, J. M., and Kazan, K. (2007). MYC2 differentially modulates diverse jasmonate-dependent functions in Arabidopsis. The Plant Cell, 19(*7),* 2225-2245.

Donnelly, R., Cunniffe, N. J., Carr, J. P., Gilligan, and C. A. (2019). Pathogenic modification of plants enhances long-distance dispersal of nonpersistently transmitted viruses to new hosts. Ecology, 100(7), e02725.

Drinnenberg, I. A., Fink, G. R., and Bartel, D. P. (2011). Compatibility with killer explains the rise of RNAi-deficient fungi. Science, 333(6049), 1592.

Drucker, M., and Then, C. (2015). Transmission activation in non-circulative virus transmission: A general concept? Current Opinion in Virology, 15, 63-68.

Du, Z., Chen, A., Chen, W., Liao, Q., Zhang, H., Bao, Y., Roossinck, M. J., and Carr, J. P. (2014). Nuclear-cytoplasmic partitioning of cucumber mosaic virus protein 2b determines the balance between its roles as a virulence determinant and an RNA-silencing suppressor. Journal of Virology, 88(10), 5228-5241.

Du. Z., Chen, A., Chen, W., Westwood, J. H., Baulcombe, D. C., and Carr, J. P. (2014b). Using a viral vector to reveal the role of miR159 in disease symptom induction by a severe strain of *Cucumber mosaic virus*. Plant Physiology, 164, 1378-1388.

Duan, C. G., Wang, C. H., and Guo, H. S. (2012). Application of RNA silencing to plant disease resistance. Silence, *3*(1), 5.

Elad, Y., and Pertot, I. (2014). Climate change impacts on plant pathogens and plant diseases. Journal of Crop Improvement, 28, 99-139.

Ellis, C., Karafyllidis, I., and Turner, J. G. (2002). Constitutive activation of jasmonate signaling in an Arabidopsis mutant correlates with enhanced resistance to *Erysiphe cichoracearum*, *Pseudomonas syringae*, and *Myzus persicae*. Molecular Plant-Microbe Interactions,15(10), 1025-1030.

Eulalio, A., Behm-Ansmant, I., Schweizer, D., Izaurralde, E. (2007). P-body formation is a consequence, not the cause of RNA-mediated gene silencing. Molecular Cell Biology, 27, 3970-3981.

Eystathioy, T., Jakymiw, A., Chan, E. K., Séraphin, B., Cougot, N., and Fritzler, M. J. (2003). The GW182 protein colocalizes with mRNA degradation associated proteins hDcp1 and hLSm4 in cytoplasmic GW bodies. RNA, 9(10), 1171–1173.

Fereres, A. (2015). Insect vectors as drivers of plant virus emergence. Current Opinion in Virology, 10, 42-46.

Fernández-Calvino, L., Goytia, E., López-Abella, D., Giner, A., Urizarna, M., Vilaplana, L., and López-Moya, J. J. (2010). The helper-component protease

transmission factor of tobacco etch potyvirus binds specifically to an aphid ribosomal protein homologous to the laminin receptor precursor. The Journal of General Virology, 91, 2862-2873.

Ferrari, S., Savatin, D. V, Sicilia, F., Gramegna, G., Cervone, F., and Lorenzo, G. De (2013). Oligogalacturonides: plant damage-associated molecular patterns and regulators of growth and development. Frontiers in Plant Science, 4, 49.

Fess, T.L., Kotcon, J.B., and Benedito, V.A. (2011). Crop breeding for low input agriculture: A sustainable response to feed a growing world population. Sustainability, 3, 1742-1772.

Filipowicz, W. (2005). RNAi: The nuts and bolts of the RISC machine. Cell, 122, 17-20.

Fontes, E. P. B., Santos, A. A., Luz, D. F., Waclawovsky, A. J., and Chory, J. (2004). The geminivirus nuclear shuttle protein is a virulence factor that suppresses transmembrane receptor kinase activity. Genes and Development, 18, 2545-2556.

Frerigmann, H., Piolewska-Bednarek, M., Sanchez-Vallet, A., Molina, A., Glawischnig, E., Gigolashvili, T., and Bednarek, P. (2016). Regulation of Pathogen-Triggered Tryptophan Metabolism in *Arabidopsis thaliana* by MYB Transcription Factors and Indole Glucosinolate Conversion Products. Molecular Plant, 9, 682-695.

Fukudome, A., and Fukuhara, T. (2017). Plant dicer-like proteins: double-stranded RNA-cleaving enzymes for small RNA biogenesis. Journal of Plant Research, 130(1), 33-44.

Gal-On, A., Canto, T., Palukaitis, P. (2000). Characterisation of genetically modified cucumber mosaic virus expressing histidine-tagged 1a and 2a proteins. Archives of Virology, 145(1), 37-50.

Gal-On, A., Kaplan, I., Roossinck, M.J., and Palukaitis, P. (1994). The kinetics of infection of zucchini squash by cucumber mosaic virus indicate a function for RNA 1 in virus movement. Virology, 205, 280-289.

Gao, M., Wang, X., Wang, D., Xu, F., Ding, X., Zhang Z., Bi, D., Cheng, Y.T., Chen, S., Li, X., and Zhang, Y. (2009). Regulation of cell death and innate immunity by two receptor-like kinases in Arabidopsis. Cell Host and Microbe, 6, 34-44.

Garcia-Ruiz, H., Takeda, A., Chapman, E. J., Sullivan, C. M., Fahlgren, N., Brempelis, K. J., and Carrington, J. C. (2010). Arabidopsis RNA-dependent RNA polymerases and dicer-like proteins in antiviral defense and small interfering RNA biogenesis during *Turnip Mosaic Virus infection*. The Plant Cell, 22(2), 481-496.

Garcia-Ruiz, H., Carbonell A., Hoyer J. S., Fahlgren, N, Gilbert, K. B., Takeda, A., Giampetruzzi, A., Garcia Ruiz, M. T., McGinn, M. G & Lowery, N. (2015). Roles and Programming of Arabidopsis ARGONAUTE Proteins during Turnip Mosaic Virus Infection. PLoS Pathogens. 2015;11:e1004755.

Gershoni, J. M., and Palade, G. E. (1982). Electrophoretic transfer of proteins from sodium dodecyl sulfate-polyacrylamide gels to a positively charged membrane filter. Analytical Biochemistry, 124, 396-405.

Gigolashvili, T., Yatusevich, R., Berger, B., Müller, C., and Flügge, U. I. (2007a). The R2R3-MYB transcription factor HAG1/MYB28 is a regulator of methionine-derived glucosinolate biosynthesis in *Arabidopsis thaliana* . The Plant Journal : for cell and molecular biology, 51(2), 247-261.

Gigolashvili, T., Berger, B., Mock, H. P., Müller, C., Weisshaar, B., and Flügge, U. I. (2007b). The transcription factor HIG1/MYB51 regulates indolic glucosinolate biosynthesis in *Arabidopsis thaliana* . The Plant Journal : for cell and molecular biology, 50(5), 886-901.

Gilliland, A., Singh, D. P., Hayward, J. M., Moore, C. A., Murphy, A. M., York, C. J., Slator, J., and Carr, J. P. (2003). Genetic modification of alternative respiration has

differential effects on antimycin A-induced versus salicylic acid-induced resistance to *Tobacco mosaic virus.* Plant Physiology 132, 1518-1528.

Gómez-Gómez, L., Felix, G., and Boller, T. (1999). A single locus determines sensitivity to bacterial flagellin in *Arabidopsis thaliana* . The Plant Journal : for cell and molecular biology, 18(3), 277-284.

Gonda, T. & Symons, R. H. (1979). Cucumber Mosaic Virus Replication in Cowpea Protoplasts: Time Course of Virus, Coat Protein and RNA Synthesis. Journal of General Virology, 45:3, doi.org/10.1099/0022-1317-45-3-723

González, I., Martínez, L., Rakitina, D. V, Lewsey, M.G., Atencio, F. A., Llave, C., Kalinina, N.O., Carr, J.P., Palukaitis, P., and Canto, T. (2010). *Cucumber mosaic virus* 2b protein subcellular targets and interactions: their significance to RNA silencing suppressor activity. Molecular Plant-Microbe Interactions, 23, 294-303.

González, I., Rakitina, D., Semashko, M., Taliansky, M., Praveen, S., Palukaitis, P., Carr, J.P., Kalinina, N., and Canto, T. (2012). RNA binding is more critical to the suppression of silencing function of *Cucumber mosaic virus* 2b protein than nuclear localization. RNA, 18, 771-782.

Goto, K., Kobori, T., Kosaka, Y., Natsuaki, T., Masuta, C. (2007). Characterization of silencing suppressor 2b of cucumber mosaic virus based on examination of its small RNA-binding abilities. The Plant Cell Physiology, 48, 1050-1060.

Gouveia, B. C., Calil, I. P., Machado, J. P. B., Santos, A. A., and Fontes, E. P. B. (2017). Immune Receptors and Co-receptors in Antiviral Innate Immunity in Plants. Frontiers in Microbiology, 7, 1-14.

Gray, S., Cilia, M., and Ghanim, M. (2014). Circulative, “Nonpropagative” virus transmission: An orchestra of virus-, insect-, and plant-derived instruments. Advances in Virus Research, 89, 141-199.

Groen, S. C., Jiang, S., Murphy, A. M., Cunniffe, N. J., Westwood, J. H., Davey, M. P., Bruce, T. J., Caulfield, J. C., Furzer, O. J., Reed, A., Robinson, S. I., Miller, E., Davis, C. N., Pickett, J. A., Whitney, H. M., Glover, B. J., and Carr, J. P. (2016). Virus Infection of Plants Alters Pollinator Preference: A Payback for Susceptible Hosts?. PLoS Pathogens, 12(8), e1005790.

Groen, S. C., Wamonje, F. O., Murphy, A. M., Carr, J. P. (2017). Engineering resistance to virus transmission. Current Opinion in Virology, 26, 20-27.

Groen, S. C., Tungadi, T., Du, Z., Westwood, J. H., Murphy, A. M., Labadie, T., Lucas, G., Powell, G. and Carr, J. P. (2020). Jasmonic acid and BAK1 are required in CMV-medicated plant defence against *Myzus persicae* in *Arabidopsis thaliana* . (Manuscript in preparation).

Habili, N. and Francki, R. I. B. (1974a). Comparative studies on tomato aspermy and cucumber mosaic viruses. I. Physical and chemical properties. Virology, 57, 392-401.

Habili, N. and Francki, R. I. B. (1974b). Comparative studies on tomato aspermy and cucumber mosaic viruses. II. Virus stability. Virology, 60, 29-36.

Hamera, S., Song, X., Su, L., Chen, X., Fang, R. (2012). *Cucumber mosaic virus* suppressor 2b binds to AGO4-related small RNAs and impairs AGO4 activities. The Plant Journal, 69, 104-115.

Handford, M. G., and Carr, J. P. (2006) Plant metabolism associated with resistance and susceptibility. In: Loebenstein, G., Carr, J.P., editors. Natural resistance mechanisms of plants to viruses. Berlin: Springer; pp. 315-340.

Hannon, G. J. (2002). RNA interference. Nature, 418(6894), 244-251.

Hartley, J. L., Temple, G. F., and Brasch, M. A. (2000). DNA Cloning Using *In Vitro* Site-Specific Recombination. Genome Research, 10, 1788-1795.

Harvey, J. J., Lewsey, M. G., Patel, K., Westwood, J., Heimstädt, S., Carr, J. P., and Baulcombe, D. C. (2011). An antiviral defense role of AGO2 in plants. PloS One, 6(1), e14639.

Hayes, R., Buck, K. (1990). Complete replication of a eukaryotic virus RNA *in vitro* by a purified RNA-dependent RNA polymerase. Cell, 63(2), 363-8.

He, K., Gou, X., Yuan, T., Lin, H., Asami, T., Yoshida, S., Scott, R., and Jia, L. (2007). BAK1 and BKK1 Regulate Brassinosteroid-Dependent Growth and Brassinosteroid-Independent Cell-Death Pathways. Current Biology, 17, 1109-15.

Heese, A., Hann, D. R., Gimenez-Ibanez, S., Jones, A. M. E., He, K., Li, J., Schroeder, J. I., Peck, S. C., and Rathjen, J. P. (2007). The receptor-like kinase SERK3/BAK1 is a central regulator of innate immunity in plants. Proceedings of the National Academy of Sciences of the United States of America, 104, 12217-12222.

Hull, R. (2009). Mechanical inoculation of plant viruses. Current protocols in microbiology, Chapter 16.

Hunter, P. R., Craddock, C. P., Di Benedetto, S., Roberts, L. M., and Frigerio, L. (2007). Fluorescent reporter proteins for the tonoplast and the vacuolar lumen identify a single vacuolar compartment in Arabidopsis cells. Plant Physiology, 145(4), 1371-1382.

Hwang, M. S., Kim, K. N., Lee, J. H., and Park, Y. I. 2007. Identification of amino acid sequences determining interaction between the *Cucumber mosaic virus*-encoded 2a polymerase and 3a movement proteins. Journal of General Virology, 88, 3445-3451.

Hwang, M. S., Kim, S. H., Lee, J. H., Bae, J. M., Paek, K. H. and Park, Y. I. (2005). Evidence for interaction between the 2a polymerase protein and the 3a movement protein of *Cucumber mosaic virus*. Journal of General Virology, 86, 3171-3177.

Hwang, M. S., Kim, S. H., Lee, J. H., Bae, J. M., Paek, K. H., and Park, Y. I. (2005). Evidence for interaction between the 2a polymerase protein and the 3a movement protein of Cucumber mosaic virus. Journal of General Virology, 86, 3171-3177.

Ilardi, V., and Nicola-Negri, E. D. (2011). Genetically engineered resistance to *Plum pox virus* infection in herbaceous and stone fruit hosts. GM Crops, 2(1), 24-33.

Inaba, J., Kim, B. M., Shimura, H., & Masuta, C. (2011). Virus-induced necrosis is a consequence of direct protein-protein interaction between a viral RNA-silencing suppressor and a host catalase. Plant physiology, 156(4), 2026–2036.

Ingelfinger, D., Arndt-Jovin, D. J., Luhrmann, R., and Achsel, T. (2002). The human LSm1-7 proteins colocalise with the mRNA-degrading enzymes Dcp1/2 and Xrnl in distinct cytoplasmic foci. RNA, 8, 1489-14501.

Ingwell, L. L., Eigenbrode, S. D., and Bosque-Pérez, N. A. (2012). Plant viruses alter insect behavior to enhance their spread. Scientific Reports. 2, 578.

Jacquemond, M. (2012). *Cucumber mosaic virus*. Advances in Virus Research, 84, 439-504.

Jaspars, E. M. J., Gill, D. S., and Symons, R. H. (1986). Viral RNA synthesis by a particulate fraction from cucumber seedlings infected with cucumber mosaic virus. Virology, 144, 410-425.

Jaubert, M., Bhattacharjee, S., Mello, A. F., Perry, K. L., and Moffett, P. (2011). ARGONAUTE2 mediates RNA-silencing antiviral defenses against Potato virus X in Arabidopsis. Plant Physiology, 156(3), 1556–1564.

Jensen, S., and Thomsen, A. R. (2012). Sensing of RNA Viruses: a Review of Innate Immune Receptors Involved in Recognizing RNA Virus Invasion. Journal of Virology, 86, 2900-2910.

Bruenn J. A. (1991). Relationships among the positive strand and double-strand RNA viruses as viewed through their RNA-dependent RNA polymerases. Nucleic Acids Research, 19(2), 217-226.

Ji, L. H., and Ding, S. W. (2001). The suppressor of transgene RNA silencing encoded by *Cucumber mosaic virus* interferes with salicylic acid-mediated virus resistance. Molecular Plant-Microbe Interactions, 14, 715-724.

Jia, X., Meng, Q., Zeng, H., Wang, W., and Yin, H. (2016). Chitosan oligosaccharide induces resistance to *Tobacco mosaic virus* in Arabidopsis via the salicylic acid-mediated signalling pathway. Scientific Reports, 6, 26144.

Jones-Rhoades, M. W., and Bartel, D. P. (2004). Computational identification of plant microRNAs and their targets, including a stress-induced miRNA. Molecular Cell, 14(6), 787-799.

Jones, J. D. G., and Dangl, J. L. (2006). The plant immune system. Nature, 444, 323-329.

Kalnins, A., Otto, K., Rüther, U., and Müller-Hill, B. (1983). Sequence of the lacZ gene of Escherichia coli. The EMBO Journal, 2, 593-597.

Kang, W. H., Seo, J. K., Chung, B. N., Kim, K. H., and Kang, B. C. (2012). Helicase domain encoded by *Cucumber mosaic virus* RNA1 determines systemic infection of Cmr1 in pepper. PloS One, 7(8), e43136.

Kaplan, I. B., Gal-On, A., Palukaitis, P., Canto, T., Prior, D. A. M., Hellwald, K. H., Oparka, K. J., and Palukaitis, P. (1997). Characterization of *Cucumber Mosaic Virus*. Virology, 237, 343-349.

Karimi, M., Depicke,r A., and Hilson, P. (2007). Recombinational cloning with plant Gateway vectors. Plant Physiology, 145, 1144-1154.

Kasschau, K., Carrington, J. (1998). A counterdefensive strategy of plant viruses: suppression of posttranscriptional gene silencing. Cell, 95(4), 461-70.

Kasschau, K. D., Xie, Z., Allen, E., Llave, C., Chapman, E. J., Krizan, K. A., and Carrington, J. C. (2003). P1/HC-Pro, a viral suppressor of RNA silencing, interferes with Arabidopsis development and miRNA unction. Developmental Cell, 4(2), 205-217.

Kawai, T., and Akira, S. (2006). Innate immune recognition of viral infection. Nature Immunology, 7, 131-137.

Kazana, E., Pope, T. W., Tibbles, L., Bridges, M., Pickett, J. A., Bones, A. M., Powell, G., and Rossiter, J. T. (2007). The cabbage aphid: a walking mustard oil bomb. Proceedings of the Royal Society Biological sciences, *274*(1623), 2271-2277.

Kettles, G. J., Drurey, C., Schoonbeek, H. J., Maule, A. J., Hogenhout, S. A. (2013). Resistance of *Arabidopsis thaliana* to the green peach aphid, *Myzus persicae*, involves camalexin and is regulated by microRNAs. New Phytologist, 198, 1178-1190.

Kim, J. H., and Jander, G. (2007). *Myzus persicae* (green peach aphid) feeding on Arabidopsis induces the formation of a deterrent indole glucosinolate. The Plant Journal, 49(6), 1008-1019.

Kim, M. J., Kim, H. R., and Paek, K. H. (2006a). Arabidopsis tonoplast proteins TIP1 and TIP2 interact with the cucumber mosaic virus 1a replication protein. Journal of General Virology, 87, 3425-3431.

Kim, M. J., Ham, B. K., and Paek, K. H. (2006b). Novel protein kinase interacts with the *Cucumber mosaic virus* 1a methyltransferase domain. Biochemical and Biophysical Research Communications, 340, 228-235.

Kim, M. J., Huh, S. U., Ham, B. K., and Paek, K. H .(2008). A novel methyltransferase methylates *Cucumber mosaic virus* 1a protein and promotes systemic spread. Journal of Virology, 82, 4823-4833.

Kim, S. H., Palukaitis, P., and Park, Y.I. (2002). Phosphorylation of cucumber mosaic virus RNA polymerase 2a protein inhibits formation of replicase complex. The EMBO Journal, 21, 2292-2300.

Klement, Z. (1963). Rapid detection of the pathogenicity of phytopathogenic Pseuodomonads. Nature, 199, 299-300.

Kliebenstein, D. J., Figuth, A., and Mitchell-Olds, T. (2002). Genetic architecture of plastic methyl jasmonate responses in *Arabidopsis thaliana* . Genetics, 61(4), 1685-1696.

Koncz, C., and Schell, J. (1986). The promoter of TL-DNA gene 5 controls the tissue-specific expression of chimaeric genes carried by a novel type of Agrobacterium binary vector. Molecular and General Genetics, 204, 383-396.

Kong, J., Wei, M., Li, G., Lei, R., Qiu, Y., Wang, C., Li, Z. H., and Zhu, S. (2018). The cucumber mosaic virus movement protein suppresses PAMP-triggered immune responses in Arabidopsis and tobacco. Biochemical and Biophysical Research Communications, 498(3), 395-401.

Kørner, C. J., Klauser, D., Niehl, A., Domínguez-Ferreras, A., Chinchilla, D., Boller, T., Heinlein, M., and Hann, D. R. (2013). The immunity regulator BAK1 contributes to resistance against diverse RNA viruses. Molecular Plant-Microbe Interactions, 26, 1271-1280.

Krenz, B., Bronikowski, A., Lu, X., Ziebell, H., Thompson, J. R., and Perry, K. L. (2015). Visual monitoring of *Cucumber mosaic virus* infection in *Nicotiana benthamiana* following transmission by the aphid vector *Myzus persicae*. The Journal of General Virology, 96(9), 2904-2912.

Krol, E., Mentzel, T., Chinchilla, D., Boller, T., Felix, G., Kemmerling, B., Postel, S., Arents, M., Jeworutzki, E., Al-Rasheid, K. A., Becker, D., and Hedrich, R. (2010). Perception of the Arabidopsis danger signal peptide 1 involves the pattern recognition receptor AtPEPR1 and its close homologue AtPEPR2. The Journal of Biological Chemistry, 285(18), 13471-13479.

Kulkarni, M., Ozgur, S., and Stoecklin, G. (2010). On track with P-bodies. Biochemical Society Transactions, 38, 242-251.

Kunze, G. (2004). The N Terminus of Bacterial Elongation Factor Tu Elicits Innate Immunity in Arabidopsis Plants. The Plant Cell Online, 16, 3496-3507.

Kuśnierczyk, A., Winge, P., Jørstad, T. S., Troczyńska, J., Rossiter, J. T., and Bones, A. M. (2008). Towards global understanding of plant defence against aphids-timing and dynamics of early Arabidopsis defence responses to cabbage aphid (*Brevicoryne brassicae)* attack. Plant, Cell and Environment, 31(8), 1097-1115.

Laemmli, U.K. (1970). Cleavage of structural proteins during the assembly of the head of bacteriophage T4. Nature, 227, 680-685.

Lakatos, L., Csorba, T., Pantaleo, V., Chapman, E. J., Carrington, J. C., Liu, Y. P., Dolja, V. V., Calvino, L. F., López-Moya, J. J., and Burgyán, J. (2006). Small RNA binding is a common strategy to suppress RNA silencing by several viral suppressors. The EMBO Journal, *25*(12), 2768-2780.

Lazzaretti, D., Tournier, I., and Izaurralde, E. (2009). The C-terminal domains of human TNRC6A, TNRC6B, and TNRC6C silence bound transcripts independently of Argonaute proteins. RNA, 15(6), 1059–1066.

Leather, S. R., and Dixon, A. F. G. (1984) Aphid growth and reproductive rates. Entomologia Experimentalis et Applicata, 35, 137-140.

Lewsey, M., Surette, M., Robertson, F. C., Ziebell, H., Choi, S. H., Ryu, K. H., Canto, T., Palukaitis, P., Payne, T., Walsh, J. A., and Carr, J. P. (2009). The role of the *Cucumber mosaic virus* 2b protein in viral movement and symptom induction. Molecular Plant-Microbe Interactions*,* 22(6), 642-654.

Lewsey, M., Robertson, F.C., Canto, T., Palukaitis, P., and Carr, J.P. (2007). Selective targeting of miRNA-regulated plant development by a viral counter-silencing protein. The Plant Journal, 50, 240-252.

Lewsey, M. G., Murphy, A. M., Maclean, D., Dalchau, N., Westwood, J. H., Macaulay, K., Bennett, M. H., Moulin, M., Hanke, D. E., Powell, G., Smith, A. G., and Carr, J. P. (2010). Disruption of two defensive signaling pathways by a viral RNA silencing suppressor. Molecular Plant-Microbe Interactions, 23(7), 835-845.

Li, F., and Wang, A. (2018). RNA decay is an antiviral defense in plants that is counteracted by viral RNA silencing suppressors. PLoS Pathogens, 14(8), e1007228.

Li, F., and Ding, S. W. (2006). Virus counterdefense: diverse strategies for evading the RNA-silencing immunity. Annual Review of Microbiology, 60, 503-531.

Li, H. W., Lucy, A. P., Guo, H. S., Li, W. X., Ji, L. H., Wong, S. M., and Ding, S. W. (1999). Strong host resistance targeted against a viral suppressor of the plant gene silencing defence mechanism. The EMBO Journal, 18, 2683-2691.

Li, J., Wen, J., Lease, K. A., Doke, J. T., Tax, F. E., and Walker, J. C. (2002). BAK1, an Arabidopsis LRR receptor-like protein kinase, interacts with BRI1 and modulates brassinosteroid signaling. Cell, 110(2), 213-222.

Li, L., Zhao, Y., McCaig, B. C., Wingerd, B. A., Wang, J., Whalon, M. E., Pichersky, E., and Howe, G. A. (2004). The tomato homolog of CORONATINE-INSENSITIVE1 is required for the maternal control of seed maturation, jasmonate-signalled defence responses, and glandular trichome development. The Plant Cell, 16, 126-143.

Li, Q., and Palukaitis, P. (1996). Comparison of the nucleic acid- and NTP-binding properties of the movement protein of cucumber mosaic cucumovirus and tobacco mosaic tobamovirus. Virology, 216(1), 71-79.

Li, Y., Zhang, Q., Zhang, J., Wu, L., Qi, Y., and Zhou, J.-M. (2010). Identification of microRNAs involved in pathogen-associated molecular pattern-triggered plant innate immunity. Plant Physiology, 152, 2222-2231.

Liang, W., Li, C., Liu, F., Jiang, H., Li, S., Sun, J., Wu, X., and Li, C. (2009). The Arabidopsis homologs of CCR4-associated factor 1 show mRNA deadenylation activity and play a role in plant defence responses. Cell Research, 19(3), 307-316.

Liu, S. J., He, X. H., Park, G., Josefsson, C., and Perry, K. L. (2002). A conserved capsid protein surface domain of *Cucumber mosaic virus* is essential for efficient aphid vector transmission. Journal of Virology, 76, 9756-9762.

Liu, J., Rivas, F. V., Wohlschlegel, J., Yates, J. R., Parker, R., and Hannon, G. J. (2005). A role for the P-body component GW182 in microRNA function. Nature Cell Biology, 7(12), 1261–1266.

Loebenstein, G. (2009). Plant Virus Diseases: Economic Aspects. In Desk Encyclopedia of Plant and Fungal Virology, pp. 171-176.

Lot, H., and Kaper, J. M. (1976). Physical and chemical differentiation of three strains of cucumber mosaic virus and peanut stunt virus. Virology, 74, 209-222.

Lotze, M. T., Zeh, H. J., Rubartelli, A., Sparvero, L. J., Amoscato, A. A., Washburn, N. R., DeVera, M. E., Liang, X., Tor, M., and Billiar, T. (2007). The grateful dead: Damage-associated molecular pattern molecules and reduction/oxidation regulate immunity. Immunological Reviews, 220, 60-81.

Lucas, W. J. (1995). Plasmodesmata-intercellular channels for macromolecular transport in plants. Current Opinion in Cell Biology, 7, 673-680.

Lucy, A. P., Guo, H. S., Li, W. X., and Ding, S. W. (2000). Suppression of post-transcriptional gene silencing by a plant viral protein localised in the nucleus. The EMBO Journal, 19, 1672-1680.

Lukhovitskaya, N., and Ryabova, L. A. (2019). *Cauliflower mosaic virus* transactivator protein (TAV) can suppress nonsense-mediated decay by targeting VARICOSE, a scaffold protein of the decapping complex. Scientific Reports, 9(1), 7042.

Ma, S., Quist, T. M., Ulanov, A., Joly, R., and Bohnert, H. J. (2004). Loss of TIP1;1 aquaporin in Arabidopsis leads to cell and plant death. The Plant Journal, 40, 845-859.

Macho, A. P., and Zipfel, C. (2014). Plant PRRs and the activation of innate immune signaling. Molecular Cell, 54, 263-272.

Majumdar, R., Rajasekaran, K., and Cary, J. W. (2017). RNA interference (RNAi) as a potential tool for control of mycotoxin contamination in crop plants: Concepts and considerations. Frontiers in Plant Science, 8, 200.

Mallory, A. C., Bartel, D. P., and Bartel, B. (2005). MicroRNA-directed regulation of Arabidopsis AUXIN RESPONSE FACTOR17 is essential for proper development and modulates expression of early auxin response genes. The Plant Cell, 17(5), 1360-1375.

Mandadi, K. K., and Scholthof, K. B. G. (2013). Plant immune responses against viruses: how does a virus cause disease? The Plant Cell, 25, 1489-1505.

Martin, B., Collar, J. L., Tjallingii, W. F., and Fereres, A. (1997). Intracellular ingestion and salivation by aphids may cause the acquisition and inoculation of non-persistently transmitted plant viruses. Journal of General Virology, 78, 2701-2705.

Masclaux, C. and Expert, D. (1995). Signalling potential of iron in plant-microbe interactions: the pathogenic switch of iron transport in *Erwinia chrysanthemi*. The Plant Journal, 7(1), 121-128.

Mauck, K. E., De Moraes, C. M., Mescher, M. C. (2010). Deceptive chemical signals induced by a plant virus attract insect vectors to inferior hosts. Proceedings of the National Academy of Sciences of the United States of America, 107, 3600-3605.

Mauck, K. E., De Moraes, C. M., Mescher, M. C. (2016). Effects of pathogens on sensory-mediated interactions between plants and insect vectors. Current Opinion in Plant Biology, 32, 53-61.

Mauck, K., Bosque-Pérez, N. A., Eigenbrode, S. D., De Moraes, C. M., and Mescher, M. C. (2012). Transmission mechanisms shape pathogen effects on host-vector interactions: Evidence from plant viruses. Functional Ecology, 26, 1162-1175.

Mayers, C. N., Palukaitis, P., Carr, J. P. (2008). Subcellular distribution analysis of the cucumber mosaic virus 2b protein. Journal of General Virology, 81, 219-226.

Mewis, I., Appel, H. M., Hom, A., Raina, R., and Schultz, J. C. (2005). Major signaling pathways modulate Arabidopsis glucosinolate accumulation and response to both phloem-feeding and chewing insects. Plant Physiology, 138, 1149-1162.

Mewis, I., Khan, M. A. M., Glawischnig, E., Schreiner, M., Ulrichs, C. (2012). Water stress and aphid feeding differentially influence metabolite composition in *Arabidopsis thaliana* (L.). PloS One, 7, e48661.

Mewis, I., Tokuhisa, J. G., Schultz, J. C., Appel, H. M., Ulrichs, C., and Gershenzon, J. (2006). Gene expression and glucosinolate accumulation in *Arabidopsis thaliana* in response to generalist and specialist herbivores of different feeding guilds and the role of defense signaling pathways. Phytochemistry, 67, 2450-2462.

Mi, S., Cai, T., Hu, Y., Chen, Y., Hodges, E., Ni, F., Wu, L., Li, S., Zhou, H., Long, C., Chen, S., Hannon, G. J., and Qi, Y. (2008). Sorting of small RNAs into Arabidopsis ARGONAUTE complexes is directed by the 5' terminal nucleotide. Cell, 133, 116-127.

Miao, H., Wei, J., Zhao, Y., Yan, H., Sun, B., Huang, J., and Wang, Q. (2013). Glucose signalling positively regulates aliphatic glucosinolate biosynthesis. Journal of Experimental Botany, 64, 1097-1109.

Mikkelsen, M. D., Petersen, B. L., Glawischnig, E., Jensen, A. B., Andreasson, E., and Halkier, B. A. (2003). Modulation of CYP79 genes and glucosinolate profiles in Arabidopsis by defense signaling pathways. Plant Physiology, 131, 298-308.

Mine, A., and Okuno, T. (2012). Composition of plant virus RNA replicase complexes. Current Opinion in Virology, 2, 663-669.

Minoia, S., Carbonell, A., Di Serio, F., Gisel, A., Carrington, J. C., Navarro, B., and Flores, R. (2014). Specific argonautes selectively bind small RNAs derived from potato spindle tuber viroid and attenuate viroid accumulation in vivo. Journal of VIrology, 88(20), 11933–11945.

Mlotshwa, S., Pruss, G., Vance, V. (2008). Small RNAs in viral infection and host defense. Trends in Plant Science, 13(7), 375-382.

Mochizuki, T., and Ohki, S. (2011). *Cucumber mosaic virus*: viral genes as virulence determinants. Molecular Plant Pathology, 13(3), 217-225.

Moon, S. L., and Wilusz, J. (2013). Cytoplasmic viruses: rage against the (cellular RNA decay) machine. PLoS Pathogens, 9(12), e1003762.

Moran, P.J., and Thompson, G.A. (2001). Molecular responses to aphid feeding in Arabidopsis in relation to plant defense pathways. Plant Physiology, 125, 1074-1085.

Morel JB, Godon C, Mourrain P, Beclin C, Boutet S, Feuerbach F, Proux F, Vaucheret H. Fertile hypomorphic ARGONAUTE (ago1) mutants impaired in post-transcriptional gene silencing and virus resistance. Plant Cell. 2002;14:629–639.

Motomura, K., Le, TN.Q., Kumakura, N., Fukaya, T., Takeda, A. and Watanabe, Y. (2012) The role of decapping proteins in the miRNA accumulation in *Arabidopsis thaliana*. RNA Biology, 644-652.

Mulot, M., Monsion, B., Boissinot, S., Rastegar, M., Meyer, S., Bochet, N., and Brault, V. (2018). Transmission of *Turnip yellows virus* by *Myzus persicae* Is Reduced by Feeding Aphids on Double-Stranded RNA Targeting the Ephrin Receptor Protein. Frontiers in Microbiology, 9, 457.

Nagy, P. D., Strating, J. R., and van Kuppeveld, F. J. (2016). Building Viral Replication Organelles: Close Encounters of the Membrane Types. PLoS Pathogens, 12(10), e1005912.

Nakahara, K. S., Masuta, C., Yamada, S., Shimura, H., Kashihara, Y., Wada, T. S., Meguro, A., Goto, K., Tadamura, K., Sueda, K., Sekiguchi, T., Shao, J., Itchoda, N., Matsumura, T., Igarashi, M., Ito, K., Carthew, R. W., and Uyeda, I. (2012). Tobacco calmodulin-like protein provides secondary defense by binding to and directing degradation of virus RNA silencing suppressors. Proceedings of the National Academy of Sciences of the United States of America, 109(25), 10113-10118.

Ng, J. C. K., and Perry, K. L. (2004). Transmission of plant viruses by aphid vectors. Molecular Plant Pathology, 5, 505-511.

Nicaise, V., and Candresse, T. (2016). *Plum pox virus* capsid protein suppresses plant pathogen-associated molecular pattern (PAMP)-triggered immunity. Molecular Plant Pathology, 18(6), 878–886.

Niehl, A., Wyrsch, I., Boller, T., and Heinlein, M. (2016). Double-stranded RNAs induce a pattern-triggered immune signaling pathway in plants. New Phytologist, 211, 1008-1019.

Nishikiori, M., and Ahlquist, P. (2018). Organelle luminal dependence of (+)strand RNA virus replication reveals a hidden druggable target. Scientific Advances, 4, eaap8258.

Nitta, N., Takanami, Y., Kuwata, S., Kubo, S. (1988). Inoculation with RNAs 1 and 2 of cucumber mosaic virus induces viral replicase activity in tobacco mesophyll protoplasts. Journal General Virology, 69, 2695-700.

O'Reilly, E. K., Paul, J. D., and Kao, C. C. (1997). Analysis of the interaction of viral RNA replication proteins by using the yeast two-hybrid assay. Journal of Virology, 71(10), 7526-7532.

O'Reilly, E. K., Wang, Z., French, R., and Kao, C. C. (1998). Interactions between the structural domains of the RNA replication proteins of plant-infecting RNA viruses. Journal of Virology, 72(9), 7160-7169.

Owen, J., and Palukaitis, P. (1988). Characterization of cucumber mosaic virus I. Molecular heterogeneity mapping of RNA 3 in eight CMV strains. Virology, 166, 495-502.

Owen, J., Shintaku, M., Aeschleman, P., Ben Tahar, S., and Palukaitis, P. (1990). Nucleotide sequence and evolutionary relationships of cucumber mosaic virus (CMV) strains: CMV RNA 3. Journal of General Virology, 71, 2243-2249.

Palukaitis, P. Determinants of pathogenesis. In: Palukaitis, P., García-Arenal, F., editors. Cucumber Mosaic Virus. St Paul MN: APS Press; (2019). pp. 145-154.

Palukaitis, P., and García-Arenal, F. (2003). Cucumoviruses. Advances in Virus Research, 62, 241–323.

Park, C. J., Caddell, D. F., and Ronald, P. C. (2012). Protein phosphorylation in plant immunity: insights into the regulation of pattern recognition receptor-mediated signaling. Frontiers in Plant Science, 3, 1-9.

Parry, G., Calderon-Villalobos, L. I., Prigge, M., Peret, B., Dharmasiri, S., Itoh, H., Lechner, E., Gray, W. M., Bennett, M., and Estelle, M. (2009). Complex regulation of the TIR1/AFB family of auxin receptors. Proceedings of the National Academy of Sciences of the United States of America, 106(52), 22540-22545.

Pazhouhandeh, M., Dieterle, M., Marrocco, K., Lechner, E., Berry, B., Brault, V., Hemmer, O., Kretsch, T., Richards, K. E., Genschik, P., and Ziegler-Graff, V. (2006). F-box-like domain in the polerovirus protein P0 is required for silencing suppressor function. Proceedings of the National Academy of Sciences of the United States of America, 103(6), 1994-1999.

Peden, K. W., and Symons, R. H. (1973). *Cucumber mosaic virus* contains a functionally divided genome. Virology, 53(2), 487-492.

Perry, K. L., Zhang, L., and Palukaitis, P. (1998). Amino acid changes in the coat protein of cucumber mosaic virus differentially affect transmission by the aphids *Myzus persicae* and *Aphis gossypii*. Virology, 242, 204-210.

Perry, K. L., Zhang, L., Shintaku, M. H., and Palukaitis, P. (1994). Mapping determinants in cucumber mosaic virus for transmission by *Aphis gossypii*. Virology, 205, 591-595.

Pfalz, M., Vogel, H., and Kroymann, J. (2009). The gene controlling the INDOLE GLUCOSINOLATE MODIFIER1 quantitative trait locus alters indole glucosinolate structures and aphid resistance in Arabidopsis. The Plant Cell, 21, 985-999.

Pirone, T. P., and Blanc, S. (1996). Helper-dependent vector transmission of plant viruses. Annual Review of Phytopathology, 34, 227-247.

Pomeranz, M. C., Hah, C., Lin, P. C., Kang, S. G., Finer, J. J., Blackshear, P. J., and Jang, J. C. (2010). The Arabidopsis tandem zinc finger protein AtTZF1 traffics between the nucleus and cytoplasmic foci and binds both DNA and RNA. Plant Physiology, 152(1), 151-165.

Powell, G. (2005). Intracellular salivation is the aphid activity associated with inoculation or non-persistently transmitted viruses. Journal of General Virology, 86, 469-472.

Prince, D. C., Drurey, C., Zipfel, C., and Hogenhout, S. A. (2014). The Leucine-Rich Repeat Receptor-Like Kinase BRASSINOSTEROID INSENSITIVE1-ASSOCIATED KINASE1 and the Cytochrome P450 PHYTOALEXIN DEFICIENT3 Contribute to Innate Immunity to Aphids in Arabidopsis. Plant Physiology, 164, 2207-2219.

Provvidenti, R., Robinson, R. W., and Shail, J. W. (1980). A source of resistance to a strain of Cucumber mosaic virus in *Lactuca saligna* L. Hortscience, 15, 528-529.

Fereres, A. and Raccah, B. (2015). Plant Virus Transmission by Insects. In eLS, John Wiley and Sons, Ltd (Ed.).

Qiu, Y., Zhang, Y., Wang, C. (2018). Cucumber mosaic virus coat protein induces the development of chlorotic symptoms through interacting with the chloroplast ferredoxin I protein. Science Reports 8, 1205

Rashid, U. J, Hoffmann, J., Brutschy, B., Piehler, J., and Chen, J. C. H. (2008). Multiple targets for suppression of RNA interference by *Tomato aspermy virus* protein 2B. Biochemistry, 47, 12655-12657.

Ren, T., Qu, F., and Morris, T. J. (2000). HRT gene function requires interaction between a NAC protein and viral capsid protein to confer resistance to turnip crinkle virus. The Plant Cell, 12, 1917-1926.

Rhee, S., Watt, L. G., Bravo-Cazar, A. L., Tungadi, T. D., and Carr, J. P. (2020). Effects of the *cucumber mosaic virus* 2a protein on symptoms and aphid-plant interactions in Arabidopsis. (Manuscript in preparation).

Rhoades, M., Reinhart, B., Lim, L., Burge, C., Bartel, B., and Bartel, D. (2002). Prediction of plant microRNA targets. Cell, 110, 513-520.

Rice, P., Longden, I., Bleasby A. (2000). EMBOSS: the European molecular biology open software suite [J]. Trends in Genetics, 16(6), 276-277.

Riedel, D., Lesemann, D. E., and Maiss, E. (1998). Ultrastructural localisation of nonstructural and coat proteins of 19 potyviruses using antisera to bacterially expressed proteins of plum pox potyvirus. Archives of Virology, 143, 2133-2158.

Rizzo, T. M., and Palukaitis, P. (1990). Construction of full-length cDNA clones of cucumber mosaic virus RNAs 1, 2 and 3: Generation of infectious RNA transcripts. Molecular and General Genetics, 222, 249-256.

Roossinck, M. J., Bujorski, J., Ding, S. W., Hajimorad, R., Hanada, K., Scott, S., Tousignant, M. (1999). Family Bromoviridae. 923-935 in: Virus Taxonomy Seventh Report of the International Committee on Taxonomy of Viruses.

Roossinck, M. J. (2002). Evolutionary history of *Cucumber mosaic virus* deduced by phylogenetic analyses. Journal of Virology, 76, 3382-3387.

Roossinck, M. J., and Palukaitis, P. (1990). Rapid induction and severity of symptoms in zucchini squash (Cucurbita pepo) map to RNA1 of cucumber mosaic virus. Molecular Plant-Microbe Interactions, 3, 188-192.

Roossinck, M. J., and White, P. S. (1998). Cucumovirus isolation and RNA extraction. In Plant Virology Protocols, G.D. Foster and S.C. Taylor, eds (Totowa, NJ: Humana Press), pp. 189-196.

Ross, A. F. (1961). Localized acquired resistance to plant virus infection in hypersensitive hosts. Virology, 14:329-39.

Ross, A. F. (1961). Systemic acquired resistance induced by localized virus infections in plants. Virology, 14:340-58.

Roux, M., Schwessinger, B., Albrecht, C., Chinchilla, D., Jones, A., Holton, N., Malinovsky, F. G., Tör, M., de Vries, S., and Zipfel, C. (2011). The Arabidopsis leucine-rich repeat receptor-like kinases BAK1/SERK3 and BKK1/SERK4 are required for innate immunity to hemibiotrophic and biotrophic pathogens. The Plant Cell, 23(6), 2440-2455.

Sabin, L. R., Zheng, Q., Thekkat, P., Yang, J., Hannon, G. J., Gregory, B. D., Tudor, M., and Cherry, S. (2013). Dicer-2 processes diverse viral RNA species. PloS One, 8(2), e55458.

Sambrook, J., Fritsch, E. F., Maniatis, T. (1989). Molecular Cloning: A Laboratory Manual. Cold Spring Harbor, NY, U.S.A. Cold Spring Harbor Laboratory Press.

Sanger, F., Nicklen, S., and Coulson, A.R. (1977). DNA sequencing with chain-terminating inhibitors. Proceedings of the National Academy of Sciences of the United States of America, 74(12), 5463-7.

Santos, A. A., Carvalho, C. M., Florentino, L. H., Ramos, H. J. O., and Fontes, E. P. B. (2009). Conserved threonine residues within the A-loop of the receptor NIK differentially regulate the kinase function required for antiviral signaling. PloS One, 4(6), e5781.

Schlaeppi, K., Abou-Mansour, E., Buchala, A., and Mauch, F. (2010). Disease resistance of Arabidopsis to *Phytophthora brassicae* is established by the sequential action of indole glucosinolates and camalexin. The Plant Journal, *62*, 840-851.

Scholthof, K. B., Adkins, S., Czosnek, H., Palukaitis, P., Jacquot, E., Hohn, T., Hohn, B., Saunders, K., Candresse, T., Ahlquist, P., Hemenway, C., and Foster, G. D. (2011). Top 10 plant viruses in molecular plant pathology. Molecular Plant Pathology, 12(9), 938-954.

Schuck, J., Gursinsky, T., Pantaleo, V., Burgyán, J., and Behrens, S.E. (2013). AGO/RISC-mediated antiviral RNA silencing in a plant *in vitro* system. Nucleic Acids Research, 41, 5090-5103.

Schwessinger, B., Roux, M., Kadota, Y., Ntoukakis, V., Sklenar, J., Jones, A., and Zipfel, C. (2011). Phosphorylation-dependent differential regulation of plant growth, cell death, and innate immunity by the regulatory receptor-like kinase BAK1. PLoS Genetics, 7(4), e1002046.

Seibel, N. M., Eljouni, J., Nalaskowski, M. M., and Hampe, W. (2007). Nuclear localization of enhanced green fluorescent protein homomultimers. Analytical Biochemistry, 368(1), 95-99.

Seo, J. K., Kwon, S. J., Kim, K. H. Replication and the replicase. In: Palukaitis P, García-Arenal F, editors. Cucumber Mosaic Virus. St Paul MN: APS Press; (2019). pp. 123-131.

Seo, J. K., Kwon, S. J., Choi, H. S., & Kim, K. H. (2009). Evidence for alternate states of Cucumber mosaic virus replicase assembly in positive- and negative-strand RNA synthesis. Virology, 383(2), 248–260.

Seth, R. B., Sun, L., and Chen, Z. J. (2006). Antiviral innate immunity pathways. Cell Research, 16(2), 141-147.

Shabalina, S. A., and Koonin, E. V. (2008). Origins and evolution of eukaryotic RNA interference. Trends in Ecology and Evolution, 23(10), 578-587.

Singh, R. K., Gase, K., Baldwin, I. T., and Pandey, S. P. (2015). Molecular evolution and diversification of the Argonaute family of proteins in plants. BMC plant biology, 15, 23.

Smith, C. M., and Boyko, E.V. (2006). Mini Review: The molecular bases of plant resistance and defense responses to aphid feeding: current status. Entomologia Experimentalis et Applicata, 122, 1-16.

Smith, L. M., Sanders, J. Z., Kaiser, R. J., Hughes, P., Dodd, C., Connell, C. R., Heiner, C., Kent, S. B., and Hood, L. E. (1986). Fluorescence detection in automated DNA sequence analysis. Nature, 321(6071), 674-679.

Soto-Suárez, M., Baldrich, P., Weigel, D., Rubio-Somoza, I., and San Segundo, B. (2017). The Arabidopsis miR396 mediates pathogen-associated molecular pattern-triggered immune responses against fungal pathogens. Scientific reports, 7, 44898.

Souret, F. F., Kastenmayer, J. P., and Green, P. J. (2004). AtXRN4 degrades mRNA in Arabidopsis and its substrates include selected miRNA targets. Molecular Cell, 15(2), 173-183.

Stewart, S. A., Hodge, S., Ismail, N., Mansfield, J. W., Feys, B. J., Prosperi, J. M., Huguet,, T., Ben, C., Gentzbittel, L., Powell, G. (2009). The RAP1 gene confers effective, race-specific resistance to the pea aphid in *Medicago truncatula* independent of the hypersensitive reaction. Molecular Plant-Microbe Interactions, 22, 645-1655.

Sun, Y., Li, L., Macho, A. P., Han, Z., Hu, Z., Zipfel, C., Zhou, J. M., and Chai, J. (2013). Structural basis for flg22-induced activation of the Arabidopsis FLS2-BAK1 immune complex. Science, 342(6158), 624-628.

Takeda, K., and Akira, S. (2004). TLR signaling pathways. Seminars in Immunology 16, 3-9.

Takeda, A., Iwasaki. S., Watanabe. T., Utsumi, M., and Watanabe Y. (2008). The mechanism selecting the guide strand from small RNA duplexes is different among argonaute proteins. Plant Cell Physiology, 49: 493–500.

Tharun, S., He, W., Mayes, A. E., Lennertz, P., Beggs, J. D., and Parker, R. (2000). Yeast Sm-like proteins function in mRNA decapping and decay. Nature, 404, 515-518.

Tornero, P. and Dangl, J. L. (2001). A high-throughput method for quantifying growth of phytopathogenic bacteria in *Arabidopsis thaliana*. The Plant Journal, 28(4), 475-481.

Towbin, H., Staehelin, T., and Gordon, J. (1979). Electrophoretic transfer of proteins from polyacrylamide gels to nitrocellulose sheets: procedure and some applications. Proceedings of the National Academy of Sciences of the United States of America 76, 4350-4354.

Traynor, P., Young, B. M., and Ahlquist, P. (1991). Deletion analysis of brome mosaic virus 2a protein. Effects on RNA replication and systemic spread. Journal of Virology, 65, 2807-2815.

Tungadi, T., Groen, S. C., Murphy, A. M., Pate, A. E., Iqbal, J., Bruce, T., Cunniffe, N. J., and Carr, J. P. (2017). *Cucumber mosaic virus* and its 2b protein alter emission of host volatile organic compounds but not aphid vector settling in tobacco. Virology Journal, 14(1), 91.

Tungadi, T., Donnelly, R., Qing, L., Iqbal, J., Murphy, A. M., Pate, A. E., Cunniffe, N. J., and Carr, J. P. (2020). Cucumber mosaic virus 2b proteins inhibit virus-induced aphid resistance in tobacco. Molecular Plant Pathology, 21(2), 250-257.

Uhrig, J. F., Canto, T., Marshall, D., MacFarlane, S.A. (2004). Relocalisation of nuclear ALY proteins to the cytoplasm by the tomato bushy stunt virus P19 pathogenicity protein. Plant Physiology, 135, 2411-2423.

Untergasser, A., Cutcutache, I., Koressaar, T., Ye, J., Faircloth, B.C., Remm, M. and Rozen, S.G. (2012). Primer3-new capabilities and interfaces. Nucleic Acids Research, 40, e115.

Uzest, M., Gargani, D., Dombrovsky, A., Cazevieille, C., Cot, D., and Blanc, S. (2010). The "acrostyle": a newly described anatomical structure in aphid stylets. Arthropod Structure and Development, 39(4), 221-229.

Uzest, M., Gargani, D., Drucker, M., Hébrard, E., Garzo, E., Candresse, T., Fereres, A., and Blanc, S. (2007). A protein key to plant virus transmission at the tip of the insect vector stylet. Proceedings of the National Academy of Sciences of the United States of America, 104(46), 17959-17964.

van Loon, L.C., Rep, M., and Pieterse, C.M.J. (2006). Significance of inducible defense-related proteins in infected plants. Annual Review of Phytopathology, *44*, 135-162.

Vaquero, C., Sanz, A. I., Serra, M. T., García-Luque, I. (1996). Accumulation kinetics of CMV RNA 3-encoded proteins and subcellular localization of the 3a protein in infected and transgenic tobacco plants. Archives of Virology, 141, 987-999.

Vaquero, C., Liao, Y. C., Nähring, J., and Fischer, R. (1997). Mapping of the RNA-binding domain of the cucumber mosaic virus movement protein. The Journal of General Virology, 78, 2095-2099.

Vaquero, C., Turner, A. P., Demangeat, G., Sanz, A., Serra, M. T., Roberts, K., and García-Luque, I. (1994). The 3a protein from cucumber mosaic virus increases the gating capacity of plasmodesmata in transgenic tobacco plants. The Journal of General Virology, 75, 3193-3197.

Várallyay, E., and Havelda Z. (2013). Unrelated viral suppressors of RNA silencing mediate the control of ARGONAUTE1 level. Molecular Plant Pathology, 14 567-575.

Várallyay, E., Válóczi, A., Agyi, A., Burgyán, J., Havelda, Z. (2010). Plant virus-mediated induction of miR168 is associated with repression of ARGONAUTE1 accumulation. The EMBO Journal, 29, 3507-3519.

Vargason, J. M., Szittya, G., Burgyán, J., Hall, T. M. (2003). Size-selective recognition of siRNA by an RNA silencing suppressor. Cell, 115, 799-811.

Vaucheret, H. (2008). Plant ARGONAUTEs. Trends in Plant Science, 13, 350-358.

Vaucheret, H., Vazquez, F., Crété, P., and Bartel, D. P. (2004). The action of ARGONAUTE1 in the miRNA pathway and its regulation by the miRNA pathway are crucial for plant development. Genes and Development, 18(10), 1187-1197.

Vos, I. A., Verhage, A., Schuurink, R. C., Watt, L. G., Pieterse, C. M. J., Van Wees, S. C. M. (2013). Onset of herbivore-induced resistance in systemic tissue primed for jasmonate dependent defenses is activated by abscisic acid. Frontiers in Plant Science, 4, 539.

Wang, X., Lee, W. M,, Watanabe, T., Schwart, M., Janda, M., Ahlquist, P. (2005). *Brome mosaic virus* 1a nucleoside triphosphatase/helicase domain plays crucial roles in recruiting RNA replication templates. Journal of Virology, 79, 13747-13758.

Wang, X., Kota, U., He, K., Blackburn, K., Li, J., Goshe, M. B., Huber, S. C., and Clouse, S. D. (2008). Sequential transphosphorylation of the BRI1/BAK1 receptor kinase complex impacts early events in brassinosteroid signaling. Developmental cell, 15(2), 220-235.

Wang, X. B., Wu, Q., Ito, T., Cillo, F., Li, W. X., Chen, X., Yu, J.L., and Ding, S. W. (2010). RNAi- mediated viral immunity requires amplification of virus-derived siRNAs in *Arabidopsis thaliana* . Proceedings of the National Academy of Sciences of the United States of America, 107, 484-489.

Watt, L. G., Crawshaw, S., Rhee, S. J., Murphy, A., Pate, A., Canto, T., and Carr, J. P. (2020). The cucumber mosaic virus 1a protein regulates interactions between the 2b protein and ARGONAUTE 1 while maintaining 2b's silencing suppressor activity. PloS Pathogens, (Manuscript in review).

Weigel, D., and Glazebrook, J. (2006). Transformation of agrobacterium using the freeze-thaw method. Cold Spring Harbour Protocols, doi:10.1101/pdb.prot4666.

Westwood, J. H., Groen, S. C., Du, Z., Murphy, A. M., Anggoro, D. T., Tungadi, T., Luang-In, V., Lewsey, M. G., Rossiter, J. T., Powell, G., Smith, A. G., and Carr, J.

P. (2013a). A trio of viral proteins tunes aphid-plant interactions in *Arabidopsis thaliana* . PloS One, 8(12), e83066.

Westwood, J. H., McCann, L., Naish, M., Dixon, H., Murphy, A. M., Stancombe, M. A., Bennett, M. H., Powell, G., Webb, A. A. R., and Carr, J. P. (2013b). A viral RNA silencing suppressor interferes with abscisic acid-mediated signalling and induces drought tolerance in *Arabidopsis thaliana* . Molecular Plant Pathology, 14, 158-170.

Westwood, J. H., Lewsey, M. G., Murphy, A. M., Tungadi, T., Bates, A., Gilligan, C. A., and Carr, J. P. (2014). Interference with jasmonic acid-regulated gene expression is a general property of viral suppressors of RNA silencing but only partly explains virus-induced changes in plant-aphid interactions. The Journal of General Virology, 95, 733-739.

Whitham, S., Dinesh-Kumar, S. P., Choi, D., Hehl, R., Corr, C., Baker, B. (1994). The product of the tobacco mosaic virus resistance gene N: similarity to toll and the interleukin-1 receptor. Cell, 78(6): 1101-15.

Wu, D., Qi, T., Li, W. X., Tian, H., Gao, H., Wang, J., Ge, J., Yao, R., Ren, C., Wang, X. B., Liu, Y., Kang, L., Ding, S. W., and Xie, D. (2017). Viral effector protein manipulates host hormone signaling to attract insect vectors. Cell Research, 27(3), 402-415.

Wu, M. F., Tian, Q., and Reed, J. W. (2006). Arabidopsis microRNA167 controls patterns of ARF6 and ARF8 expression, and regulates both female and male reproduction. Development, 133(21), 4211-4218.

Xu, A., Zhao, Z., Chen, W., Zhang, H., Liao, Q., Chen, J., Carr, J. P., and Du, Z. (2013). Self-interaction of the cucumber mosaic virus 2b protein plays a vital role in the suppression of RNA silencing and the induction of viral symptoms. Molecular Plant Pathology, 14(8), 803-812.

Xu J, Yang JY, Niu Q. W, Chua N. H. (2006). Arabidopsis DCP2, DCP1, and VARICOSE form a decapping complex required for postembryonic development. The Plant Cell, 18(12), 3386-3398.

Xu, J., and Chua, N. H. (2009). Arabidopsis decapping 5 is required for mRNA decapping, P-body formation, and translational repression during postembryonic development. The Plant Cell, 21(10), 3270-3279.

Xu, J., Meng, J., Meng, X., Zhao, Y., Liu, J., Sun, T., Liu, Y., Wang, Q., and Zhang, S. (2016). Pathogen-responsive MPK3 and MPK6 reprogram the biosynthesis of indole glucosinolates and their derivatives in Arabidopsis immunity. The Plant Cell, 28(5), 1144-1162.

Yang, H., Gou, X., He, K., Xi, D., Du, J., Lin, H., and Li, J. (2010). BAK1 and BKK1 in *Arabidopsis thaliana* confer reduced susceptibility to turnip crinkle virus. European Journal of Plant Pathology, 127, 149-156.

Yang, J. Y., Iwasaki, M., Machida, C., Machida, Y., Zhou, X., and Chua, N. H. (2008). betaC1, the pathogenicity factor of TYLCCNV, interacts with AS1 to alter leaf development and suppress selective jasmonic acid responses. Genes and Development, 22, 2564-2577.

Ye, K., Malinina, L., and Patel, D. (2003). Recognition of small interfering RNA by a viral suppressor of RNA silencing. Nature, 426, 874-878.

Yi, H., and Richards, E. J. (2007). A cluster of disease resistance genes in Arabidopsis is co-ordinately regulated by transcriptional activation and RNA silencing. The Plant Cell, 19, 2929-2939.

Yoneyama, M., and Fujita, T. (2010). Recognition of viral nucleic acids in innate immunity. Reviews in Medical Virology, 20, 4-22.

Yoon, J. Y, Palukaitis P, Choi, S. K. Host Range. In: Palukaitis P, García-Arenal F, editors. Cucumber Mosaic Virus. St Paul MN: APS Press; (2019). pp. 15-18.

Zaitlin, M., Anderson, J.M., Perry, K.L., Zhang, L., and Palukaitis, P. (1994). Specificity of replicase-mediated resistance to cucumber mosaic virus. Virology, 201, 200-205.

Zhang, X., Yuan, Y. R., Pei, Y., Lin, S. S., Tuschl, T., Patel, D. J., and Chua, N. H. (2006). *Cucumber mosaic virus*-encoded 2b suppressor inhibits Arabidopsis Argonaute1 cleavage activity to counter plant defense. Genes and Development, 20(23), 3255-3268.

Zhang, X., Zhao, H., Gao, S., Wang, W. C., Katiyar-Agarwal, S., Huang, H. D., Raikhel, N., and Jin, H. (2011). Arabidopsis Argonaute 2 regulates innate immunity via miRNA393(∗)-mediated silencing of a Golgi-localized SNARE gene, MEMB12. Molecular Cell, 42(3), 356–366.

Zhang, Z., Hu, F., Sung, M. W., Shu, C., Castillo-González, C., Koiwa, H., Tang, G., Dickman, M., Li, P., Zhang, X. (2017). RISC-interacting clearing 39-59 exoribonucleases (RICEs) degrade uridylated cleavage fragments to maintain functional RISC in *Arabidopsis thaliana.* eLife, 6, e24466

Zhang, L., Handa, K., and Palukaitis, P. (1994). Mapping local and systemic symptom determinants of cucumber mosaic cucumovirus in tobacco. Journal of General Virology, 75, 3185-3191.

Zhou, T., Murphy, A. M., Lewsey, M. G., Westwood, J. H., Zhang, H. M., González, I., Canto, T., and Carr, J. P. (2014). Domains of the cucumber mosaic virus 2b silencing suppressor protein affecting inhibition of salicylic acid-induced resistance and priming of salicylic acid accumulation during infection. The Journal of General Virology, 95, 1408-1413.

Zhou, N., Tootle, T.L., and Glazebrook, J. (1999). Arabidopsis PAD3, a gene required for camalexin biosynthesis, encodes a putative cytochrome P450 monooxygenase. The Plant Cell, 11, 2419-2428.

Ziebell, H., Murphy, A. M., Groen, S. C., Tungadi, T., Westwood, J. H., Lewsey, M. G., Moulin, M., Kleczkowski, A., Smith, A. G., Stevens, M., Powell, G., and Carr, J. P. (2011). *Cucumber mosaic virus* and its 2b RNA silencing suppressor modify plant-aphid interactions in tobacco. Scientific Reports, 1, 187.

Zilberman, D., Cao, X.F., and Jacobsen, S.E. (2003). ARGONAUTE4 control of locus-specific siRNA accumulation and DNA and histone methylation. Science, 299, 716-719.

Zipfel, C. (2008). Pattern-recognition receptors in plant innate immunity. Current Opinion in Immunology, 20, 10-16.

Zorzatto, C., Machado, J. P., Lopes, K. V., Nascimento, K. J., Pereira, W. A., Brustolini, O. J., Reis, P. A., Calil, I. P., Deguchi, M., Sachetto-Martins, G., Gouveia, B. C., Loriato, V. A., Silva, M. A., Silva, F. F., Santos, A. A., Chory, J., and Fontes, E. P. (2015). NIK1-mediated translation suppression functions as a plant antiviral immunity mechanism. Nature, 520(7549), 679-682.

Zust, T., Heichinger, C., Grossniklaus, U., Harrington, R., Kliebenstein, D.J ., and Turnbull, L. A. (2012). Natural Enemies Drive Geographic Variation in Plant Defenses. Science, 338, 116-119.